Optimal Deployment of Green Hydrogen Plants in Ontario Electricity System

Part I: Integration with Power Distribution and Bulk Transmission Systems

2024-08-30

Smart Grid Research Laboratory, York University

Version 1.1

This project was supported by the financial contribution of the Independent Electricity System Operator.

This project is supported by the financial contribution of the Independent Electricity System Operator (IESO), through its Hydrogen Innovation Fund. However, the views, opinions and learnings expressed in this report are solely those of The York University.

Table of Contents

Acronyms

PtH	Power to Hydrogen
HtP	Hydrogen to Power
GHP	Green Hydrogen Plant
CoH	Cost of Hydrogen
LCOH	Levelized Cost of Hydrogen
PEME	Proton Exchange Membrane Electrolysis
PEM	Proton Exchange Membrane
AE	Alkaline Electrolysis
UHV	Ultra-High Voltage
CAPEX	Capital Expenditure
OPEX	Operating Expenditure
CAES	Compressed-Air Energy Storage
PHES	Pumped-Hydro Energy Storage
RES	Renewable Energy Sources
IRA	Inflation Reduction Act
ITC	Investment Tax Credit
PTC	Production Tax Credit
IESO	Independent Electricity System Operator
LDC	Local Distribution Company
HOEP	Hourly Ontario Energy Prices
BESS	Battery Energy Storage Systems
BoP	Balance of Plant
HRS	Hydrogen Refueling Station
PtHtP	Power-to-Hydrogen-to-Power
FCEV	Fuel Cell Electric Vehicle
Mt	Million Tonnes
CCUS	Carbon Capture, Usage and Storage
SOEC	Solid Oxide Electrolysis Cell

PDF	Probability Distribution Function
SoH	State of Hydrogen
CEH	Carbon Emission per kg of Hydrogen
SQP	Sequential Quadratic Programming
PPA	Power Purchase Agreement
CBDR	Capacity-Based Demand Response
NPV	Net Present Value
IRR	Internal Rate of Return
RDG	Renewable Distributed Generation
ADS	Active Distribution System
DSO	Distribution System Operator
DSCM	Distribution System Congestion Management
ANSI	American National Standards Institute
BREV	Base Revenue
HfG	Hydrogen-Fired Generator
DR	Demand Response
OR	Operating Reserve
ICE	Internal Combustion Engine
EH	Energy Hub
SoC	State of Charge
GOF	Grid Operation Fee
SoH	State of Hydrogen
FCEV	Fuel Cell Electric Vehicle
DER	Distributed Energy Resource

Executive Summary

This report starts with a survey on green hydrogen production and storage technologies. The concepts of operation, research activities, and pilot projects are given and discussed. Various technologies for generation of hydrogen are discussed and compared. The technical and economic opportunities and challenges for integration of hydrogen generation and storage technologies with power systems are discussed, and the features of hydrogen storage are compared with other forms of energy storage.

Hydrogen utilization means, types, and economy of hydrogen are discussed. The technical and economic data in the public for hydrogen production and storage is collected and discussed. In addition, the data required for modeling, simulation, and analysis of Green Hydrogen Plants (GHPs) and their integration with the Ontario electricity market is collected and categorized. Where applicable, Ontario market data are used for simulation and studies to evaluate the feasibility and integration of GHP in Ontario. Modeling and simulation procedure of Proton Exchange Membrane Electrolysis (PEME) and Alkaline is given. The application of Power to Hydrogen (PtH) and Hydrogen to Power (HtP) conversion technologies for provision of ancillary services to the grid is investigated, and their technical and economic benefits are discussed. Further, the application of GHPs for serving Local Distribution Companies (LDCs) via resolving distribution grid issues is discussed.

The report is structured as follows:

Section 1 presents the introduction covering the background, survey on the relevant reports and articles, identifying the research gaps, and opportunities and challenges for integration of GHPs with the power grid. This section also narrows down the discussions to the barriers and opportunities for integration of GHPs specifically with the Ontario electricity market.

Section 2 discusses hydrogen supply chain including various technologies for hydrogen production, storage, and utilization. Different features of electrolyzers are presented and compared. Hydrogen production plants powered by renewable resources are discussed. The findings of this section can be summarized as follows:

- Primarily, there are three electrolyzer technologies (Alkaline, PEME, and solid oxide electrolyzer cell) with different performances.

- The alkaline water electrolyzer is a mature technology and has a stack lifetime (60,000 operating hours), the lowest degradation rate (0.1%/1000 hr.), and a low electricity consumption (48-53 kWh/kg H_2). It also has the widest capacity range (1-700 Nm^3/hr.) and the lowest capital expenditure (CAPEX) ($500-$1400/kW), but it offers a low efficiency in the range of 63-70%. It also offers a low response time up to 10 minutes and slow ramp rate of around 0.2-2% per second.

- The PEME is at the commercial stage and presents a stack lifetime of 50,000-60,000 operating hours, degradation rate of 0.2%/1000 hr, and electricity consumption of 46-55 kWh/kg H_2. It has a low-capacity range (1-100 Nm^3/hr) and a relatively high CAPEX ($1100-$1800/kW). It offers an efficiency of around 60-72%, a very fast start time of up to 1 minutes, and a ramp rate of 100% per second.

- The solid oxide electrolyzer cell is at the demonstration stage and has the highest efficiency (74-86%), but it operates at a higher temperature range (700-900°C) and introduces a shorter stack lifetime (<20,000 operating hours). It comes with the highest degradation cost (1.9%/1000 hr), and the electricity consumption of 40-45 kWh/kg H_2, provided that a heat source is made available. It offers the lowest capacity (1-10 Nm^3/hr) and the highest CAPEX ($2800-5600/kW).

- The geographical location is also a crucial factor affecting the Levelized Cost of Hydrogen (LCOH), even within the same country. This is because the potential for deployment of various renewable energy resources for green hydrogen production, such as solar or wind units, varies for different locations. For instance, the LCOH, the wholesale cost for producing hydrogen, varies from $3.883 to $10.887/kg within different locations according to a study. Another study suggests that the LCOH varies across the cities, ranging from $4.54 to $7.48/kg.

Section 3 discusses the modeling and simulations of GHP elements. It then presents the feasibility analysis of the hydrogen and storage plants for various applications including provision of ancillary services to the grid and resolving distribution system issues. The section discusses the distributed and centralized forms of hydrogen generation and storage. It is indicated how the optimal sizing and rating of hydrogen storage plants can be determined based on the available opportunities in the market. The findings of this section can be summarized as follows:

- The electrolyzer efficiency impacts the electricity consumption, and in turn the operating schedule and electricity usage cost. This would impact the LCOH values. It is indicated that as the efficiency increases, the LCOH decreases but the relationship between the LCOH and the efficiency values are non-linear.

- Despite the fact that mass production at central hydrogen generation plants is more economical, the transportation cost of the hydrogen to the consumption areas could escalate the overall cost. For the compressed hydrogen, the transportation cost is around $0.3-0.5/kg of hydrogen per 100km. If the production of hydrogen takes place within the utilization center, the transportation cost can be alleviated, and the reliability of hydrogen availability increases since the issues associated with transportation of hydrogen from the production facility to the utilization centers are eliminated.

- In the context of power and natural gas, Energy Hubs (EHs) can be formed using the emerging PtH and Hydrogen-Fired Generator (HfG) technologies. Such an EH can be used to serve the LDCs via loss reduction, voltage regulation, reverse power flow management, and congestion relief.

- **Section 4, 5, and 6** present final remarks, lessons learned, and next steps. The mathematical formulation for modeling and optimization is given in the appendix.

1. Introduction

1.1. Background

Hydrogen is playing a critical role in the global energy transition, where the production of low carbon hydrogen is identified as a potential long-term and reliable solution to address climate change while offering clean energy and economic growth. In response, many countries have recently developed and unveiled their national hydrogen economy strategies while there are unprecedented global efforts to scale up the clean hydrogen economy through unifying its fast developing and multi-faceted value chain. The global hydrogen demand is expected to reach 130 Million Tonnes (Mt) by 2030, compared to 94 Mt in 2019 [1].

In the meantime, there are different ways of producing hydrogen, where hydrogen production is classified based on the source or the process used to generate it and the associated amount of carbon emissions [1]. Among different types of resources, production of hydrogen from clean and/or low carbon electricity systems using water electrolysis is the most prominent. Hydrogen is labelled green when it is produced from Renewable Energy Sources (RES) such as solar and wind. To propel the mass deployment of clean hydrogen technologies, governments are offering new policies to enhance the economic viability of clean hydrogen production in comparison to conventional fuel. For example, the

USA approved the Inflation Reduction Act (IRA) in August 2022, which creates a new tax credit to subsidize low carbon hydrogen producers with either Investment Tax Credit (ITC) or Production Tax Credit (PTC) on the kg of produced hydrogen [2]. In 2023, Canada introduced refundable tax credits for net zero clean technologies worth up to 40% of the investment costs [3]. Similarly, the European Union announced a pilot auction program to provide subsidized contracts to green hydrogen producers. This auction is set to allocate a total of 800 million Euros to renewable hydrogen producers within the European economic area. The support will be structured as a fixed premium offered in kg of the generated renewable hydrogen [4].

Several MW-scale green hydrogen projects have been recently deployed and/or announced to be commissioned around the globe [5]—[7]. With continuous advancements in the electrolysis sizes and stacking, GHPs will have the potential to be rapidly scaled up to GW plants producing tons of hydrogen per day [8]. Yet, GHPs are categorized as complex and high cost systems, and thus, their mass deployment and integration with electricity systems necessitate the development of appropriate modelling tools: techno-economic analysis, optimal operation, and optimal design [9]—[10].

1.2. Survey of Existing Works

In this section, the main features of the analysis and studies conducted by typical detailed optimization and techno-economic analysis are given and compared. The main features of the above-mentioned reports and articles are given in Table 1 and are compared with the offerings of the current project.

Table 1 | Main Features of Analysis and Studies Conducted by Sample Reports or Articles

	Transmission System Support Feasibility	LDC Support Feasibility	Various Configurations of GHP	Co-Location of GHP&DERs	Detailed Techno-Economic Study	Cost-Benefit Analysis of Different Configurations	Different Electrolysis Technologies	Various Storage Technologies	Policy Considerations	Barriers Towards Green Hydrogen Production	Carbon Pricing/Taxation Mechanisms	Hydrogen Production Process
Proposed Project	X	X	X	X	X	X	X	x	X	X	X	X
Report [11]	X	X							X	X	X	X
Report [12]									X	X		X
Report [13]									X			X
Report [14]	X	X						X	X			
Article [15]				X		X				X		X
Article [16]			X	X						X		X
Article [17]				X		X				X		X
Article [18]				X						X		X

Article [19]	X	X
Article [20]	X	X

The technical report in [11] aims to guide policy makers in the design and implementation of policy to support green hydrogen as one of the feasible methods of decarbonising the energy sector. The guide focuses on the status and drivers of green hydrogen and the barriers it faces. It also explores the pillars of the national policy making to support hydrogen, and the third presents the main policy recommendations in different segments of the green hydrogen value chain.

The report in [12] explores the challenges that green hydrogen faces in the industrial sector and the options available to policy makers to address such challenges. It would discuss potential green uses in industry and identify barriers towards green hydrogen deployment.

The report in [13] focuses on the supply side of that value chain. It examines the policies that are needed to support the production of green hydrogen by water electrolysis, its transport to locations where it will be consumed, and the options for storage.

The report in [14] discusses different energy storage technologies, including mechanical, electrochemical, electrical, chemical and thermal energy storage technologies and are at different levels of development. It would also discuss the technologies for hydrogen storage.

The study in [15] is concerned with a multi-energy trading framework for a hybrid renewable-to-hydrogen provider to coordinate the interaction and trading of electricity and hydrogen while promoting the accommodation of renewable energy resources. The hydrogen provider can harvest renewables for green hydrogen production and generate stacked profits from both the electricity and hydrogen markets.

This article in [16] presents a multi-renewable-to-hydrogen production algorithm to improve the green hydrogen production efficiency in the presence of renewables. A hydrogen demand forecasting model is given to project the gas load for hydrogen fueling stations via extracting the spatial features and temporal dependencies of traffic flows in the transit network. A coordinated control strategy is presented to suppress high fluctuations in electrolysis current caused by sporadic availability of wind and solar outputs using model predictive control frameworks.

This study in [17] presents a bi-level strategic operation model for hydrogen service providers. At the operation level, the bidding, hydrogen generation and hydrogen transportation are coordinated to minimize the overall cost for hydrogen service providers. At the market level, the market clearing is

simulated to estimate the impact of hydrogen service providers behaviour on electricity prices in the market. A mechanism is developed to make connections between the discrete-time based hydrogen production and continuous-time based hydrogen transportation.

The authors in [18] present a hydrogen pricing method based on marginal pricing theory. The method is focused on hydrogen systems where renewables are used for hydrogen production. A hydrogen energy market is formed to define the industrial chain of hydrogen and the hydrogen trading mechanism. The calculation method for the locational marginal hydrogen price is given with respect to the prices in the electricity markets. Case studies and discussions are given to evaluate the performance of the methods.

This article in [19] proposes a reliability evaluation model for the integrated gas and electricity systems taking into account the effects of hydrogen. The PtH and methane process is given to convert the surplus renewable energy to hydrogen and methane. The produced gas is then injected into the natural gas pipelines. An optimal energy shedding model is presented to account for the impact of hydrogen on the energy flow. To consider the temporal feature of renewable energy, a Monte Carlo simulation method is applied to evaluate the reliability of the methods and processes.

This study in [20] discusses the process for hydrogen generation from renewables and injection to gas pipelines. It presents a gas security management scheme for hydrogen injection into natural gas systems generated from excessive wind power. It introduces gas security indices for the integrated electricity and gas system considering the coordinated operation of tightly coupled infrastructures. To maintain gas security within an acceptable range, the mixture of nitrogen and liquid petroleum gas with hydrogen is used to address the gas security violation caused by hydrogen injection.

The planning and operational impacts associated with the mass deployment of GHPs based on either centralized or distributed way of production on the electric grid have not been yet addressed. It is also not clear which entity or entities will own and operate the hydrogen infrastructure (generation, storage, transportation, and utilization). Further, the pricing mechanism (regulated versus competitive) of selling hydrogen to the hydrogen market and its impact on the electricity market have not been discussed. The costs of GHPs and the pricing mechanisms of selling hydrogen could significantly impact the cost of ownership and feasibility studies of adopting centralized and distributed GHPs.

1.3. Opportunities and Challenges for Integration of GHP with Power Grids

Market Price Arbitrage Opportunities - Inexpensive electricity during off-peak periods can be converted to hydrogen via electrolysis, stored, and released back to the grid using HtP conversion technologies during peak periods when the electricity price is high. This would benefit the grid by

partially shifting the demand from peak to off-peak periods and at the same time allow the hydrogen plant operator to benefit from market price variations.

Ancillary Services Opportunities - GHPs can be used for provision of various grid services including Demand Response (DR), Operating Reserve (OR), and smoothing of variable/renewable power generators. These grid services will benefit energy stakeholders including transmission system operators, distribution utilities, independent green hydrogen producers, and end customers. This is done via utilization of the GHPs capacity in full for enhancing the grid's resiliency and improving the financial profile of GHPs via stacked revenue from multiple sources.

Challenges for Integration of GHPs - There are several challenges towards utilization of GHPs for large-scale hydrogen production, as listed in the following [21]:

- **Cost of Hydrogen Compared to Existing Fossil-Based Fuels**

The cost for hydrogen production and utilization significantly exceeds the cost for production and generation of fossil fuels. As the technology materializes, however, the capital and operating expenditure for deployment and utilization of GHPs will alleviate.

- **Technological Uncertainties**

There are various technologies for production of clean hydrogen, many of which are still at the research or pilot stage and are yet to be proven to gain the trust of investors and become accepted for widespread deployment.

- **Policy and Regulatory Issues**

Deployment and utilization of GHPs are still new to policy makers and regulatory bodies. Various policies and regulations are yet to be developed for revenue support, technology incentivization, safety, etc.

- **Infrastructure Issues**

While there are already infrastructures in place for utilization of various energy resources such as electricity and gas, such infrastructures are not sufficient to facilitate widespread deployment of GHPs. There are still various issues for preparing the required infrastructures for efficient utilization of GHPs, including capital cost, social challenges, and technical issues.

- **Supply and Demand Issues**

Deployment of GHPs for production and storage of hydrogen does not necessarily lead to its utilization as an alternative source of energy. There are various challenges at the demand side that need to be addressed to create a balance between the supply and demand.

1.4. GHPs Deployment in Ontario

1.4.1. Background

Based on the Hydrogen Strategy unveiled in December 2020, Canada aims to position itself as a world-leading producer, user, and exporter of clean hydrogen. In response, Ontario has developed its provisional strategy for a low-carbon hydrogen economy, which was published in April 2022. Ontario has planned out multiple immediate actions to rapidly increase production capacity of low-carbon hydrogen to meet its need. Recently, Canada and Germany signed an agreement to enhance German energy security with clean Canadian hydrogen. The alliance will build on Canada's Hydrogen Strategy and mark a step towards Canada's objective of becoming a top global supplier of clean hydrogen. In its recent "*Pathways to Decarbonization*" report, the Independent Electricity System Operator (IESO) has referred to low-carbon hydrogen and renewable natural gas as a potential enabler towards the seamless decarbonization of the electricity system in the province. In this context, the province of Ontario has an economic and environmental opportunity to become a world-leader producer of hydrogen from its clean electricity supply.

1.4.2. Barriers in Ontario's Electricity System

In Ontario's power system, all coal power plants have been already phased out. The major power generation in Ontario is provided by nuclear power plants, which cannot quickly ramp down or up to track demand changes. Thus, they are operated for base-load generation. The trend of integrating more non-dispatchable renewable sources into the electric grid and phasing out more dispatchable fossil-fueled power plants reduces the operational flexibility of the grid and increases the chance of transmission congestion, as noted in the Bruce Transmission line.

As shown in Figure 1, historical public-domain data in Ontario's electricity market over the past several years has been analyzed to better understand the market behaviour. It is worth noting that as Ontario enters a state of both the capacity and energy needs in the near future, the historical data may not reflect the state of the Ontario's energy market in the future.

Figure 1 | Historical Ontario and Market Power and Prices Over the Past Ten Years

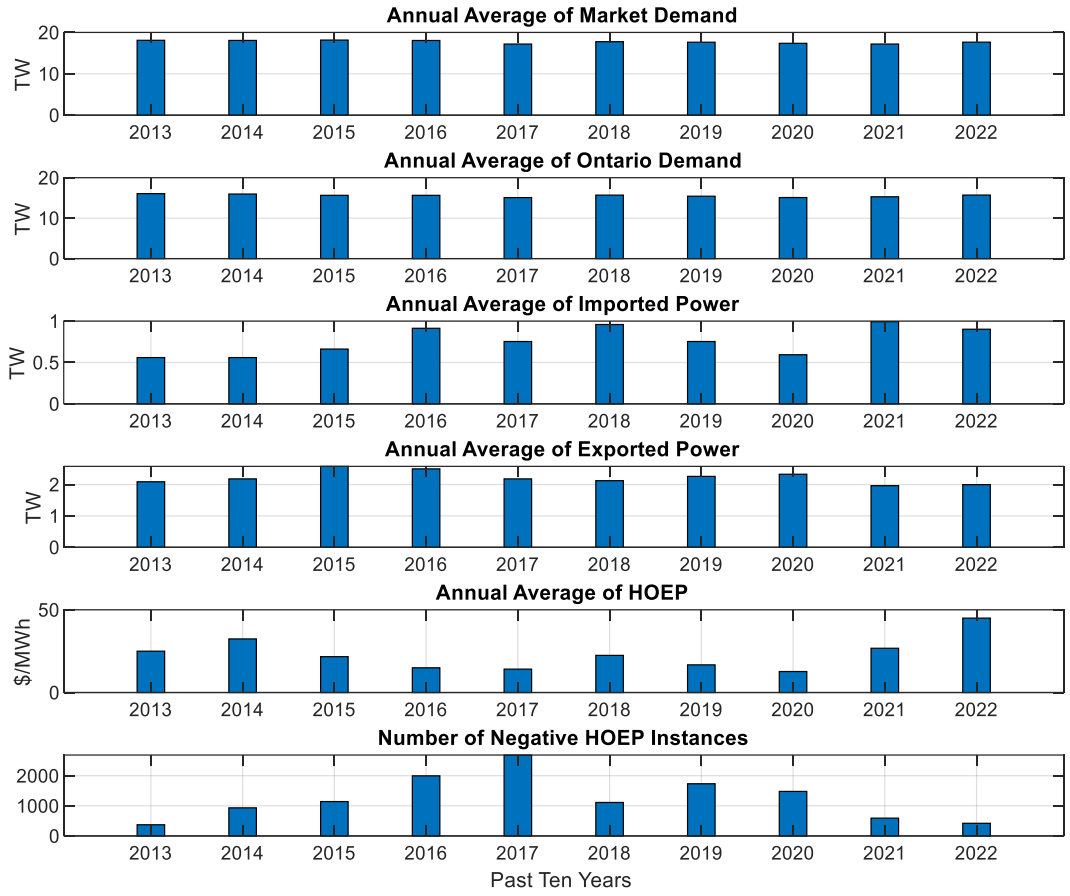

The results given in Figure 1 indicate that:

- Market and energy demands have been consistent over the past several years.
- Exported and imported powers have been variable over the years with export being significantly higher than the import in each year.
- Hourly Ontario Energy Prices (HOEP) values have also varied over the past several years with an increasing trend in recent years.
- The number of negative HOEP instances have been fluctuating where it has been on a decreasing trend recently.

From the data analysis, it can be concluded that:

- Even though very low or negative HOEP is an indication of higher supply than demand in the market, when HOEP goes low, it does not necessarily result in lower import. This means that even though there is excess power that drives the HOEP low, the market still needs to import power since excess generation (and negative prices) happen primarily at a time period when power is not needed.

It is worth noting that energy storage can be utilized as a fast-ramping dispatchable resource to help meet the future capacity needs. Ontario, however, is in the process of procuring Battery Energy Storage System (BESS) as dispatchable resources to ensure the flexibility and resiliency of the grid. By 2028, Ontario's entire BESS fleet is expected to consist of 26 facilities with total capacity of 2,916 MW, including the 390 MW Skyview 2 Battery Energy Storage System, which is expected to be the single largest storage facility procured in Canadian history. Utilization of GHPs and storage units can be considered as a promising solution for conversion of inexpensive/surplus electricity during off-peak hours to hydrogen through electrolysis. However, with the deployment of grid-connected hydrogen production units, another barrier that has to be overcome is to ensure that such hydrogen units will not lead to increased marginal emissions from more gas-powered generators being dispatched to meet marginal loads from electrolyzers.

Other barriers to the deployment of hydrogen generation units include climate consequences of hydrogen emissions, hydrogen gas management, safety, leakage, combustion dynamics, and low round-trip efficiency. Although hydrogen production is recognized as a promising alternative to the fossil fuel-based energies, it can indirectly cause adverse environmental and climate impacts. Hydrogen is known to have an indirect warming impact once it is related into the air. Safe storage, transportation, and utilization of hydrogen could pose some challenges to its widespread usage. Besides, as the technology for hydrogen production and utilization materializes more, the round-trip efficiency of the hydrogen units is yet to be optimized.

Yet, without appropriate investigation for the mass adoption of GHPs and evaluation of their impacts on the electricity system and hydrogen economy, creation of governments' policies and investment plans might reach a point of diminishing returns. Depending on the resources available and the capacity of the grid, actions can take place in the second half of the decade to address various challenges for the GHPs deployment that the grid operators in Ontario are facing.

Ontario is moving towards securing more storage capacities which helps with decarbonization and fulfilling the generation capacity requirements in the future. Distributed Energy Resources (DERs) are also expected to be utilized more in the near future to provide local generation. DERs can provide many benefits including providing customers control, reducing the system costs, and enhancing energy

security. DERs can reduce the dependency to large power plants and change how the supply mix is formulated.

1.4.3. The Expected Role of GHPs

While Ontario currently produces low-carbon energy, because of the near-term capacity requirements, the emissions of the system could increase due to increased frequency of dispatching a marginal gas unit. Hydrogen shows considerable promise to help Ontario reduce such system emissions. Hydrogen can be produced using clean energy in Ontario's grid and position Ontario to support the large-scale production of low-carbon hydrogen. GHPs can play a major role in Ontario in the second half of the decade and help the energy sectors to meet their needs. In the near future, green hydrogen can be used as a clean form of fuel to replace traditional fossil fuels and help Ontario move faster towards reduction of greenhouse gas emissions. According to the IESO's 2024 Annual Planning Outlook, it is predicted that Ontario's electricity demand will increase by 60% over the next 25 years. Deployment of 2,916 MW of BESS in Ontario by 2028 is a great step towards ensuring a reliable electric grid that could support the demand increase and help reduce emissions. BESS can provide various services to the Ontario's grid including energy shifting from off-peak to peak periods and provision of ancillary services. GHPs can work alongside BESS to utilize the surplus power for production of green hydrogen to meet the hydrogen demand in the near future. They can also provide various ancillary services to the grid similar to the BESS.

Electrolysis-based hydrogen plants are dispatchable units that can adjust their electricity demand to avoid congestion in the grid, contribute to various DR programs, and therefore, enhance the resiliency of the grid. Other resources could be also co-located with electrolysis, such as fuel cell, combustion units, PV, wind, or battery storage to increase the resiliency and functions of the system and contribute to decarbonization via production of clean energy. GHPs can be constructed either as: 1) centralized (off-site) large-scale plants within the IESO-controlled transmission grid that would then transport/export hydrogen to utilization sites, or 2) distributed small-scale plants (usually less than 10 MW within LDCs) for local generation, storage, and utilization.

Here it is noteworthy that the ramp rates of the electrolysis process depend on the technology which is used for hydrogen production, e.g., Alkaline or Proton Exchange Membrane (PEM). Technologies with slower ramp rates such as Alkaline are more suitable for baseload and can be utilized for production of hydrogen at nighttime using inexpensive/waste electricity. Technologies with higher ramp rates, e.g., PEM, however, are more suitable for provision of various grid services since they are able to make rapid changes in their energy consumption level. In addition, careful considerations should be given to the design and configuration aspects of GHPs to ensure that they are technically sound and economically viable solutions.

While inexpensive electricity from the grid can be considered as the most viable form of energy for hydrogen production, other energy sources show promise. Biomass, a renewable organic energy resource, such as agriculture crop residues, can be used to produce hydrogen via gasification, along with other byproducts. While biomass gasification is a mature technology and can be adopted for hydrogen production, it can also be used for electricity generation. The appropriateness of biomass for hydrogen versus electricity generation depends on the capital and operating costs and system efficiency. With the technological advancements in recent years, green hydrogen can be produced in the near future through biomass pyrolysis. The byproducts of the pyrolysis process including carbon black can be utilized in industry applications to further enhance the efficiency of the process. The successful deployment of biomass-derived hydrogen production via pyrolysis depends on the initial and running costs of the system.

1.4.4. Application of GHPs

1.4.4.1. Provision of Ancillary Services to the Grid

Feasibility-based sizing, design, and scheduling models are used for utilization of GHPs for provision of various grid services including DR, OR, and smoothing of variable/renewable power generators. These grid services will benefit energy stakeholders including IESO, distribution utilities, independent green hydrogen producers, and end users. This is because the model would allow for utilization of the GHPs capacity in full for enhancing the grid's resiliency and improving the financial profile of the GHPs via stacked revenue from multiple sources.

1.4.4.2. Resolving Various Grid Issues

The integration of dispatchable GHPs into the grid will bring several values to the grid via alleviating many existing or imminent distribution grid issues. Hydrogen generation units as dispatchable assets can be utilized for alleviating distribution losses, managing reverse power flow, voltage regulation, and congestion relief. Electrolyzers that are set up to produce hydrogen can adapt their generation according to the needs of the distribution grid and contribute to resolving various issues in the grid. This would, in turn, defer or eliminate the need of grid infrastructure upgrades in transmission and/or distribution grids and thereby alleviating huge financial burdens for ratepayers.

1.4.5. Technology Solution in Ontario

The ramp rates and start up times of the electrolysis process for hydrogen production, that would impact the type of services the technology can provide to the grid, depend on the technology which is used for hydrogen production, e.g., Alkaline or PEM.

The studies show that electrolysis technologies with slower ramp rates such as Alkaline are more suitable for managing surplus base generation and can be utilized for production of hydrogen at nighttime during events of sustained inexpensive/waste electricity. As such, the Alkaline technology would be utilized for energy shifting from off-peak to peak periods in the Ontario's grid. Technologies with higher ramp rates, e.g., PEM, however, are more suitable for provision of various grid services as they can make rapid changes in their energy consumption level.

1.4.6. The Need for Strategic Research

Research is necessary to allow for informed actions and policies to be implemented for the provisional and regional green hydrogen strategies. Agreement on the most likely scenario(s) for GHPs adoption in Ontario will help inform the stakeholders about the urgency of specific actions. The outcomes of the research will help inform provincial and municipal staff as they collectively provide input on the prioritization of possible actions. Additionally, provincial and municipal actions need to be in line with the generation capacity and other restrictions established by the IESO and LDCs. In some areas, new electrical loads (such as GHPs) may not be installed due to capacity limitations in power generation, transmission, and/or distribution systems. Also, mass deployment of GHPs could alter the existing electricity market programs and initiatives in Ontario, and thus, impact the flexibility and operability of the entire system.

2. Hydrogen Energy Supply Chain

2.1. Hydrogen Generation and Hydrogen to Power Technologies

Hydrogen can be generated either centrally in large scale and then be transported to hydrogen utilization point, or produced on site (i.e., near consumption areas). Despite the fact that mass production at central hydrogen generation plants is more economical, the transportation cost of hydrogen to consumption areas could escalate the overall cost. For the compressed hydrogen, the transportation cost is around $0.3-0.5/kg of hydrogen per 100km. In the case of the fueling stations for instance, it has been argued that the production of hydrogen should take place within the fueling station facility in order to alleviate the transportation cost and increase the reliability of hydrogen availability. In what follows, various technologies for hydrogen generation and power generation using hydrogen are discussed.

2.1.1. Electrolyzer Technologies

An electrolyzer produces hydrogen by electrochemically converting water into hydrogen and oxygen. Primarily, there are three electrolyzer technologies with different performances as indicated in Table 2. Relatively, the alkaline water electrolyzer offers the longest stack lifetime (60,000 operating hours), the lowest degradation rate (0.1%/1000 hr.), and the lowest electricity consumption (48-53 kWh/kg H_2). It also has the widest capacity range (1-700 Nm^3/hr.) and the lowest CAPEX ($500-1400/kW), but it offers a lower efficiency. The PEM electrolyzer introduces the fastest start response time (5 sec. up to 1 min.). While the solid oxide electrolyzer cell offers the highest efficiency (74-86%), it however, operates at a higher temperature range (700-900°C) and has a shorter stack lifetime (<20,000 operating hours) [22] - [24].

Table 2 |Comparison Between Electrolyzer Technologies

	Alkaline Water Electrolyzer	**Proton Exchange Membrane Electrolyzer**	**Solid Oxide Electrolyzer Cell**
Technological Maturity	Mature (TRL: 10)	Commercial (TRL: 9)	Demonstration (TRL:7)
Efficiency	63-70%	60-72%	74-86%
Operating Temperature (°C)	<60	50-80	700-900
Operating Pressure Range (bar)	1-30	1-30	8-50
Start Response	Up to 10 mins	5 seconds up to 1 min	NA
Ramp Up/Down	0.2-2% per second	100% per second	NA
Capacity (Nm^3/hr)	1-700	1-100	1-10
Stack Lifetime (Operating Hours)	60,000	50,000-80,000	<20,000
Degradation (%/1000 hr)	0.1	0.2	1.9
Electricity Consumption (kWh/kg H_2)	48-53	55-60	40-45 (with heat source)
Plant Scale (kg/day) in 2020	Up to 70,000	Up to 50,000	Pilot Scale
CAPEX ($/kW)	500-1400	1100-1800	2800-5600

It is worth noting that the electrolyzer efficiency varies depending on the power input of the electrolyzer as depicted in Figure 2 [25].

Figure 2 | Electrolyzer Power, Conversion Efficiency, Hydrogen Production Rate, and CoH as Functions of Power

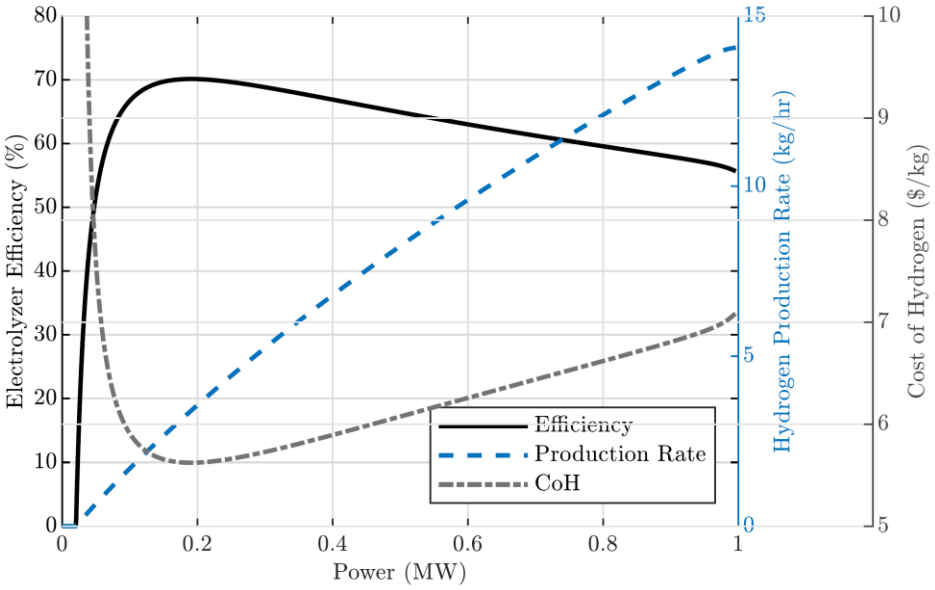

Figure 2 shows the relationship between the conversion efficiency, hydrogen production rate, and Cost of Hydrogen (CoH) production for a 1-MW electrolyzer with a fixed electricity cost of $100/MWh. The electrolyzer efficiency increases with increasing the electrolyzer loading to a certain level, and then it starts decreasing. For the example given, an operating point of 15-25%, the electrolyzer produces its maximum efficiency at 70%, and the CoH would be minimum at around $5.6/kg. At very low operating points, near zero, the efficiency is set to zero, where the CoH represents the cost of operating the electrolyzer in the standby mode. Once the electrolyzer is operated at its maximum capacity, the efficiency and CoH reach to around 55% and $7/kg, respectively. The hydrogen production rate almost linearly increases with the increase of the electrolyzer power consumption from zero to around 14 kg/hr.

In general, the figure shows the trade-off between the system efficiency and the hydrogen production cost. A high hydrogen production cost is associated with a lower system efficiency, meaning there are higher power losses. Operating an electrolyzer at the maximum efficiency mandates oversizing of the electrolyzer, and thus, increases its capital cost significantly. The production of hydrogen typically involves a higher Operating Expenditure (OPEX) at lower system efficiency values, necessitating the optimization of the system to determine the optimum operating point that balances the system cost and efficiency [25].

In addition to cell stacks, an electrolyzer requires the use of additional equipment to operate effectively. The term Balance of Plant (BoP) in electrolyzer systems refers to the subsystems and components essential for supplying and recirculating water to the electrolytes, regulating heat, purifying and

separating the produced hydrogen and oxygen, and establishing a connection between the electrolyzer stack and the power source [24].

2.1.2. Hydrogen Generation Plants Powered by Renewable Resources

The integration of power and hydrogen systems commonly involves two scenarios: coupling at the power source side and coupling at the load side. The former involves hydrogen production system located at the power source, while the latter focuses on centralized renewable power generation bases that transmit energy to hydrogen production units at the load side via Ultra-High Voltage (UHV) transmission lines.

PtH coupling at the source side offers several advantages such as peak regulation support and high utilization of renewable energy. Hydrogen production can be used for local consumption, hydrogen fuel cells, and providing grid services. This maximizes the utilization of renewable energy and ensures stable power transmission through UHV lines. However, the transportation cost of hydrogen is considered one of the potential drawbacks of this coupling scenario [26].

PtH coupling at the load side offers various advantages such as flexible site selection for hydrogen production. By constructing centralized renewable power generation bases in regions with rich renewable resources, the excess power is transmitted to hydrogen production unit via UHV lines. This scenario allows for the proximity of hydrogen production facilities to regions with high hydrogen demand, reducing the costs associated with conversion, storage, and long-distance transport. It also eliminates potential safety risks associated with transporting hydrogen over long distances. However, this scenario faces potential challenges, including the high system cost due to the extra investment in adjustable power sources (e.g. coal power or batteries), and the limited utilization of dynamic response capabilities of electrolyzers due to the stable power transmission at the load side [26].

The investigation of PtH coupling scenario from an economic perspective has gained significant attention in the literature. In [27], the researchers consider four different PtH coupling configurations of Hydrogen Refueling Stations (HRSs) in Croatia as illustrated in Figure 3.

Figure 3 |Four Different PtH Coupling Configurations of HRSs [27]

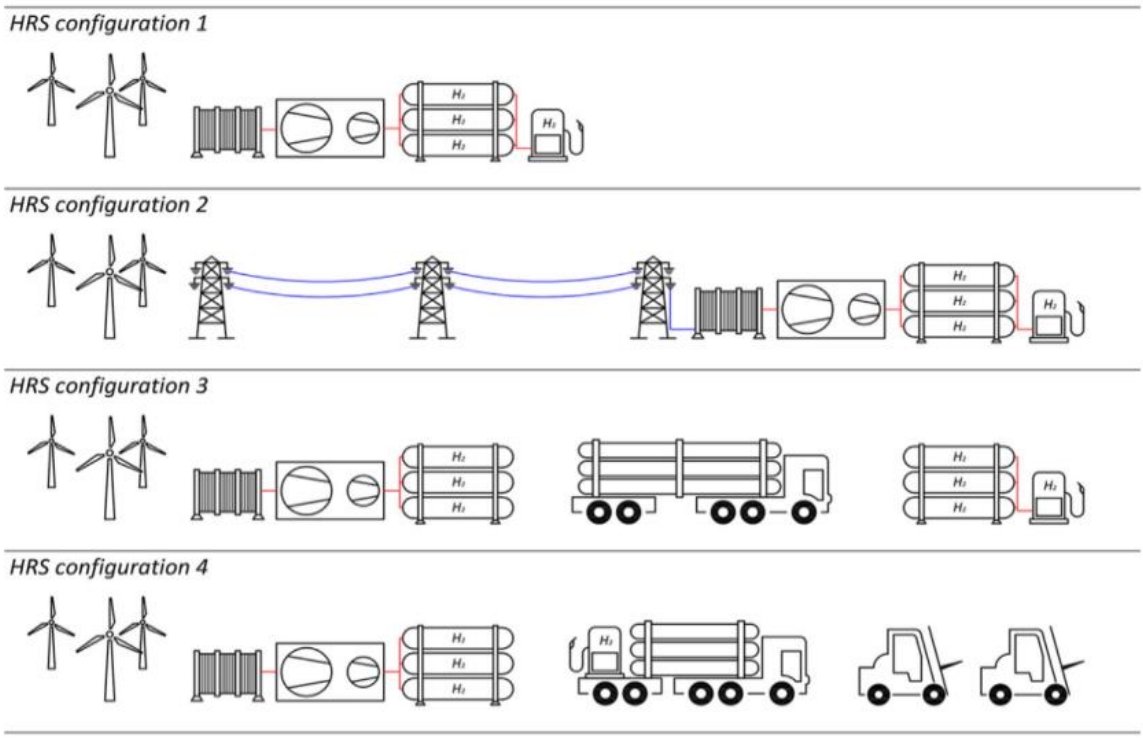

The first configuration involves hydrogen production and charging station within one existing wind farm in Croatia or both nearby the users. The second configuration involves hydrogen production near the consumption area where the wind farm power generations is transmitted to the hydrogen production plant. The third configuration includes hydrogen production within the wind farm and the charging station nearby the users, while hydrogen is delivered to the station with a tube trailer. The last configuration includes hydrogen production within the wind farm with a mobile charging station for several users in different locations. The LCOH is evaluated for each configuration, and the findings indicate that the first configuration exhibits the most favorable LCOH in comparison to the other configurations.

The CoH production and efficiency differ for different renewable energy sources. A comprehensive assessment of large-scale green hydrogen production facilities employing PEM electrolyzers in Poland reveals that offshore wind turbines exhibit a significantly lower LCOH ranging from $6.37 to $9.70/kg, compared to PV panels which yield a higher LCOH of $12.64 to $13.48/kg [28]. Additionally, the technology employed for harnessing energy from a specific renewable resource (e.g., solar energy) has a substantial impact on the LCOH of hydrogen. In [29], the authors focus on hydrogen production using solar energy in Algeria and found that the concentrated solar power-based technique

demonstrates greater competitiveness in terms of LCOH when compared to the conventional PV-based hydrogen production techniques. The geographical location is also a crucial factor affecting the LCOH, even within the same country. The transportation mechanism of hydrogen is a key factor affecting the LCOH. In cases where hydrogen is produced using renewable energies including PV or wind turbines, the climate conditions in a location significantly affects the LCOH. In Afghanistan, the researchers in [30] investigate the potential for wind power and hydrogen production. The findings reveal that the LCOH varies from $3.883 to $10.887/kg within different locations in the same country. Similarly, in [31], the authors carry out a techno-economic optimization of a solar photovoltaic power plant for dual production of electricity and hydrogen at five diverse locations across India. The findings reveal that LCOH across five locations fell within the range of $3 to $3.22/kg. Moreover, five different cities in Egypt are assessed through a techno-economic analysis of a hybrid renewable energy system comprising wind turbines and PV panels for hydrogen production and storage. The results indicate that LCOH varies across the cities, ranging from $4.54 to $7.48/kg [32].

Hydrogen can serve various applications, categorized into PtH and Power to Hydrogen to Power (PtHtP) applications. When hydrogen is employed as an energy storage system in PtHtP applications, the LCOH ranges from $21.9 to $56.5/kg H_2 [33], [34]. On the contrary, when hydrogen is utilized to meet PtH such as hydrogen refueling stations, the LCOH is considerably lower, ranging from $3 to $11.12/kg H_2 [31], [32], [35]. These findings underscore the importance of considering the intended application when assessing the economic viability of hydrogen as an energy source. Table 3 summarizes various configurations of hydrogen production and storage systems in different regions. The table reveals significant variation in LCOH values, based configuration, locations, and applications. It is worth noting that in Table 3, a capacity factor lower than 35% is considered low, between 35% and 65% is considered medium, and higher than 65% is considered high.

Table 3 | A Summary of Renewable Energy-Based GHPs in the Literature

Region	Renewable Resources						BSS	Grid	Electrolyzer Type	Capacity Factor	Application	LCOH ($/kg)
	PV	ST	Wind	Hydro	Geothermal	Biomass						
Eastern Canada [33]	✓		✓				✓	off	PEM	High	PtHtP + PtH	21.9-37.7
Saudi Arabia [34]	✓		✓				✓	off	PEM	N/A	PtHtP	43.2-56.2
Poland [28]	✓							off	PEM	N/A	PtH	12.64-13.48*
India [31]	✓		✓				✓	off		High	PtHtP + PtH	3.00-3.22
Malaysia [35]	✓		✓					off	PEM	High	PtH	11.12
Egypt [32]	✓		✓					off	Alkaline	N/A	PtH	4.54 -7.48
Sweden [36]	✓							off	Not defined	Low	PtH	28.4-30.4

Region	Renewable Resources						BSS	Grid	Electrolyzer Type	Capacity Factor	Application	LCOH ($/kg)
	PV	ST	Wind	Hydro	Geothermal	Biomass						
Badakhshan [30]			✓					off	PEM	N/A	PtH	3.887-10.827
Algeria [29]		✓						off	PEM	Low	PtH	6.1-6.8
Germany [37]	✓							on	PEM/ Alkaline	N/A	PtH	6.83-8.1 *
Croatia [27]			✓					on	PEM	High	PtH	17.1-27.2*
Oman [38]	✓							on	PEM	N/A	PtH + PtHtP	6.8
Iran [39]		✓			✓			off	PEM	Low	PtH + PtP	-

* LCOH in €/kg is converted to $/kg (1€ = 1.10 $)

2.1.3. Electrolysis-Based Hydrogen Types

Hydrogen production techniques differ in terms of energy source, feedstock, technology, production cost, and the level of carbon emissions. In the literature, a color spectrum is often used to illustrate mature hydrogen production techniques. Figure 4 shows different hydrogen colors and the corresponding energy source, production technology, and the type of emissions. It is worth noting that in addition to the three colors discussed in this report, there are colors associated with the production techniques using sources other the electricity including brown, grey, and blue that are not discussed in this section.

Figure 4 | Hydrogen Colors

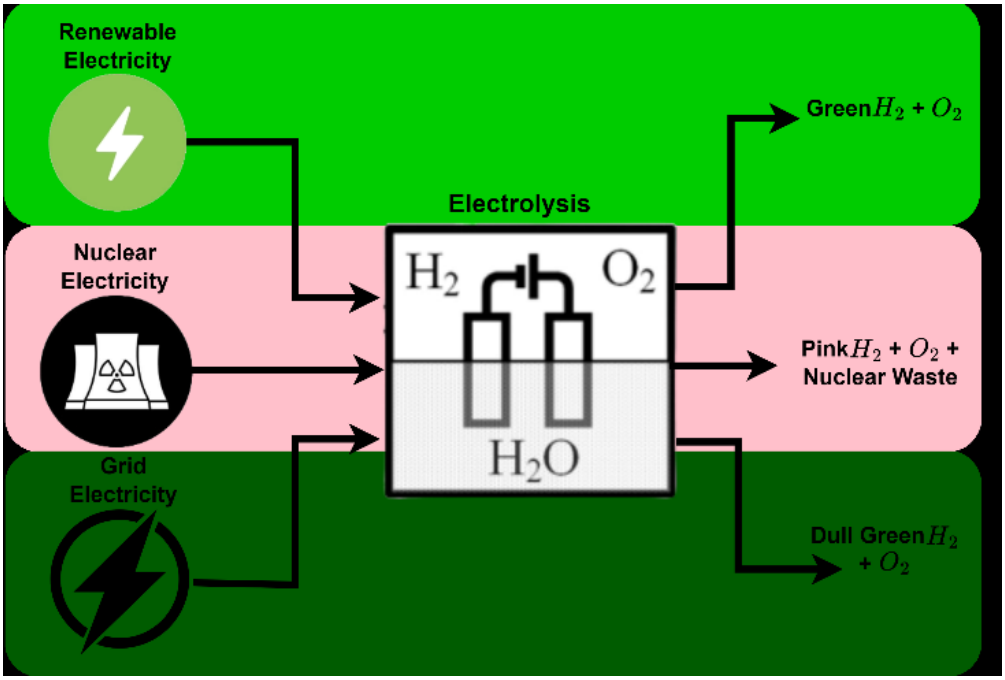

2.1.3.1. Green Hydrogen

Green hydrogen refers to the hydrogen produced from water using electrolysis powered by RES. Green hydrogen technologies offer the lowest carbon intensity alternatives for hydrogen production. Electrolysis technology employs direct current electricity to split water molecules into hydrogen and oxygen. Approximately 9 liters of freshwater are necessary for each 1 kilogram of hydrogen and 8 kilograms of oxygen generated. Considering the electrolyzer inefficiencies, the amount of the required water can increase by about 50% in practice. The produced hydrogen is of high purity and can be utilized directly in transportation and other applications without the need for additional treatment. The oxygen produced as a byproduct can be discharged into the air or utilized for medical or industrial purposes [40].

Currently, there are three main electrolysis technologies named: Alkaline Electrolysis (AE), PEME, and Solid Oxide Electrolysis Cell (SOEC). AE is the most well-established technology that has been used over a century and accounts for approximately 70% of the market share [41]. The AE technology offers the lowest capital cost and relatively a long lifespan. However, AE necessitates continuous operation to prevent damage, making it unsuitable for relying solely on the intermittent RES [42]. Further, AE systems face challenges in operating at high current densities and handling corrosive conditions [43].

PEME relies on the same technology used in the PEM fuel cell. The PEME technology is in operation since the mid of the previous century and it offers a higher power density, better efficiency, and faster response compared to AE. Thus, PEME is more suitable for urban areas, and for coupling with RES [43]. Further, PEME can produce hydrogen at high pressure, which may avoid the use of mechanical compressor. Nevertheless, the PEME technology necessitates initial investment costs due to costly electrode catalysts and membrane materials [44].

The SOEC technology is projected to offer lower capital costs and higher efficiency as compared to other electrolysis technologies [45]. The operating temperatures of SOEC range from 700 to 1000 °C which is advantageous in terms of electricity conservation due to improved thermodynamic conditions for the reaction, and the possibility of introducing heat into the process [46]. Yet, SOEC suffers from electrode's delamination, instability, and some safety concerns [45], and is still in the commercializing phase [44].

Table 4 summarizes the main technical differences between the three pre-mentioned electrolysis technologies [47].

Table 4 | Comparison Between Electrolysis Technologies

Characteristics	AE	PEME	SOEC
Cell temperature (°C)	60–90	50–80	700–900
Load flexibility (% of nominal load)	20–100	0–100	-100/+100
Cold start-up time	1–2 h	5–10 min	hours

Warm start-up time	1–5 min	<10 s	15 min
Nominal system efficiency (LHV)	51–60%	46–60%	76–81%
Specific energy consumption (kWh/Nm^3)	5.0–5.9	5.0–6.5	3.7–3.9
Max. nominal power per stack (MW)	6	2	<0.01
Cell area (m^2)	<3.6	<0.13	<0.06
Investment costs ($/kW)	950–1750	1650–2500	(>2400)
Maintenance costs (% of investment costs per year)	2–3	3–5	N/A

2.1.3.2. Pink Hydrogen

When an electrolysis system is powered from a nuclear power source, the produced hydrogen is named pink hydrogen. Incorporating a hydrogen production plant could potentially alleviate the curtailment of nuclear power plants [48], while presenting an additional avenue for energy storage, particularly when the need for seasonal storage arises. Pink hydrogen is also considered a low carbon intensity hydrogen type. Large reactors could be employed to operate with centralized hydrogen plants, while small reactors would be useful for distributed hydrogen generation.

2.1.3.3. Dull Green Hydrogen

When water electrolysis is integrated with the electric grid, the level of carbon emissions within the grid would determine the environmental cleanliness of the generated hydrogen. Some research works in the literature have classified hydrogen produced from grid-connected electrolysis as yellow hydrogen. However, the term yellow hydrogen has also been applied to hydrogen produced through electrolysis powered by solar energy. To resolve this ambiguity, this report introduces the term dull green hydrogen to describe hydrogen generated from grid-connected electrolysis. It is worthwhile to note that the carbon intensity of the electric grid is extremely critical, as it can lead to the production of dull green hydrogen with carbon emissions exceeding those of grey or even brown hydrogen. The work in [49] indicates that when the carbon intensity of the electric grid exceeds 165 kg CO_2/MWh, the carbon emissions associated with dull green hydrogen potentially exceed the emissions level of grey hydrogen produced through steam methane reforming.

2.1.4. Economical and Environmental Impacts of Hydrogen Production

Energy transition to hydrogen is controlled by three main aspects: cost of hydrogen production; level of carbon emissions; and the capability of hydrogen to be utilized in different applications. This section compares different hydrogen production technologies in terms of the cost of production and the level of carbon emissions. It also discusses the opportunity for utilizing hydrogen in various applications.

In the foreseeable future, the economic advantage of fossil fuels is expected to persist in most regions. Hydrogen derived from natural gas without Carbon Capture, Usage and Storage (CCUS) is projected to cost approximately USD 1–2 per kilogram of hydrogen depending on local gas prices. The most substantial component of hydrogen production cost is fuel prices except for the case of coal-based hydrogen as illustrated in Figure 5.

Figure 5 |Price for Hydrogen Production for Different Hydrogen Colors

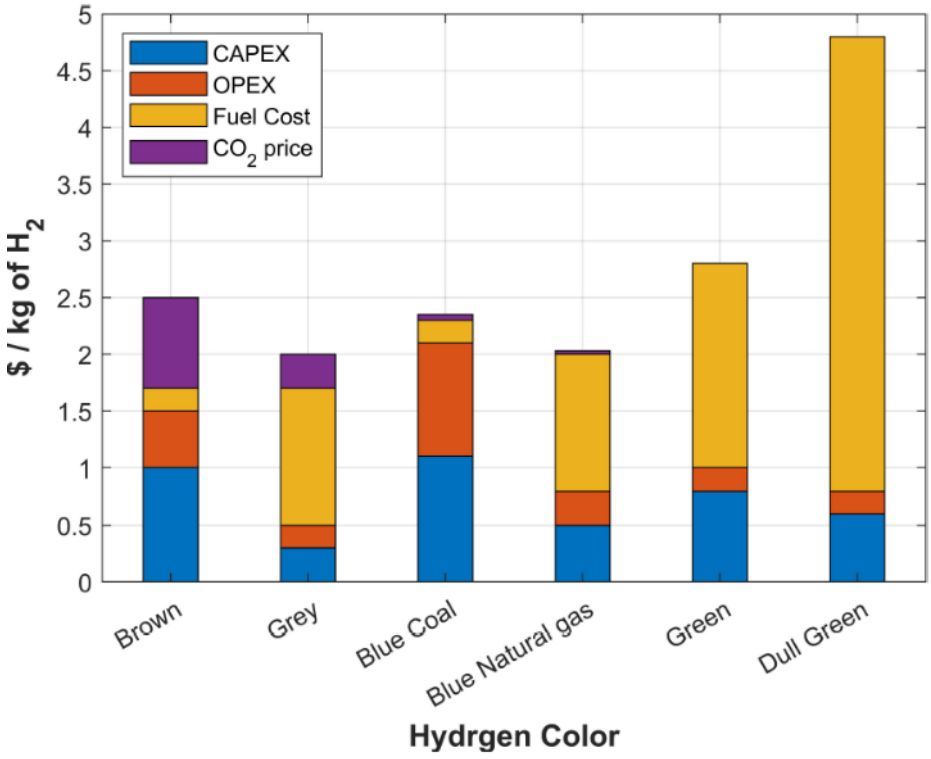

It is worth noting that the cost of the electricity from locally-generated renewable units is considered half of the cost of the electricity of the grid. Therefore, the fuel cost for green hydrogen production is less than that for dull green hydrogen production. The difference in CAPEX for green and dull green hydrogen production is due to the low-capacity factor of the green hydrogen production plant.

Further, the factors which affect fuel cost such as operating efficiency will also dominate the cost of hydrogen production [23]. The capital cost of renewable-powered electrolysis (green hydrogen plants) is higher than that of grid operated electrolysis (dull green hydrogen plants), as the renewable-powered electrolysis runs at partial load for long periods.

Specific to Ontario, the CAPEX, OPEX, and fuel cost for hydrogen production have been illustrated in Figure 6 for three different years, representing three different conditions of the electricity market. The results are presented for the market in the following years: i) 2005 when gas was on the margin for a

significant portion of the time; ii) 2017 when there was significant base load generation; and iii) 2023 when various measure has been taken to minimize the emissions and alleviate base load generation.

Figure 6 |Price for Hydrogen Production for Different Hydrogen Colors in Ontario

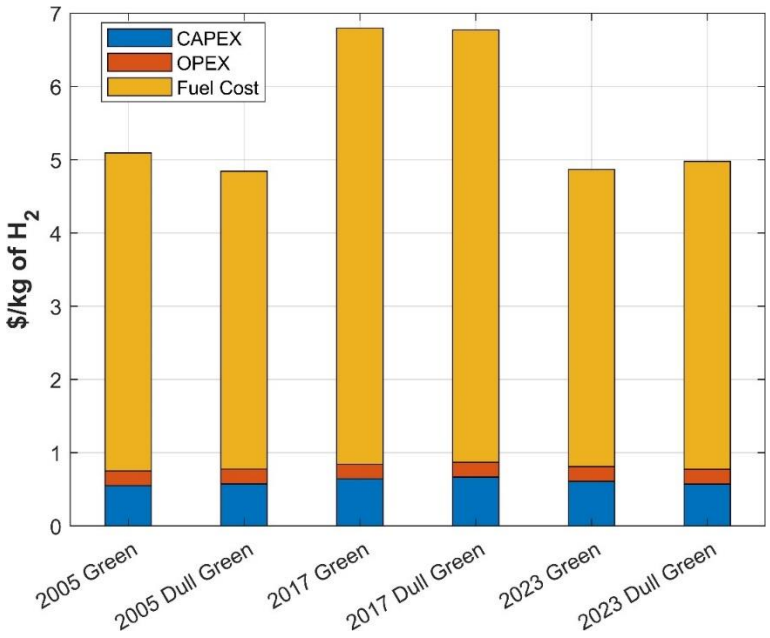

The production cost is not the only factor that determines the opportunity of certain hydrogen production technologies. The level of carbon emissions is also a key factor in this regard. As depicted in Figure 7, the carbon footprint of grey hydrogen (produced from natural gas), is approximately half that of brown hydrogen (produced from coal).

Figure 7 |Carbon Emissions of Different Hydrogen Production Technologies

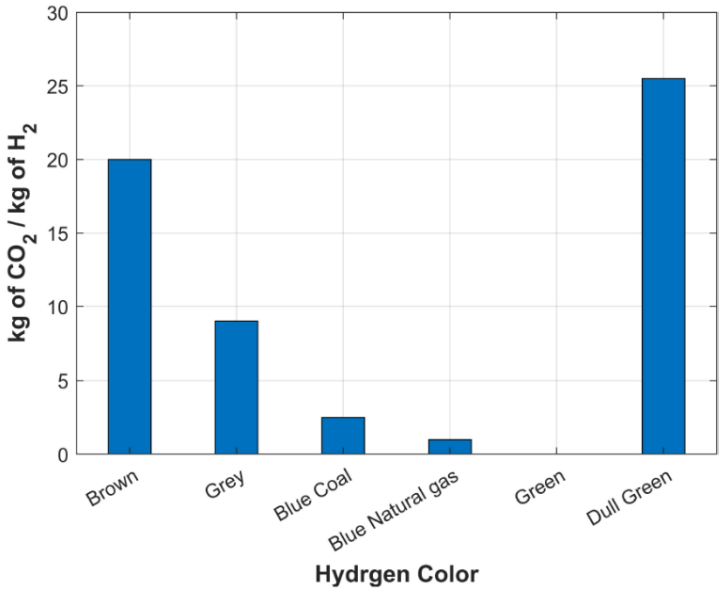

The use of CCUS significantly reduces the level of carbon emissions. Yet, the green hydrogen technology is superior with zero carbon emissions. The dull green hydrogen could result in carbon emissions more than those of grey and brown hydrogen based on the carbon intensity of the electric grid. Figure 7 considers the current global average grid carbon intensity which results in carbon emissions level exceeding the level of the grey hydrogen.

2.1.5. Hydrogen-to-Power

In the power division, hydrogen has a slight share of the electricity generation (0.2%) around the globe. Hydrogen-based electricity generators are commercially available, mainly as fuel cell units. Some forthcoming projects that involve natural gas-fired power generation, take into consideration either partially blended hydrogen or transition to using hydrogen exclusively at a later stage, but the technology is yet to be fully materialized. The electrical efficiency of fuel cells is around 50% even when operating at partial load, making it attractive for flexible operation with the power system. Figure 8 and

Table **5** show the detailed specification of an industrial fuel cell unit.

Figure 8 |Fuji Electric Fuel Cell [50]

Table 5 | Specification of Fuji Electric Fuel Cell [50]

	City gas type	Biogas type	Pure hydrogen type
Type	Phosphoric acid, normal pressure, water-cooled type (PAFC)		
Model	FP-100i	FP-100iB	FP-100iH
Structure	Package type		
Rated output	105 kW (gross), 100 kW (net)		

Operation mode		Fully automatic operation, grid interconnection		
Size		5.5 m (length) × 2.2 m (width) × 3.4 m (height)		
Mass		14t	14t	13.5t
Rated voltage, number of phases, frequency		210/220 VAC, three phases, 50/60 Hz		
Heat output		Medium temperature, waste heat recovery type: 123 kW (15°C ⇒ 60°C)	Medium temperature, waste heat recovery type: 116 kW (15°C ⇒ 60°C)	Medium temperature, waste heat recovery type: 99 kW (15°C ⇒ 60°C)
Efficiency	**Power generation efficiency**	42%	40%	48%
	Total efficiency	91%	84%	93%
Fuel type		City gas 13A	Biogas (CH_4: 60%, CO_2: 40%) (CH_4:60%, CO_2:40%)	Pure hydrogen gas (99.9% or more)
Fuel consumption		22m^3/ h (Normal)	44m^3/ h (Normal)	74m^3/ h (Normal)
Environmental performance	**Exhaust gas**	NOx: 5 vol.ppm or less SOx: Not detected Dust concentration: Not detected	NOx: 5 vol.ppm or less SOx: Not detected Dust concentration: Not detected	NOx: Not detected SOx: Not detected Dust concentration: Not detected
	Noise	65 dB (A) or less		

As reported in

Table **5**, the unit can generate up to 100kW power with the power generation efficiency of up to 48%, and the total efficiency of up to 93%. Such a high efficiency value can place the fuel cell unit in a great position for power generation. While fuel cells started being used in 1960s in space missions and thereafter in various other applications, there are still barriers to their widespread adoption and practical use. The CAPEX of fuel cell units is considerably higher than that of conventional generators, making it the most important barrier towards utilization of large-scale fuel cells. The high cost of

materials used for fuel cells production, the complexity of the production process, and the limited production volume of fuel cells compared to other alternative sources for electricity generation are the main factors driving up the fuel cell CAPEX. As the technology materializes, it is expected that their initial cost starts decreasing. Currently, the largest grid-scale fuel cell unit, the Shinincheon Bitdream fuel cell power plant is located in South Korea, which has a total capacity of 78.96 MW and is able to produce 700 GWh of electricity annually. The technology for using hydrogen as the sole fuel for gas turbines is yet to be fully materialized, but that could be another avenue for production of power using hydrogen in the near future.

2.2. Storage Systems

Hydrogen, with its impressive gravimetric energy content of 120 MJ/kg H_2, faces a unique challenge due to its low volumetric energy density. At ambient conditions (1 atm and 25°C), hydrogen's density is merely 0.0824 kg/m^3, resulting in a low volumetric energy density of 0.01 MJ/L H_2. In comparison, gasoline, under the same conditions, achieves a significantly higher volumetric energy density of 32 MJ/L [51]. Stationary applications (e.g., on-site hydrogen storage) prioritize volumetric hydrogen density, whereas on-board applications (e.g., hydrogen fuel cell vehicles) demand a delicate balance between gravimetric and volumetric densities to enable extended travel without frequent refueling. Navigating these challenges necessitates an exploration of diverse hydrogen storage techniques [51], [52].

Hydrogen storage is classified into physical-based and chemical-based storage technologies. Physical storage composed of compressed gas, liquid hydrogen, and cryo-compressed hydrogen. Compressed hydrogen and liquefied hydrogen focus on achieving compact storage through high pressure or low temperature (below hydrogen's cryogenic temperature, -253℃), respectively. While cryo-compressed hydrogen combines aspects of both approaches (compressed and liquified hydrogen), optimizing storage conditions [52].

On the other hand, chemical-based storage can be achieved via metal hydrides, complex hydrides, and Liquid Organic Hydrogen Carriers (LOHCs) [51]. Metal hydrides and complex hydrides provide chemically bonded storage with metals such as magnesium. Liquid organic hydrogen carriers introduce a chemical binding of hydrogen to organic compounds. Moreover, hydrogen can be transformed into another chemical product such as ammonia. The choice among these methods involves trade-offs in terms of applicability to specific use, duration of storing, technological readiness level, energy efficiency, system losses, cost effectiveness, and public acceptance [51].

Hydrogen storage offers various features compared to conventional forms of storage including Pumped-Hydro Energy Storage (PHES) and batteries. Table 6 reports the high-level comparative results of various energy storage technologies.

Table 6 |High Level Comparison of Storage Technologies [14]

Technologies / Features	CAPEX ($/kW)	CAPEX ($/kWh)	OPEX (% of CAPEX)	Efficiency (%)
Long-term storage, large scale (hydrogen)	3253	11	33	30
Medium-term storage, large scale (PHES)	2053	513	31	80
Short-term storage, large scale (lithium-ion batteries)	1474	377	0.5-1	88-95
Short-term/long-term storage, large scale (lead-acid batteries)	1092	437	1-2.7	85
Short-/medium-term storage, large scale (Redox-flow batteries)	1638	437	1	70
Short-term storage, large scale (sodium-based batteries)	650	737	1.6	85
PV-home storage systems (lithium-ion batteries)	1310	1092	1-2	88
Electromobility (lithium-ion batteries)	82	175	2	90

As reported in Table 6, the initial cost for deployment of hydrogen storage in kW compared with other storage systems, including PHES and battery is considerably higher. If the CAPEX is computed per kWh, the cost is significantly lower. The hydrogen storage OPEX, however, is comparable to PHES but higher than that of battery storage as expected since battery storage does not demand higher costs for maintenance. The efficiency of hydrogen storage, on the other hand, is significantly lower than other storage technologies, but this could be improved in the future as hydrogen generation technologies materialize.

2.3. Hydrogen Utilization Means, Types, and Economy of Hydrogen

Hydrogen has a long history as an energy source. It was utilized to run the first Internal Combustion Engines (ICEs) and to lift balloons and airships 200 years ago. Later, hydrogen became a part of energy industry and oil refining. Under the pressure of climate change, the global demand of hydrogen has

significantly increased. In this context, low-carbon hydrogen emerges as a reliable energy carrier and a clean fuel. However, the majority of low-carbon hydrogen production technologies are still in their infancy. Additionally, the production of low-carbon hydrogen encounters big challenges in terms of competing with the prices of conventional fossil fuel.

While hydrogen is recognized as a means for development of green transportation, it has many other applications such as producing fertilizer and other chemicals, refining petroleum, treating metals, and processing foods. For instance, ammonia is produced using hydrogen from fossil sources and used for fertilization. Such an approach for production of fertilizers offers many benefits including lowering the carbon footprint across the food chain and reducing the dependency on fossil sources. Hydrogen could also be used for nearly emissions-free steel production and help alleviate the environmental issues. This is done by replacing fossil fuels with hydrogen in the production stage.

2.3.1. Hydrogen Utilization

As compared to 2020, the global hydrogen demand reached approximately 94 Mt in 2021 with a 5% rise Mt. Most of that increase was due to conventional hydrogen applications such as refining and industry. However, some new applications for hydrogen utilization have also experienced a rapid increase. New steel projects in which pure hydrogen is directly used for iron reduction have also increased. In the transportation sector, the global stock of Fuel Cell Electric Vehicle (FCEV) increased from 33000 in 2020 to 51000 by the end of 2022. Although, the majority of FCEVs are passenger cars, China led the production of 800 fuel cell trucks in 2021. Further, Germany started the operation of the first hydrogen fuel cell train. Also, more than 100 pilot projects have announced to use hydrogen or its derivatives in shipping. In the power sector, about 3.5 GW are announced to use hydrogen and ammonia by the end of 2030. The hydrogen demand around the globe is estimated to approach 130 Mt by 2030 to meet the climate commitments already announced by the governments around the world. However, to meet net-zero emissions by 2050, the global hydrogen demand has to reach 200 Mt in 2030 [1].

Figure 9 shows the annual variation in hydrogen demand for different applications from 2019 to 2021. It also shows the projected demand by the end of 2030.

Figure 9 | **Annual Hydrogen Demand for Different Applications**

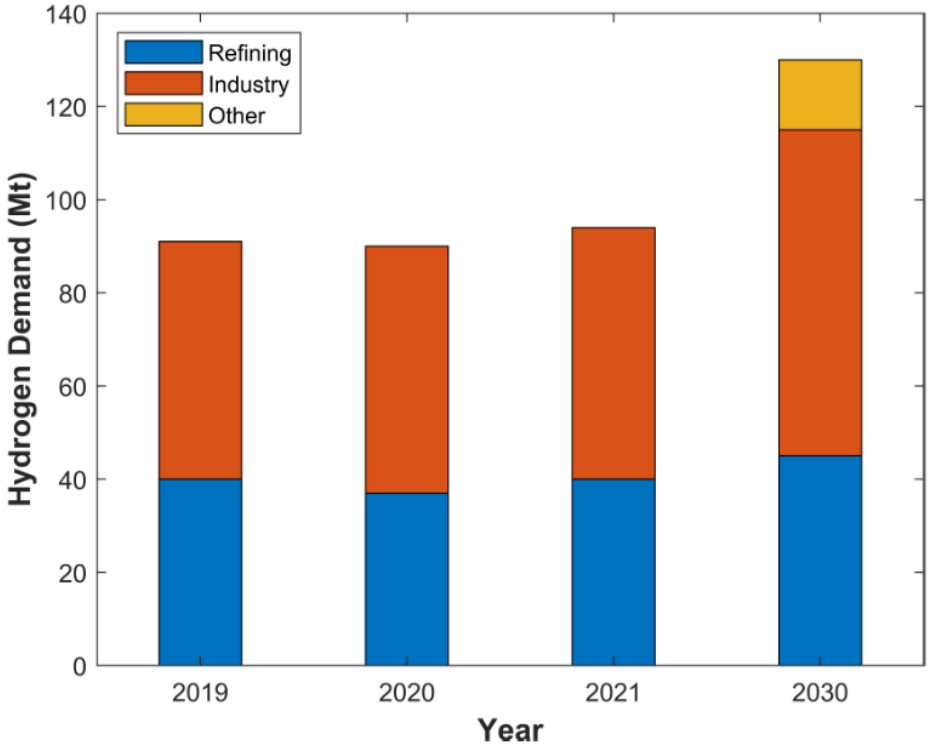

2.3.1.1. Refining

Oil refineries are industrial plants that transform crude oil into other petroleum products such as gasoline, diesel, aviation fuel, and naphtha. In this process, hydrogen is used to remove impurities such as sulphur and also in converting heavy oil into lighter products [53]. The use of hydrogen in refining

approached 40 Mt in 2018 and then dropped sharply to reach 38 Mt, due to the pandemic, in 2020 before restoring to the 40 Mt level by the end of 2021. In 2021, the majority of hydrogen utilized in refining is produced from fossil fuel, leading to the release of over 200 Mt of CO_2 [1]. Some new applications for hydrogen are expected to rise in the short-term including upgrade of biofuels and high-temperature heating. In Canada, the Varennes Carbon Recycling project aims to convert more than 200,000 tonnes of non-recyclable waste into 125 million litres of biofuels. The project deploys a 90 MW electrolysis for clean hydrogen production and is expected to start the commissioning phase in 2025 [54]. The first pure hydrogen operated furnace is deployed in Essar's Stanlow refinery in UK. The furnace operation would initially be based on natural gas and will be operated by hydrogen later in 2026 when the HyNet Northwest project for clean hydrogen production begins [55].

2.3.1.2. Industry

Currently, the primary uses of hydrogen in industry are for ammonia production, methanol production, and steel industry application that annually accounts for 34, 15, and 5 Mt of hydrogen usage, respectively. Other applications such as glassmaking, electronics, and chemical industries account to relatively a small volume of hydrogen [1].

In 2021, almost all hydrogen utilized within the industry sector is produced from fossil fuels (natural gas, and coal), resulting in 630 Mt of CO_2 that accounts for 7% of industrial emissions. Due to the economic expansion, hydrogen-derived products are expected to rise in the medium term, which, in turn, will increase the industrial demand for hydrogen. Therefore, the industrial hydrogen demand is expected to reach 65 Mt in 2030. To achieve the climate goals of different governments around the globe, low-emission new hydrogen production technologies are projected to account for 13 Mt of industrial hydrogen production by the end of 2030 [1].

2.3.1.3. Transportation

In the transportation sector, hydrogen demand exceeded 30 kilo tonnes in 2021, marking 60% growth as compared to 2020. However, hydrogen accounts for only 0.003% of the total energy used in transportation. Among various modes of transportation, road vehicles, particularly trucks and buses, are the primary driver for hydrogen demand because of its high annual mileage and heavy weight [1]. Additionally, hydrogen presents a viable solution for decarbonizing diesel-based rail lines, especially when the electrification is not feasible, and the distance exceeds the electric batteries capabilities. In August 2022, Germany succeeded in deployment of the first fuel cell train fleet in Lower Saxony [56]. The maritime and aviation sectors also witnessed a growing interest for utilizing hydrogen and synthetic fuels derived from hydrogen. It is worth noting that the technologies for utilizing hydrogen in these sectors are not mature yet. However, there is a considerable number of ongoing pilot projects including about 45 projects focusing on utilizing hydrogen, 40 pertaining to ammonia, and 25 exploring the use of methanol in shipping. Most of the hydrogen projects concentrate on smaller vessels, while the

ammonia projects focus on larger vessels. The methanol projects are distributed between both the small and large vessels. In the aviation sector, there are two key development areas: the manufacturing of a hydrogen-based sustainable aviation fuel, and the hydrogen-powered aircraft for flights covering short to medium distances. The progress of hydrogen-based sustainable aviation fuel is more mature, with cost emerging as the primary obstacle to implementation. On the other hand, the realization of hydrogen-powered aviation faces greater challenges, as the associated technologies are still in the initial phase of the development [1].

2.3.1.4. Buildings

The contribution of hydrogen in satisfying the energy demand in the buildings sector is still negligible. The use of natural gas in cooking and heating is about 25% of the energy demand in the buildings sector. Given the current energy crisis and the global drive to attain net zero emissions, a number of countries prohibited the utilization of fossil fuels in new constructions. For instance, France has enforced such a ban since 2022. The existing reliance on fossil fuels for generating energy for buildings is expected to transfer to environmentally friendly alternatives such as electricity, district heating, and decentralized renewable sources, prior to adopting hydrogen usage. Hydrogen technologies in buildings suffers from low efficiency as compared to other viable solutions due to the energy losses during hydrogen conversion, transportation, and utilization [1].

Yet, there are some opportunities for hydrogen utilization in buildings particularly in cases where there are existing natural gas infrastructure and challenges in decarbonization. This could be especially relevant in scenarios involving cold climates, historical city centers, and structures with inadequate insulation. Hydrogen demand in the building sector could increase up to 2 Mt by 2030, accounting for only 0.2% of the buildings' total energy demand [1].

2.3.1.5. Electricity Generation

In the power sector, hydrogen has a much-reduced share of the electricity generation around the globe, i.e., 0.2%. The majority of this generation uses a mix of gases with high hydrogen content. Hydrogen-based electricity generators are commercially available and appear in many forms such as reciprocating gas engines, fuel cells and gas turbines. Many forthcoming projects that involve natural gas-fired power generation, take into consideration either partially blended hydrogen or transition into using hydrogen exclusively at a later stage. The electrical efficiency of fuel cells is around 50-60% even when operating at the partial load, making it attractive for flexible operation with the electricity system. During the year of 2021, a total of 348 megawatts of stationary fuel cell capacity was globally introduced [1]. Table 7 reports the stationary fuel cell types, their ratings, and their geographical distribution.

Table 7 | Fuel Cell Applications and Ratings

Stationary Fuel Cell Types	Residential	Small Commercial	Medium-Sized	Large Commercial and Industrial	Utility-Scale
Ratings	1 - 5 kW	5 - 100 kW	100 kW – 1 MW	1 - 10 MW	Greater than 10 MW
Geographical Distribution	North America Europe	North America Europe Asia-Pacific	North America Europe	Europe Asia-Pacific	Asia-Pacific

3. Techno-Economic Analysis and Discussion

3.1. Methodology for Modeling and Studies

This section presents the modeling and simulation approaches for the GHP and identifies case studies and scenarios. The mathematical modeling for the optimal design and operation of the PEM and Alkaline technologies is given in the appendix Sections 7.1 and 7.2.

3.1.1. Model Framework

In this section, the sizing and optimal operation management models that are formed using the toolboxes developed by the Smart Grid Research team at York University are described. The models are used to investigate the optimal design and operation of the GHPs that would achieve the following primary objectives: 1) optimal design of the GHP components, 2) help meet the decarbonization target of Ontario electricity system via increase of renewables penetration, 3) improve the flexibility and durability of the electricity system via provision of ancillary services, 4) minimize the GHP facility's OPEX, 5) meet certain target of green hydrogen production to supply projected hydrogen demand, and 6) meet profit target for GHP private investors. Figure 10 shows the model for optimal sizing of the GHPs.

As shown in Figure 10, there are various inputs to the model including operating parameters and constraints. Different factors and functions are taken into consideration for optimal sizing including electrolysis operation and safety factors, hydrogen production and storage process, electrolyzer models, and BESS as an optional component. The electrolyzer efficiency and costs have been calculated

where the optimization algorithm aims to minimize the LCOH. Finally, the storage, electrolyzer, fuel cell, and BESS ratings are determined at the minimal LCOH where all the operational needs and constraints are met.

Figure 11 shows a schematic diagram of the framework modeled for operation management of the GHP, which is incorporated as a sub-problem into the optimal sizing described in Figure 10.

Figure 10 | Optimal Sizing of Green Hydrogen Plants

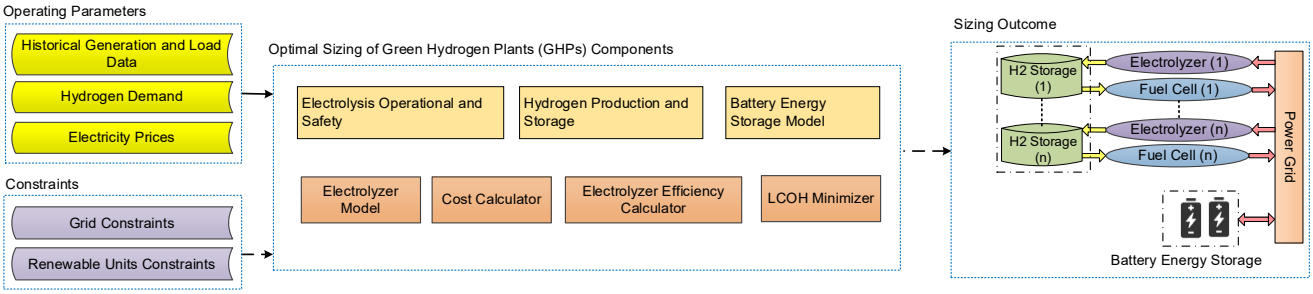

Figure 11 | Optimal Operation Management of GHPs

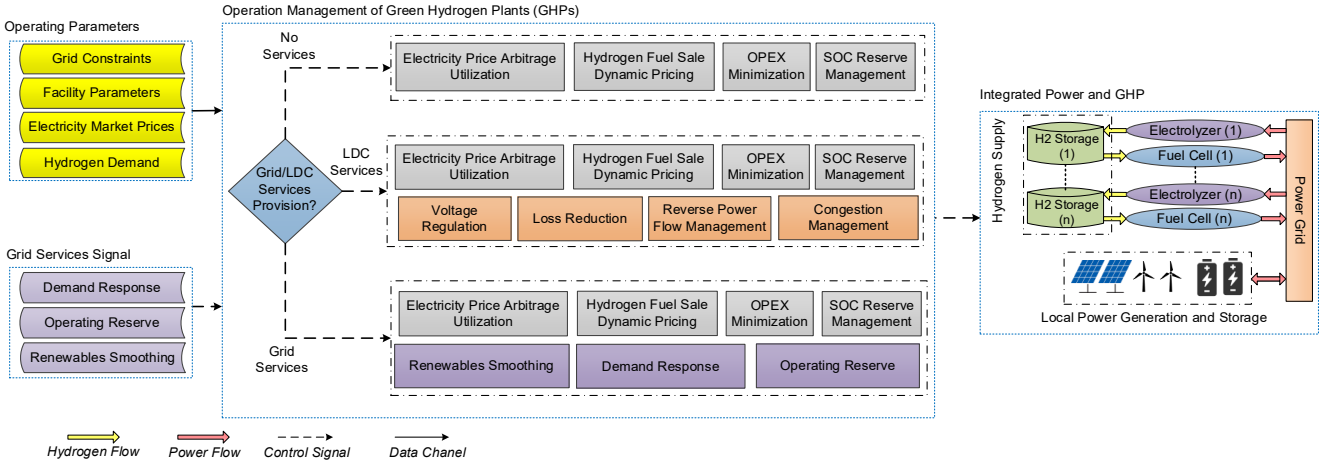

As shown in Figure 11, the following operating parameters are collected and fed to the model: grid constraints, GHP facility parameters, electricity prices, and hydrogen demand. In addition, various grid signals are inputted to the model. These are defined as the optimization parameters used for optimal

operation management of the GHP. The optimization-based model for operation management of the GHP is formulated considering all the grid and facility constraints to ensure that the optimal solution is viable. The figure shows that there are three operating modes defined in order to generate the results for various cases: 1) no grid services as the base case, 2), provision of ancillary services to the grid, and 3) provision of LDC services. There are various features associated with these operating modes as follows:

- **No Grid Service as the Base Case –** the model is scheduled to optimize the operation of the GHP for base cases including price arbitrage, hydrogen fuel price determination, OPEX minimization, and State of Charge (SoC) management.
- **Provision of Ancillary Services –** In addition to the base cases functions, the model schedules the GHP for provision of the grid services by following the ancillary services inputted to the model.
- **Provision of LDC Services –** In addition to the base case features, the model schedules the GHP for serving the LDC via voltage regulation, loss reduction, reverse power flow management, and congestion management.

The optimal sizing and operation management models are coded and simulated in the MATLAB environment where the historical market data in Ontario are used for numerical studies. The formulated optimization problems to run the techno-economic feasibility studies are solved using Sequential Quadratic Programming (SQP) that is available as a built-in function in MATLAB's optimization toolbox. The convergence constraints and decision variables tolerances are set to 10^{-6}. The specification of the platform used to conduct the simulations are as follows: Core i7-10700K, 3.8 GHz CPU, 32 GB RAM, and 64 bits system.

3.1.2. Scenarios and Case Studies

3.1.2.1. Optimal Sizing Scenarios

Two possible scenarios are considered for sizing the GHP facility as follows:

- **Scenario 1**: the facility is sized and rated based on the opportunities available for contribution to the ancillary services in addition to its base application to fulfill the hydrogen demand in the market.
- **Scenario 2**: the facility is sized and rated according to the hydrogen demand in the market but not for provision of ancillary services to the electricity market.

In Scenario 1, the facility's components would be associated with higher ratings in order to ensure that the facility can fulfill both the requirements for contribution to the ancillary services and hydrogen supply to consumers; this would result in higher CAPEX of the facility.

In Scenario 2, the facility's components would be rated only to fulfill the hydrogen demand, thereby resulting in lower CAPEX. In this case, the optimal scheduling algorithm schedules the facility in an optimal faction and use the storage as a buffer to fulfill the requirements for both the hydrogen supply to the market and provision of ancillary services.

For each of the optimal sizing scenarios, multiple case studies are defined as described hereunder.

3.1.2.2. Case Studies for Operation Management

Based on the above scenarios for sizing of GHP components, six case studies are carried out to evaluate the optimal operation management of the designed GHP facility as summarized in Table 8. As depicted in the table, case study 1 considers a simple model of the electrolyzer, where aspects such as safety limits and optimized electrolyzer parameters (membrane thickness, cross section area of stacks, and output pressure) are not taken into consideration. Cases 2 to 5 consider a detailed modeling of the electrolyzers. Also, the optional co-location of the GHP with a BSS to enhance the overall performance of the system is considered in case 6.

Table 8 | Summary of Case Studies

Case No.	BESS	GHP Parameters	Safety Constraints	GHP Model
1 [17]	✗	✗	✗	Constant Efficiency and kg/kWh
2	✗	✗	✗	Detailed Model
3 [27]	✗	✓	✗	
4	✗	✗	✓	
5	✗	✓	✓	
6	✓	✓	✓	

Using these different case studies, the application of the PEM and Alkaline based GHPs without and with contribution to ancillary services are evaluated. In addition, the impact of CAPEX and efficiency variations on the LCOH is evaluated for each technology. The studies also are extended to investigate the aggregation of multiple and distributed GHPs (owned and operated by private entities) fed by the distribution system to serve the LDC.

3.2. Optimal Deployment of PEM Based GHP

The IEEE 30-bus bulk transmission system shown in Figure 12 is used to validate the effectiveness of the proposed design of a GHP.

Figure 12 | Single Line Diagram of the IEEE 30-Bus System Under Study

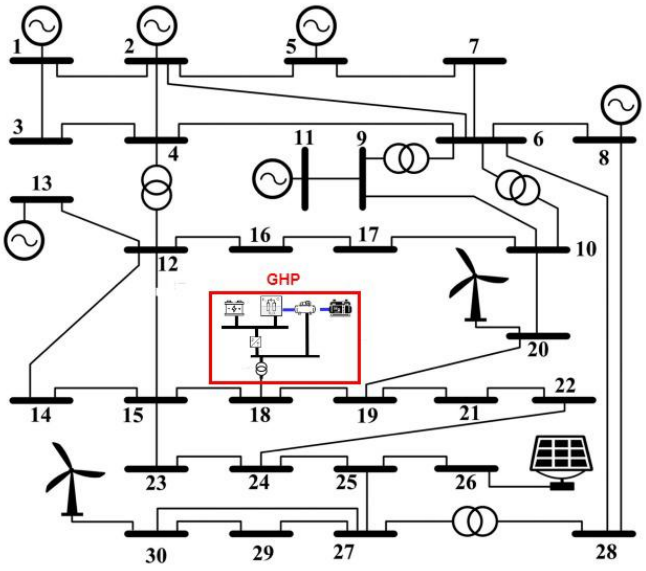

Two wind power plants, sized at 600 MW each, are connected to Buses 20 and 30. Also, a 500-MW solar PV plant is connected to Bus 26. The GHP under design is assumed to be arbitrary connected to Bus 18.

The optimal deployment of PEM based GHP includes the sizing of its components under the six case studies reported in Table 8. In the first case, as depicted in the table, the PEME is modeled by a constant conversion rate in kWh/kg. The other five cases utilize the detailed steady state model described in the appendix. In Case 2, predefined PEME internal parameters (obtained from a manufacturer technical sheet) are utilized without considering the safety constraints. In the third case, PEME parameters are optimized concurrently with the sizing of the GHP without considering the PEME safety constraints. The fourth case considers predetermined PEME parameters, as in Case 2, but takes into consideration its safety constraints. The fifth case considers both the optimal design of the PEME parameters and the safety constraints into account. In the sixth case, the GHP is equipped with a BESS where the PEME parameters are optimized as in Case 5 while considering the PEME safety constraints.

Five years hourly historical data for solar irradiation and wind speed in the province of Ontario, Canada [59] has been collected. The historical data is then used to generate the hourly solar irradiation and wind speed profiles of four typical days representing the four seasons of the year. Each hour is represented by five states for both the solar irradiation and wind speed. Hence, there are 25 (5x5) combined states for each hour. Also, the historical electrical demand in the province of Ontario [60] is used to calculate the mean of hourly demand for four typical days of the four seasons as given in Figure 13 (a).

At each hour, the weighted average of maximum available power of the 25 combined states is calculated at the selected bus (Bus = 18) to obtain the available power for green and dull green hydrogen production as demonstrated in Figure 13.

Figure 13 |(a) Electrical demand profile, (b) Available power at Bus 18, available renewable power at Bus 18, and total connected renewable power, (c) Hydrogen demand profile of the four typical days.

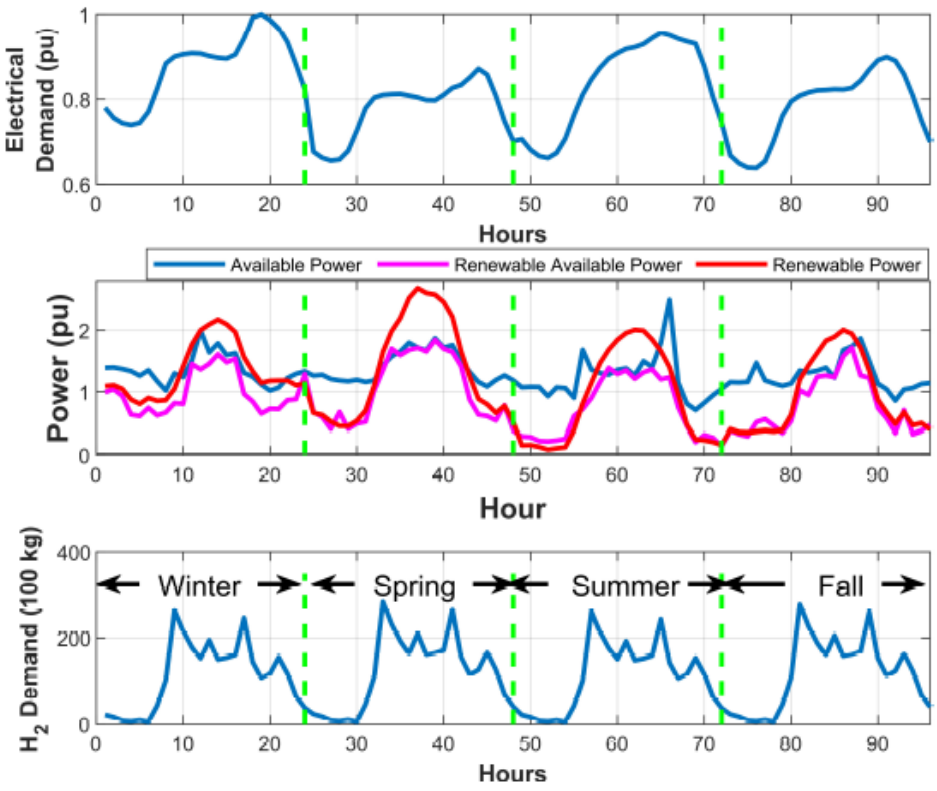

As shown in Figure 13, the available power profile to produce dull green hydrogen at Bus 18 is significantly different from the renewable available power to produce green hydrogen at the same bus. The latter is capped by both grid constraints and maximum renewable generation connected to the studied network. As depicted in Figure 13 (b), renewable power generation limits the maximum

renewable available power for green hydrogen production during nighttime while other grid constraints cap the available power during daytime.

Historical data for the electricity market price given by the IESO [32] in Ontario is used to generate 1000 cases, where each case has its own probability. High power consumers are charged with multiple components that include HOEP and Grid Operation Fees (GOFs) such as regulatory services, delivery charges, and supply services. When a renewable Power Purchase Agreement (PPA) is used, the energy price is set at a fixed rate while the same GOFs are applied. In this work, it is assumed that the energy price for PPA is set at 20 $/MWh as given in [61] and [62]. The subsidy term, is assumed to be set based on the PTC, which is modeled as a function of the Carbon Emission per kg of Hydrogen (CEH) as given below, where the subsidy values are chosen as announced by the USA federal government in [2]:

$$\Upsilon = \begin{cases} 3\,\$ & , 0 \leq CEH \leq 0.45 \\ 1\,\$ & , 0.45 < CEH \leq 1.5 \\ 0.75\,\$ & , 1.5 < CEH \leq 2.5 \\ 0.6\,\$ & , 2.5 < CEH \leq 4 \\ 0\,\$ & , CEH > 4 \end{cases}$$

The CEH is a function of the hourly carbon intensity and can be obtained as below, where the used hourly carbon intensity is the mean of the historical hourly carbon intensity of Ontario electrical grid.

$$CEH = \frac{\sum_{t=1}^{T} CI^t P^t_{grid}}{\sum_{t=1}^{T} L^t_{elz}}$$

The hydrogen demand profile is derived from the aggregation of demand at hydrogen refueling stations [10]. The aggregated demand is then used to find four typical days of hydrogen demand to represent the entire year by finding the mean of the hydrogen demand profile as shown in Figure 13 (c). Other simulation parameters listed in Table 9 are imported from previous techno-economic studies in the literature [25], [63].

Table 9 |Simulation Parameters

Parameter	Value	Parameter	Value
C_{elz}	600 $k\$/MW$	k	1.4
C_{BESS}	100 $k\$/MW$	η_{BESS}	97.5%
C_{Cmp}	7.52 $k\$/MW$	$\gamma_{BESS}, \gamma_{HS}$	0.006%
C_{HS}	124 $\$/kg$	α	0.43
O_w	0.08 $\$/kg$	a_x	$1.2x10^{-5}$
O_{elz}	17 $k\$/MWh$	$Pr_{H_2,T}$	$5.31x10^{-16}$ $mole/sPa$
O_{Cmp}	$1.5\%C_{Cmp}$ $k\$/MWh$	R_o	$27m\Omega cm^2$
O_{HS}	$2\%C_{HS}\$/kg$	ΔH_{vap}	$41572J/mole$
D_{elz}	$40\%C_{Stack}$ $k\$/MWh$	π_{H_2O}, π_{O_2}	$0.48bar, 1bar$
C_{Conv}	120 $k\$/MVA$	π_{HS}, $\Psi^{max}_{H_2inO_2}$	500 bar, 10%
V_{LHV}	$1.25V$	η_{Cmp}	63%
ΔH_{LHV}	$241kJ/mole$	a, b, δ_m	2744, 1.665, 1.15

In what follows, the results obtained for Cases 1, 2, and 3 are presented and analyzed. **In Case 1**, the PEME is modeled with a constant conversion rate in kg/kWh, i.e., without consideration of i) the detailed model provided in this report, or ii) the design of the PEME internal parameters, and iii) safety constraints. In this case, the cathodic pressure π_{H2} needs to be predetermined to facilitate the design of other components in the GHP, e.g., the mechanical compressor. Therefore, and without loss of generality, the cathodic pressure π_{H2} is set in this case at 30 bars as given in most commercially available PEME [64]. Table 10 reports the obtained optimal sizes of the GHP components for pure green and dull green hydrogen.

Table 10 | Parameters of the Optimally Designed GHP for Cases 1 To 4 with Consideration of the US Subsidy

Item	Parameter	Green				Dull Green (Dg3)			
		Case 1	Case 2	Case 3	Case 4	Case 1	Case 2	Case 3	Case 4
PEME	l_m	–	N212	N211	N212	–	N212	N212	N212
	$\pi_{H_2(bar)}$	30	30	28	30	30	30	54	30
	$A_{elz}(m^2)$	–	2124	1888	1102	–	1877	1968	1368
	$P_{elz}^{rate}(MW)$	113	121	104	63	115	107	112	78
Elec. Devices	$P_{Conv}^{rate}(MW)$	116	124	107	65	118	110	116	80
	$P_{Cmp}^{rate}(MW)$	18	21	19	11	18	18	14	13
H_2 Storage	$Cap_{HS}(100kg)$	224	240	228	216	247	247	247	213
Cost	$LCOH(\$/kg)$	4.88	4.5	4.3	5.9	7	6.7	6.4	7.9

As shown in Table 10 the rated power of different components in the designed dull GHP is higher than those in the pure GHP since the dull green case suffers from larger variations in electricity prices compared to the green case that obtains electricity through a PPA. Hence, higher power ratings are required to minimize/avoid the operation of the dull GHP at high electricity prices. As reported in the table, the LCOH in the pure GHP case is 30% lower than the dull GHP. The produced dull green hydrogen is labeled as Dg3 as the resultant CEH equals 1.82 CO2kg/H2kg. Thus, the dull GHP qualifies for a $0.75 subsidy.

It is worth noting that the results given in Table 10 for Cases 1 to 4 are presented with consideration of the US subsidy for the green hydrogen production, thereby green hydrogen production has become more economical. Table 11 reports the GHP optimal parameters for Cases 1 to 4 where the LCOH has been computed with consideration of the Canadian subsidy for the green hydrogen production and for dull green production where the grid supply mix results in low emissions. In addition, the electrolyzer capacity factor has been reported for various cases.

Table 11 | Parameters of the Optimally Designed GHP for Cases 1 To 4 with Consideration of the Canadian Subsidy

Item	Parameter	Green				Dull Green (Dg3)			
		Case 1	Case 2	Case 3	Case 4	Case 1	Case 2	Case 3	Case 4
PEME	l_m	–	N212	N211	N212	–	N212	N212	N212
	$\pi_{H_2(bar)}$	30	30	28	30	30	30	54	30
	$A_{elz}(m^2)$	–	2124	1888	1102	–	1877	1968	1368
	$P_{elz}^{rate}(MW)$	113	121	104	63	115	107	112	78
Elec. Devices	$P_{Conv}^{rate}(MW)$	116	124	107	65	118	110	116	80
	$P_{Cmp}^{rate}(MW)$	18	21	19	11	18	18	14	13
H_2 Storage	$Cap_{HS}(100kg)$	224	240	228	216	247	247	247	213
Cost	$LCOH(\$/kg)$	7.88	7.5	7.3	8.9	7.75	7.4	7.15	8.63
	$Min\ LCOH(\$/kg)$	-	-	-	-	7.0	6.7	6.56	7.78
	$Max\ LCOH(\$/kg)$	-	-	-	-	8.56	8.06	7.8	9.56
	$Std\ LCOH(\$/kg)$	-	-	-	-	0.24	0.2	0.2	0.28
	$LCOH(\$/kg)$ with ITC	7.56	7.15	7	8.76	7.5	7.18	6.95	8.49
Capacity Factor	-	Med	Med	Med	High	Med	Med	Med	High

Figure 14 (a) shows the total imported power and PEME power consumption for the pure green hydrogen production of Case 1. As depicted in Figure 14 (a), the total power consumption is kept within the limits of the maximum available renewable power. The corresponding PEME efficiency is given in Figure 14 (c). As illustrated in the figure, the efficiency is constant over the entire time window (the four typical days) under study. Modeling the PEME with a constant conversion rate does not reflect the impact of PEME loading (power consumption) variation on its operating efficiency. As such, the PEME efficiency does not change during the four typical days. Further, ignoring the detailed modeling of PEME makes it impossible to calculate the hydrogen in oxygen percentage, and hence, the safe operation of PEME during the studied time window cannot be explored and is not guaranteed.

Figure 14 |(A) Imported and PEME Power Of Case 1, (B) Imported and PEME Power of Case 2, (C) PEME Efficiency of Cases 1 And 2, (D) PEME Current Density of Cases 2 and 4, and (E) Hydrogen in Oxygen Percentage of Cases 2 and 4.

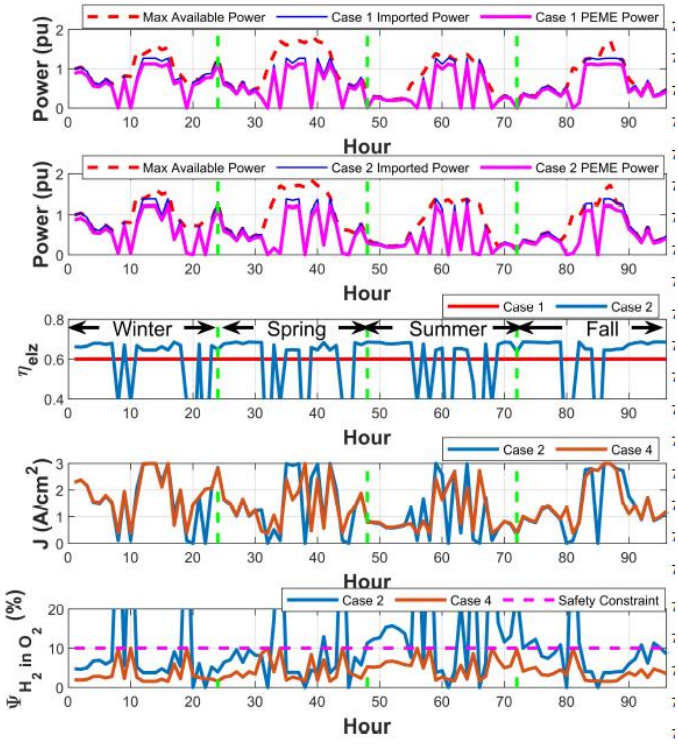

Case 2: In Case 2, the PEME detailed model is considered. However, membrane thickness and cathodic pressure are not considered as a part of the optimization problem, i.e., these two PEME parameters are chosen as utilized in the most commercially available units instead of being optimized within the optimization problem. The Nafion membrane thickness is chosen to be N212, which is known to be one of the economic options [65]. The cathodic pressure Π_{H2} is set at 30 bars according to the most commercially available PEME [64].The cell area is determined by the optimization algorithm since the rated power (sizing) of PEME depends on the selection of the cell area, i.e., the PEME rated power cannot exceed the capability (maximum current) of the chosen cell area, and thus, the cell area cannot be predefined while optimizing the PEME rating. As stated in Table 10, the utilization of the PEME model has resulted in different LCOH values. Specifically, the LCOH has been decreased by 8% and 4% for pure and dull green hydrogen, respectively. Figure 14 (b) depicts the total imported power and PEME power consumption for the pure green hydrogen production in Case 2. Figure 14 (c) shows the changes of the PEME efficiency with the change of loading. In contrast to Case 1, where the PEME efficiency remains constant regardless of loading, Figure 14 (c) highlights that in Case 2, the efficiency of PEME varies with its loading. As such, Case 2 properly considers the impact of loading level on PEME efficiency and, hence, on the LCOH.

Case 3: In Case 3, the detailed model of PEME is considered and the eleven PEME internal parameters are optimized in accordance with the design of the GHP. It is important to mention that the membrane thickness is optimized among the four commercially available Nafion membrane thickness options

(N211 – 25.4μm, N212 –51μm, N115 – 127μm, N117 – 183μm). Compared to Case 2, optimizing the PEME parameters decreases the LCOH by 4.4% and 4.5% for green and dull green hydrogen, respectively, as stated in Table 10 . For the pure green hydrogen, the optimal PEME design incorporates a thin membrane, N211, and a 28 bars cathodic pressure that keeps a relatively high PEME efficiency at both the low and high current densities to fit the large variations of the available renewable power profile. For the dull green hydrogen, the available power profile exhibits a more uniform distribution, requiring a shift of the peak of the PEME efficiency curve to a relatively high current density, and hence, a thicker membrane, N212, with the 54-bar cathodic pressure are employed. For the pure GHP of case 3, Figure 15 (a) shows that the total imported power fulfills the constraint of maximum available power. The State of Hydrogen (SoH) illustrated in Figure 15 (b) varies mainly with the hydrogen demand and slightly affected by other factors such as the electricity price. Figure 15 (c) shows large variations in the PEME current density that leads to corresponding fluctuations in the level of hydrogen in oxygen percentage as depicted in Figure 15 (d). Since Case 3 ignores the PEME safety constraints, the hydrogen in oxygen percentage freely exceeds the safe limit, 10%, as shown in Figure 15 (d).

Figure 15 |(A) Imported Power, (B) SoH, (C) Current Density, (D) Hydrogen in Oxygen Percentage of the Optimal GHP Of Cases 3 and 5.

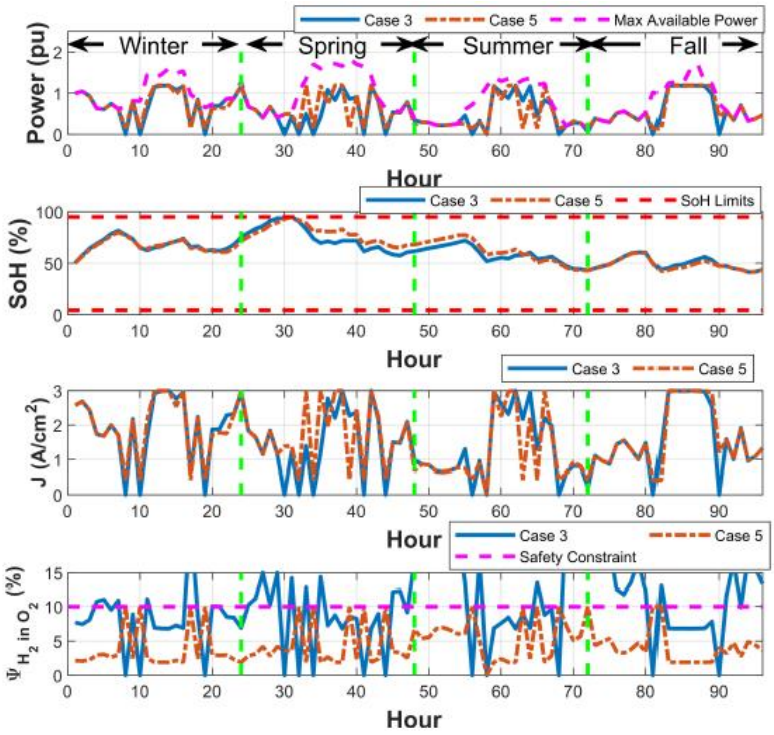

Case 4: In what follows, the design of the GHP employs the detailed PEME model without optimizing its internal parameters. Further, in this case, i.e., Case 4, considers the safety constraints of the PEME.

It is reminded that in Case 2 discussed above, the Nafion membrane thickness and the cathodic pressure are chosen to be N212, and 30 bars, while the cell area is determined by the optimization algorithm. As provided previously in Table 10, the green and dull green hydrogen LCOH is, respectively, 31% and 18% higher than that of Case 2. These results highlight the influence of considering the PEME safety constraints on the LCOH. Additionally, the incorporation of these safety constraints restricts the PEME's operation at lower current densities, resulting in the utilization of smaller PEME units when compared to the first three cases. Figure 14 (d) presented above shows the hourly variations in current densities of Cases 2 and 4. As shown in the figure, PEME current density in Case 2 ranges from 0.1 to 3 A/cm^2, while in Case 4, it fluctuates between 0.4 and 3A/cm^2. This reflects the avoidance of operating at very low current densities when safety constraints are employed as in Case 4. Figure 14 (e) shows the hydrogen in oxygen percentage for both Cases 2 and 4. As depicted in the figure, Case 2 does not ensure that the percentage of hydrogen in oxygen remains within the safe range. Conversely, Case 4 adheres to the safety constraints applied to the hydrogen in oxygen percentage.

Case 5: Case 5 considers sizing the GHP components (PEME, power converters, and compressor units) while optimizing the PEME parameters. Table 12 provides the obtained parameters of the optimally designed GHP at the four commercially available Nafion membrane thicknesses (N211 –25.4μm, N212 – 51μm, N115 –127μm, N117 – 183μm) [65]. In the case of pure GHP, the corresponding LCOH shows that the choice of medium membrane thicknesses, i.e., N212 and N115, achieves the least LCOH.

Table 12 |Parameters of the Optimally Designed GHP for Cases 5 and 6 with Consideration of the US Subsidy

	Item	Parameter	Green				Dull Green (Dg3)			
Case 5	PEME	l_m	N211	N212	N115	N117	N211	N212	N115	N117
		$\pi_{H_2(bar)}$	7	13	32	40	6	12	21	28
		$A_{elz}(m^2)$	1513	1747	1899	2156	1640	1717	1877	2170
		$P_{elz}^{rate}(MW)$	82	99	119	132	89	97	117	120
	Elec. Devices	$P_{Conv}^{rate}(MW)$	85	102	122	136	92	100	121	124
		$P_{Cmp}^{rate}(MW)$	29	26	18	17	34	27	22	19
	H_2 Storage	$Cap_{HS}(100kg)$	217	229	239	241	247	247	247	247
	Cost	$LCOH(\$/kg)$	5.1	4.7	4.8	5	7.6	7.2	7.4	7.5
Case 6	PEME	l_m	N211	N212	N115	N117	N211	N212	N115	N117
		$\pi_{H_2(bar)}$	22	45	38	54	26	50	33	52
		$A_{elz}(m^2)$	1301	1424	2098	2228	1235	1254	1842	2124
		$P_{elz}^{rate}(MW)$	71	81	132	149	68	72	115	142
	Elec. Devices	$P_{Conv}^{rate}(MW)$	153	138	169	168	158	156	236	163
		$P_{Cmp}^{rate}(MW)$	15	11	13	15	13	9	17	10
		$P_{BESS}^{rate}(MW)$	78	52	102	94	88	83	120	111
		$Cap_{BESS}(MWh)$	312	209	406	377	350	331	480	445
	H_2 Storage	$Cap_{HS}(100kg)$	195	222	186	205	226	222	221	233
	Cost	$LCOH(\$/kg)$	4.6	4.2	4.9	5.1	6.8	6.6	7.3	7.6

It is noted that PEME with thinner membrane, N211, suffers from high hydrogen crossover losses at low current densities and, and thus, its LCOH is 8.5% higher than the N212. Also, the thicker membrane, N117, suffers from high ohmic losses when it operates at high current densities, hence wider cell area is needed to limit such losses. Nevertheless, it is noted that the LCOH would be 6.4% higher than the N212. To achieve optimal operation, the PEME cathodic pressure rises when the electrolysis membrane becomes thicker, where increasing the thickness allows such rise in pressure while maintaining hydrogen crossover within the safe limits. For dull GHP, similar variations in the cathodic pressure and the cell area of the PEME can be observed with increasing the membrane thickness. Table 12 shows that the N212 membrane provides the lowest LCOH for dull GHP, which is the same as in the GHP case. For all membrane thicknesses, the produced hydrogen is labeled as Dg3 based on its level of CEH. Compared to Case 4, non optimized PEME parameters, Case 5 provides 20% and 9% reduction in the LCOH for green and dull green hydrogen, respectively. The optimal cathodic pressure for both green and dull green hydrogen is much lower than that proposed in Case 4. Further, the employment of that low pressure allowed utilizing wider cell area to achieve higher efficiency without violating the PEME safety constraints.

The results given in Table 12 for Cases 5 and 6 are computed with consideration of the US subsidy for green hydrogen production, thereby green hydrogen production has become more economical. Table 13 reports the GHP optimal parameters for Cases 5 and 6 where the LCOH has been computed with consideration of the Canadian subsidy for green hydrogen production and for dull green hydrogen production where the grid supply mix results in low emissions. In addition, the electrolyzer capacity factor has been reported for various cases.

Table 13 |Parameters of the Optimally Designed GHP for Cases 5 and 6 with Consideration of the Canadian Subsidy

	Item	Parameter	Green				Dull Green (Dg3)			
Case 5	PEME	l_m	N211	N212	N115	N117	N211	N212	N115	N117
		$\pi_{H_2(bar)}$	7	13	32	40	6	12	21	28
		$A_{elz}(m^2)$	1513	1747	1899	2156	1640	1717	1877	2170
		$P_{elz}^{rate}(MW)$	82	99	119	132	89	97	117	120
	Elec. Devices	$P_{Conv}^{rate}(MW)$	85	102	122	136	92	100	121	124
		$P_{Cmp}^{rate}(MW)$	29	26	18	17	34	27	22	19
	H_2 Storage	$Cap_{HS}(100kg)$	217	229	239	241	247	247	247	247
	Cost	$LCOH(\$/kg)$	8.1	7.7	7.8	8	8.37	7.96	8.18	8.29
		$Min\ LCOH(\$/kg)$	-	-	-	-	7.64	7.3	7.46	7.52
		$Max\ LCOH(\$/kg)$	-	-	-	-	9.19	8.7	8.88	8.97
		$Std\ LCOH(\$/kg)$	-	-	-	-	0.24	0.23	0.22	0.22
		$LCOH(\$/kg)$ with ITC	7.8	7.4	7.38	7.56	8.3	7.88	7.88	8.04
	Capacity Factor	-	Med	Med	Med	Med	Med	Med	Med	Med
Case 6	PEME	l_m	N211	N212	N115	N117	N211	N212	N115	N117
		$\pi_{H_2(bar)}$	22	45	38	54	26	50	33	52
		$A_{elz}(m^2)$	1301	1424	2098	2228	1235	1254	1842	2124
		$P_{elz}^{rate}(MW)$	71	81	132	149	68	72	115	142
	Elec. Devices	$P_{Conv}^{rate}(MW)$	153	138	169	168	158	156	236	163
		$P_{Cmp}^{rate}(MW)$	15	11	13	15	13	9	17	10
		$P_{BESS}^{rate}(MW)$	78	52	102	94	88	83	120	111
		$Cap_{BESS}(MWh)$	312	209	406	377	350	331	480	445
	H_2 Storage	$Cap_{HS}(100kg)$	195	222	186	205	226	222	221	233
	Cost	$LCOH(\$/kg)$	7.5	7.2	7.9	8.1	7.4	7.35	8.05	8.35
		$Min\ LCOH(\$/kg)$	-	-	-	-	6.69	6.55	7.2	7.45
		$Max\ LCOH(\$/kg)$	-	-	-	-	8.27	8.09	8.8	9.19
		$Std\ LCOH(\$/kg)$	-	-	-	-	0.23	0.23	0.26	0.25
		$LCOH(\$/kg)$ with ITC	7.1	6.85	7.1	7.6	7.03	7	7.4	7.73
	Capacity Factor	-	High	Med	Med	Med	High	High	Med	Med

Figure 15 (a) shows the total imported power of the GHP of Case 5 with N212 membrane, indicating the optimal membrane thickness. As shown in the figure, the imported power introduces a pattern similar to that of the GHP in Case 3. Similarly, the SoH and PEME current density are similar to those of Case 3 as depicted in Figure 15 (b) and (c). However, in Case 5, the hydrogen in oxygen percentage is kept within the safe limit as illustrated in Figure 15 (d). This safe limit has been achieved as Case 5 utilizes lower cathodic pressure for both green and dull green hydrogen cases, in addition to employing a thicker membrane for the green hydrogen case when compared with Case 3.

Case 6: In what follows the effect of combing the GHP with a BESS on the PEME internal parameters is evaluated. Similar to Case 5, the cost of green hydrogen production is minimum for intermediate membrane thicknesses of N212 and N115 as depicted in Table 12. With thinner and thicker membrane thicknesses, LCOH increases by 9.5% and 21%, respectively. As the membrane becomes thicker, the PEME tends to operate at lower current densities to minimize the ohmic losses, which could also increase the electrolysis cell area. Simultaneously, the cathodic pressure rises to achieve the optimal

operation as the increase of membrane thickness allows such a rise in the pressure without surging the hydrogen crossover. However, such a described behaviour contradicts the one associated with the reduction of the operating current densities caused by increasing the cell area. It is observed that the reduction in operating current densities upsurges hydrogen crossover. For this reason, the cathodic pressure declines to 38 bars with N115 membrane. Compared to Case 5 (without BESS), the optimal cathodic pressure in Case 6 (with BESS) is higher at the same membrane thickness. This is because the BESS enables the PEME to avoid low current density operation without being forced to import power from the grid at high prices. Figure 16 (a) and (b) show the imported power from the grid, PEME consumed power, and SoH for membrane N212 that yields the minimum LCOH.

Figure 16 |(A) Imported Power, PEME Power, and (B) SoH of the Optimal GHP of Case 6; (C) Imported Power, PEME Power, and (D) SoH of the Optimal Dull GHP of Case 6.

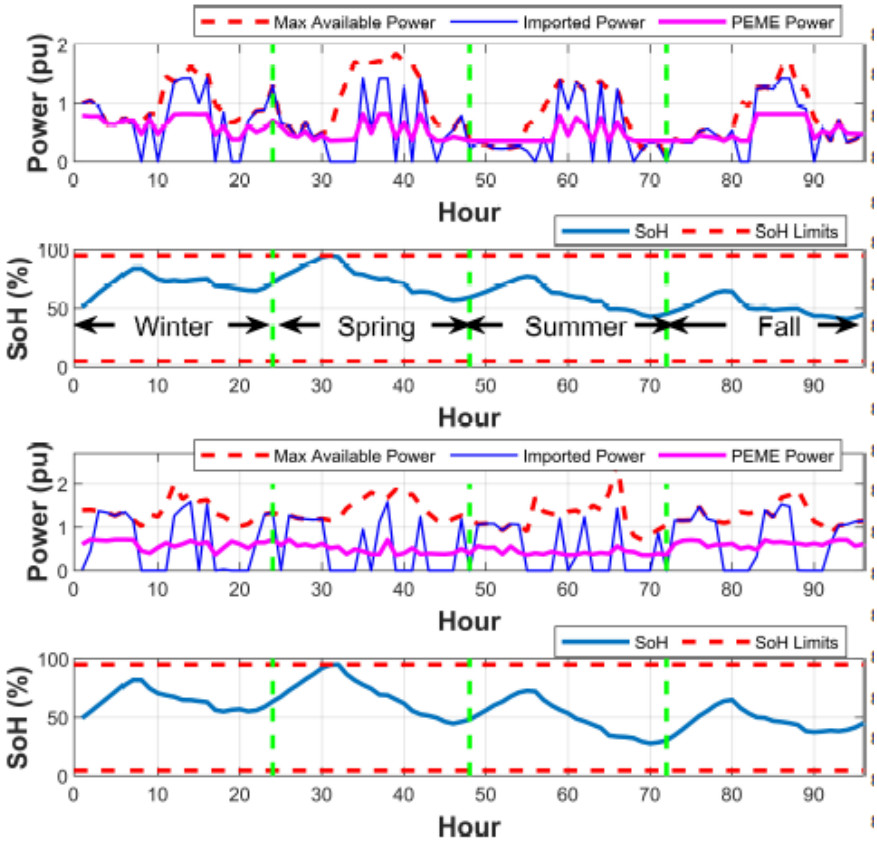

As shown in Figure 16, the imported power from the grid is kept within the envelop of the maximum available renewable power. The results show that the PEME power profile does not follow the imported power from the grid, where large fluctuations are handled by the BESS. The SoH shows a repeated pattern, where it increases during night and decreases in daytime which is consistent with the hydrogen demand profile.

Error! Reference source not found. (a) shows the variations in the SoC of the BESS that is shaped based on the power availability. The compressor power consumption shown in **Error! Reference source not found.** (b) has a similar pattern to the one shown for the PEME. **Error! Reference source not found.** (c) and (d) show the changes of the PEME operating current density and efficiency for both N212 and N117 membranes.

Figure 17 |(A) SoC, and (B) Compressor Power of the Optimal GHP of Case 6; (C) PEME Current Density, and (D) Hydrogen in Oxygen Percentage of the Optimal GHP and the N117 Membrane GHP of Case 6

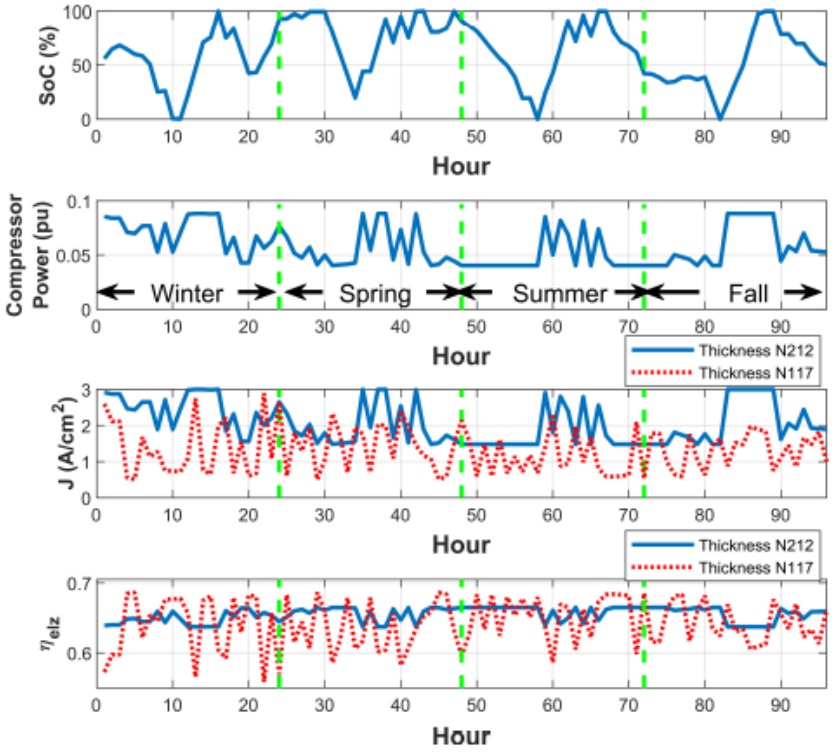

As shown **Error! Reference source not found.**, the current density of N212 is around 2A/cm^2 at most of the time, and thus, there are small variations in the efficiency. On the other hand, when membrane is employed, the current density is lower than that of N212 due to the utilization of larger cell areas. It is also noted that the efficiency fluctuations in membrane N117 is more obvious because thicker membranes offer higher resistances, and hence, the negative slope of their efficiency curve is sharper, which cause larger efficiency variations even for the same current density changes. For dull GHP, Table 12 shows that intermediate thicknesses (N212, N115) provide the minimum LCOH. The cathodic pressure shows the same pattern as the GHP case at different thicknesses. As in Case 5, the produced dull green hydrogen is categorized as Dg3 color for all membrane thicknesses. The results show that the optimal LCOH using dull GHP is 57% higher than GHP. Figure 16 (c) and (d) show the

available power profile, imported power, PEME power, and SoH for N212 membrane that are similar to the GHP case.

Clean Hydrogen Subsides: There are many announced governmental clean hydrogen subsidies. The way in which these subsidies affect the GHP design and its PEME parameters differs according to the subsidy definition. As such, the clean hydrogen ITC announced in [3] by the Canadian government is considered instead of the PTC of USA utilized in the previous case studies. Based on the clean hydrogen ITC of Canada, the new subsidy is formulated as follows:

$$\Upsilon = \begin{cases} 0.4\,CAPEX/\sum_{t=1}^{T} L_d^t \ \$ & ,0 \le CEH \le 0.75 \\ 0.25\,CAPEX/\sum_{t=1}^{T} L_d^t \ \$ & ,0.75 < CEH \le 2 \\ 0.15\,CAPEX/\sum_{t=1}^{T} L_d^t \ \$ & ,2 < CEH \le 4 \\ 0 \ \$ & ,CEH > 4 \end{cases}$$

The impact of employing the above-mentioned subsidy compared to the case without any subsidy and the case which employs the USA PTC is depicted in Figure 18 and

Figure **19**, respectively. Figure 18 shows the deviation in the LCOH, cell area, cathodic pressure, and BESS power rating as a percentage of the case without any subsidy.

Figure **19** shows the results as the percentage of the case with the USA PTC subsidy for Cases 5 and 6 for both the green and dull green hydrogen production.

Figure 18 | The Impact of Utilizing the New Subsidy on the LCOH, Cell Area, Cathodic Pressure, and BESS Power Rating of Cases 5 and 6 as the Percentage the Case without Subsidy

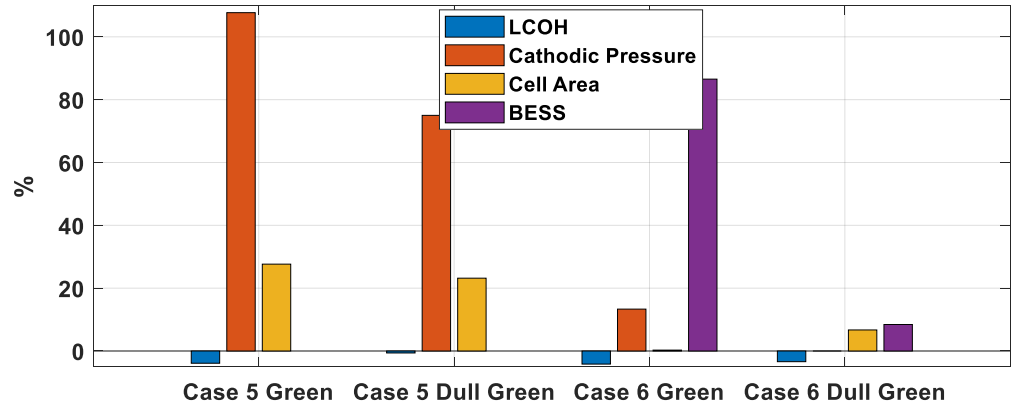

Figure 19 | The Impact of Utilizing the New Subsidy on the LCOH, Cell Area, Cathodic Pressure, and BESS Power Rating of Cases 5 and 6 as the Percentage of the Case with USA PTC Subsidy

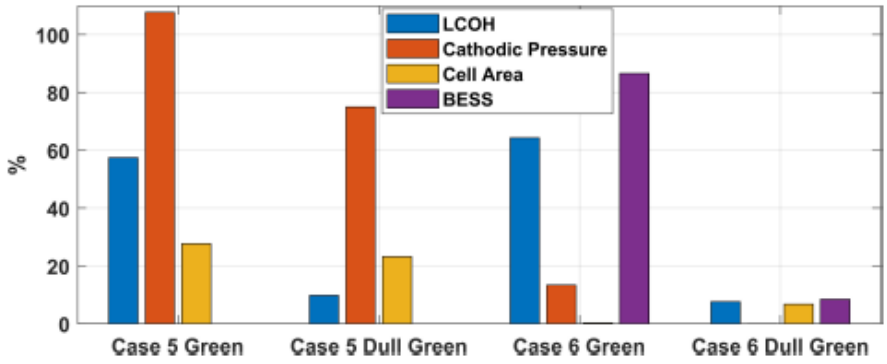

As shown in Figure 18, the LCOH is reduced marginally while other parameters are increased. Regarding the membrane thickness and compared with the case with the US PTC subsidy, Case 5 with the new subsidy utilizes a thicker membrane, N115, while Case 6 employs the same membrane as of the case with the US PTC subsidy. The new subsidy reduces the component of the capital cost especially for the green hydrogen where the capital cost is reduced by 40%. For the dull green hydrogen production, the CEH is around 1.82 CO2kg/H2kg and hence, it qualifies for 25% reduction. This capital cost reduction increases the share of the operation cost in the LCOH which, in turn, promotes rising the cathodic pressure to decrease the power consumption of the compressor. Rising the pressure could require utilizing thicker membrane to reduce the hydrogen crossover. Yet, thicker membrane increases the ohmic losses, and hence, it could employ wider cell area or and/or larger BESS to restore the efficiency. This behavior would be clearer for green hydrogen case as it offers higher reduction in the capital cost.

3.3. Optimal Deployment of AE Based GHP

The previous studies carried out for PEM based GHP is revisited for AE. Detailed modeling of AE is given in the appendix of this report. This study investigates the impact of the type of the electricity source powering the AE on the design of its parameters. The study considers two main types of sources: 1) contact source (where the AE is fed from a source providing constant/base power, e.g., nuclear generation), and 2) variable renewable energy sources (RES) such as solar, wind, or a mix. To model the RES in the design problem, the wind speed and solar radiation data of five years in Ontario, Canada [60] is used to generate a four-day typical power profile of different sizes of solar and wind power plants. The generated power profiles of solar and wind plants are depicted in Figure 20. The cost of electricity in the PPA is assumed to be fixed at a rate of 20$/MWh as discussed in [62]. AE voltage model parameters are defined in Table 14 and

Table **15** [57]. Gas crossover parameters are obtained from [58]. Other technical, cost, and simulation parameters are imported from the techno-economic study in [25] as listed in Table 14.

Figure 20 | **Solar and Wind Power Profiles of the Typical Four Days of Seasons**

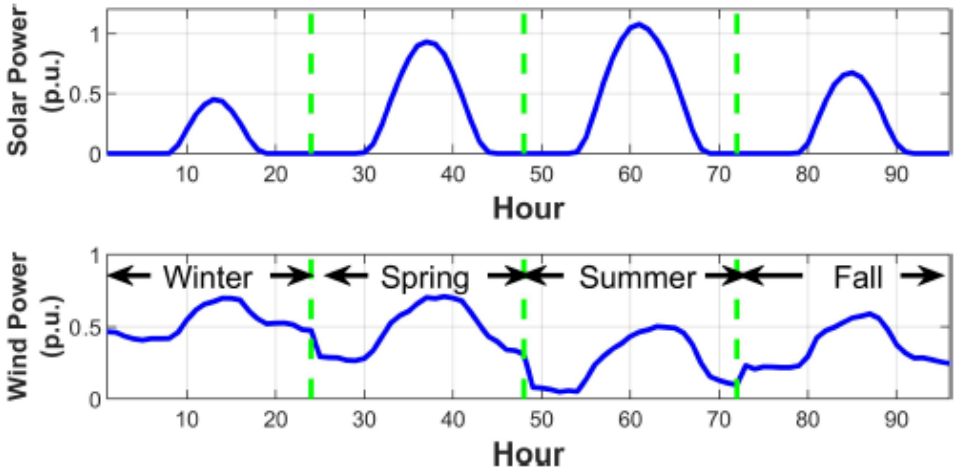

Table 14| **Simulation Parameters**

Parameter	Value	Parameter	Value
C_{AE}	600 $k\$/MW$	K	1.4
C_{Cmp}	7.52 $k\$/MW$	π_{HN}	$400bar$
C_{Conv}	120 $k\$/MW$	η_{Cmp}	63%
O_w	0.08 $\$/kg$	π_{H_2O}	$0.48bar$
D_{AE}	$40\%C_{AE}k\$/MWh$	ΔH_{LHV}	$241kJ/mole$
O_{Cmp}	$1.5\%C_{Cmp}k\$/MWh$	O_{AE}	17 $k\$/MWh$

Table 15|**Parameters of Optimized AE Based GHP with Different Power Profiles**

Power Source	Profile Type	Variable RES					Constant
	Solar Ratio (%)	100	75	50	25	0	-
	Wind Ratio (%)	0	25	50	75	100	-
AE	$\delta_s(mm)$	0.5	0.5	0.5	0.5	0.5	0.5
	π_{H_2}, $\pi_{O_2(bar)}$	1	2	4	7	10	110
	$A_{AE}(m^2)$	28603	26428	25204	24366	23354	18736
	$T_{AE}(K)$	373	373	373	373	373	373
	$M(\%)$	45	41	28	18	15	15
	$P_{AE}^{rate}(MW)$	137	126	121	118	114	95
BoP	$P_{Conv}^{rate}(MW)$	141	130	125	122	117	97
	$P_{Cmp}^{rate}(MW)$	98	73	52	42	35	7
Outcomes	LCOH ($\$/kg$)	3.2	2.6	2.3	2.1	1.9	1.5

In the analysis presented below, the optimal design of the AE based GHP with the constant power source is demonstrated. As shown in

Table **15**, the AE optimal design, when it is powered by a constant source, shows tendency to operate at high operating hydrogen and oxygen pressures. Higher operating pressures increases the hydrogen crossover that limits the safe operation and reduces the AE efficiency at low current densities. However, since the plant is running at a constant power, there is no need to run the plant at lower current densities. The plant is sized to operate near the highest capacity factor and highest current density values. The AE efficiency increases as its temperature rises. Yet, the AE temperature is limited by the corrosion levels, which increases with the temperature rise. As mentioned in [66], the 373K is the maximum practical limit for AE operating temperature. The typical electrolyte concentration falls within the range of 15% to 45%. The maximum electrolyte conductivity is attained at a concentration of 30%. However, the concentration also affects hydrogen crossover, resulting in a lower hydrogen in oxygen percentage when low concentration, i.e., 15% is employed at relatively high current density values. In this case, as the AE tends to operate at high current densities, the optimal concentration is geared towards minimizing the hydrogen crossover, especially under the conditions of high operating pressure values, which is set at 110 bars. A constant power profile cannot be easily achieved with RES, unless the excess renewable power is fed to another power user. In this case, as power is obtained through a PPA, it is assumed that the excess renewable power, not consumed by the GHP, is resold in the electricity market at the same price of the purchase. Such a strong assumption results in 1.5$/kg LCOH. Yet, in real cases this cost may change significantly.

In what follows, the optimal design of the GHP with RES power profile is evaluated, where the GHP under design is coupled with RES. Five GHP sizing simulation cases are conducted with different RES power profiles of combined solar and wind power. The obtained optimal sizing of the GHP and the corresponding AE optimal internal parameters are provided in

Table **15**. The case of pure solar power profile suffers from large variations in the generated power as shown in Figure 20 (a). Such variations force the AE to operate at different current density levels almost from zero to the maximum current density. Therefore, optimal operating pressures are kept at the minimum value of 1 bar to limit the hydrogen crossover at all current densities. The optimal electrolyte concentration is set at 45% to minimize the hydrogen cross over at low current densities, which is suitable for the solar power profile. Due to the off periods of the solar power profile, the GHP will operate at significantly low-capacity factor that results in high LCOH around 3.2$/kg.

As the wind power percentage increases (solar power percentage decreases) the resultant power profile becomes flatter and approaches the constant power profile. Therefore, the AE tends to operate at higher current densities which results in rising the optimal operating pressure and reducing the

electrolyte concentration. The separator thickness affects the ohmic overpotential, and hence, impacts the voltage efficiency. However, its effect on the voltage efficiency is insignificant compared to its impact on the hydrogen crossover. Therefore, it is kept at the thickest value for all power profiles. As in the case of the constant power profile, the AE operating temperature is always at the highest value of 373K which ensures achieving the highest voltage efficiency. The AE effective area, power rating, and power converter rating decrease as wind power percentage inclines and as the power profile peak decreases. Similarly, the compressor rating decreases due to the reduction in the AE rating and the rise of the operating pressure. The resultant LCOH declines as the capacity factor of the GHP increases with the increase of wind power percentage. Figure 21 (a), (b), and (c) show, respectively, the power profile, current density, and AE efficiency of two cases: 75% solar - 25% wind; and 100% wind.

Figure 21 | (A) Power Profiles, (B) Current Density, (C) Efficiency, (D) and Hydrogen in Oxygen Percentage of Cases 75% Solar - 25% Wind, and 100% Wind

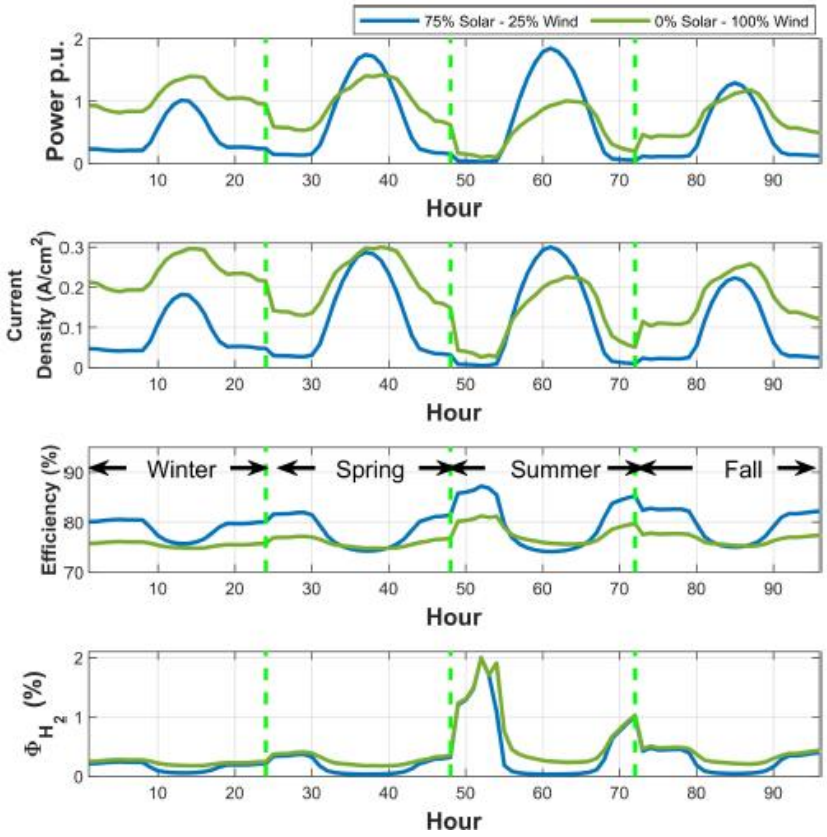

As shown in Figure 21, the latter case offers a flatter power profile, and hence, at most of the times, it tends to operate at higher current density values. Although the 100% wind case operates at lower AE efficiency at most of the time, it offers lower LCOH as it requires lower compressor consumption and

operates at a higher capacity factor. Figure 21 (d) shows that both cases comply with the safety constrains of keeping the percentage of hydrogen in oxygen less than 2%.

3.4. Result Analysis of PEME and Alkaline Considering Provision of Grid Services

For this study, the GHP facility is sized and rated based on the opportunities available for contribution to the grid services of bulk transmission systems in addition to its base application to fulfill the hydrogen demand in the market.

3.4.1. Participation in Demand Response

PEME and AE as the two main electrolysis technologies offer advantages and disadvantages depending on the application they are used for. As noted in the survey section of the report, the ramp rates of the electrolysis process depend on the technology which is used for hydrogen production. AE offers a slower ramp rate, and thus, is more suitable for baseload for production of hydrogen at nighttime using inexpensive/waste electricity. PEME offers a higher ramp rate, and thus, is more suitable for provision of grid services since it is able to make rapid changes in its energy consumption level. This section aims to compare the two technologies from the technical and economic perspectives. Figure 22 below shows the operating parameters of the PEME and AE, when they are used for provision of DR services.

Figure 22 |The Operating Parameters of Alkaline (Left-Hand Side) and PEME (Right-Hand Side) Electrolyzers, when they are Used for DR Services

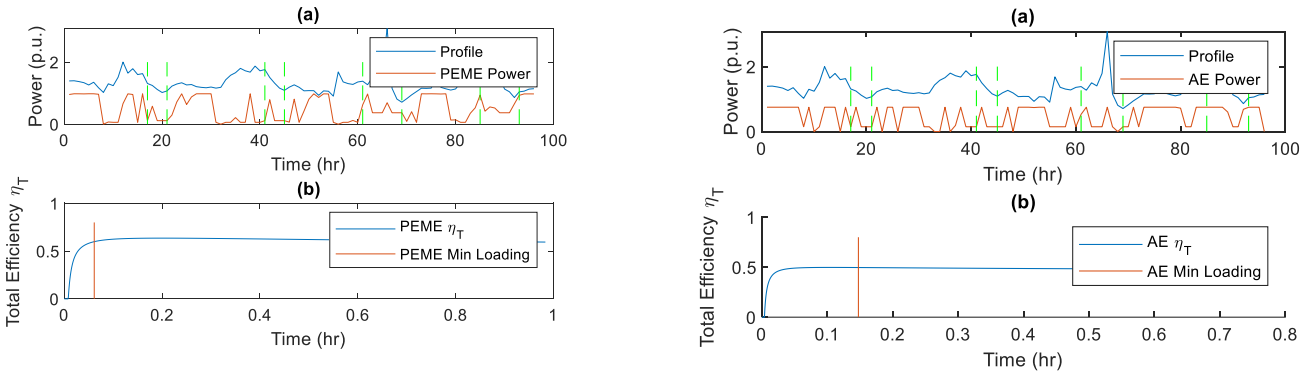

Table 16 |Optimal Sizing of Alkaline and PEME Electrolyzers with and without DR Services

Component	AE without DR	AE with DR	PEME without DR	PEME with DR
Electrolyzer Size (p.u.)	0.7494714	1.262039	1.041281	0.9834156
Converter Size (p.u.)	0.7726509	1.130885	1.073472	1.011197
Compressor Size (p.u.)	0.2402284	0.3511725	0.1263585	0.09422298
Hydrogen Storage Size (100 kg)	216.248	265.2558	277.8159	252.5706
LCOH $/kg	9.042414	8.935042	8.315092	8.48598

As shown in Figure 22 (a), for both the Alkaline and PEM, the electrolyzer power stays below the grid power profile, i.e., the maximum power limit of the grid, indicating that the grid constraints are not violated. Figure 22 (b) show that the electrolyzer's efficiency values change depending on the power consumption of the electrolyzers. This would indicate that electrolyzers need to be loaded to a certain level in order to produce hydrogen efficiently.

Table 16 reports the optimal ratings and LCOH of Alkaline and PEM electrolyzers and other components used for simulation studies, for base case (no contribution to ancillary services) and the case with contribution to DR services.

Facility ratings have been decided for cases as follows: 1) without contribution to the DR program, and 2) with contribution to the DR program. As reported in the table, larger component ratings are needed for the facility when it is scheduled to provide ancillary services to the grid. In addition, there has been marginal changes in the LCOH when the facility is operated to provide DR services. This is because the excess CAPEX needed to size the facility for DR services offsets the extra revenue collected from contribution to DR services.

3.4.2. Participation in Operating Reserve (OR) Services

Figure 23 below shows the operating parameters of the PEM and Alkaline electrolyzers, when they are used for provision of OR services.

Figure 23 |The Operating Parameters of AE (Left-Hand Side) and PEME (Right-Hand Side), when they participate in OR Services

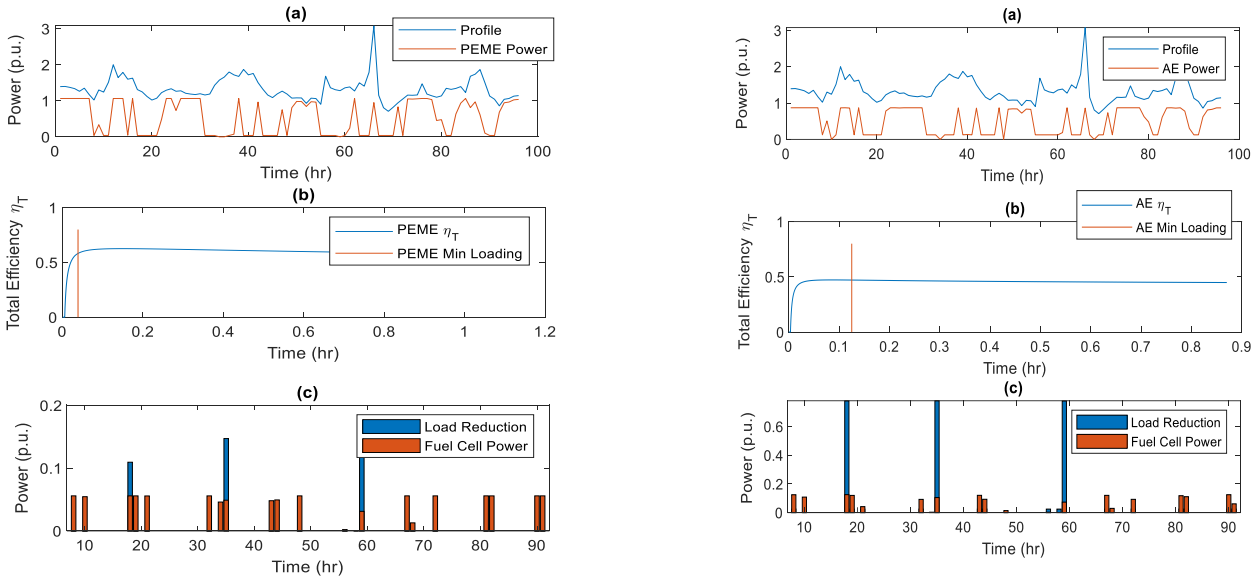

As shown in Figure 23 (a), for both the Alkaline and PEM electrolyzers, the electrolyzer power stays below the grid power profile, i.e., the maximum power limit of the grid, indicating that the grid constraints are not violated. Figure 22 (b) show that the electrolyzer's efficiency changes depending on the power consumption of the electrolyzers. This would indicate that electrolyzers need to be loaded

to a certain level to produce hydrogen efficiently. Figure 22 (c) shows how the electrolyzer reduces its consumption, or the fuel cell unit produces power injected to the grid in response to the OR signal.

Table 17 reports the optimal ratings and LCOH of Alkaline and PEM electrolyzers and other components used for simulation studies, for base case (no contribution to ancillary services) and the case with contribution to OR services. Facility ratings have been decided for cases as follows: 1) without contribution to the OR program, and 2) with contribution to the OR program. The numbers in the table show that larger ratings are needed for various components when the facility is scheduled to provide ancillary services to the grid. In addition, there have been marginal changes in the LCOH when the facility is operated to provide OR services. Similar to the case presented for the DR contribution, this is because the excess CAPEX needed to size and design the facility for OR services offsets the extra revenue collected from contribution to OR services.

Table 17 |Optimal Sizing of AE and PEME with and without OR Services

Component	AE without OR	Alkaline with OR	PEME without OR	PEME with OR
Electrolyzer Size (p.u.)	0.7494714	0.8704011	1.041281	1.065071
Fuel Cell Size (p.u.)	0	0.1251079	0	0.0558573
Converter Size (p.u.)	0.7726509	0.8973208	1.073472	1.09799
Compressor Size (p.u.)	0.2402284	0.3115919	0.1263585	0.1339508
Hydrogen Storage Size (100 kg)	216.248	256.995	277.8159	281.7167
LCOH $/kg	9.042414	8.807809	8.315092	8.318589

3.4.3. Participation in Renewable Smoothing

Figure 24 shows the operating parameters of the PEM and Alkaline, when they are used for provision of renewables smoothing services. As shown in Figure (a), similar to previous cases for both the Alkaline and PEM electrolyzers, the electrolyzer power stays below the grid power profile, i.e., the maximum

power limit of the grid, indicating that the grid constraints are not violated. Figure (b) show that the electrolyzer's efficiency values vary depending on the power consumption of the electrolyzers. Similar to utilization of electrolyzer for DR and OR services, this would indicate that electrolyzers should be loaded to a certain level to produce hydrogen efficiently. Figure (c) states that the electrolyzer reduces its energy consumption, or the fuel cell unit produces power injected to the grid as needed to compensate for the variation of renewable power generation.

Table 18 reports the optimal ratings and LCOH of Alkaline and PEM electrolyzers and other components used for simulation studies, for base case (no contribution to ancillary services) and the case with contribution to renewables smoothing services.

Figure 24 |The Operating Parameters of AE (Left-Hand Side) and PEM (Right-Hand Side) when they are Used for Renewables Smoothing

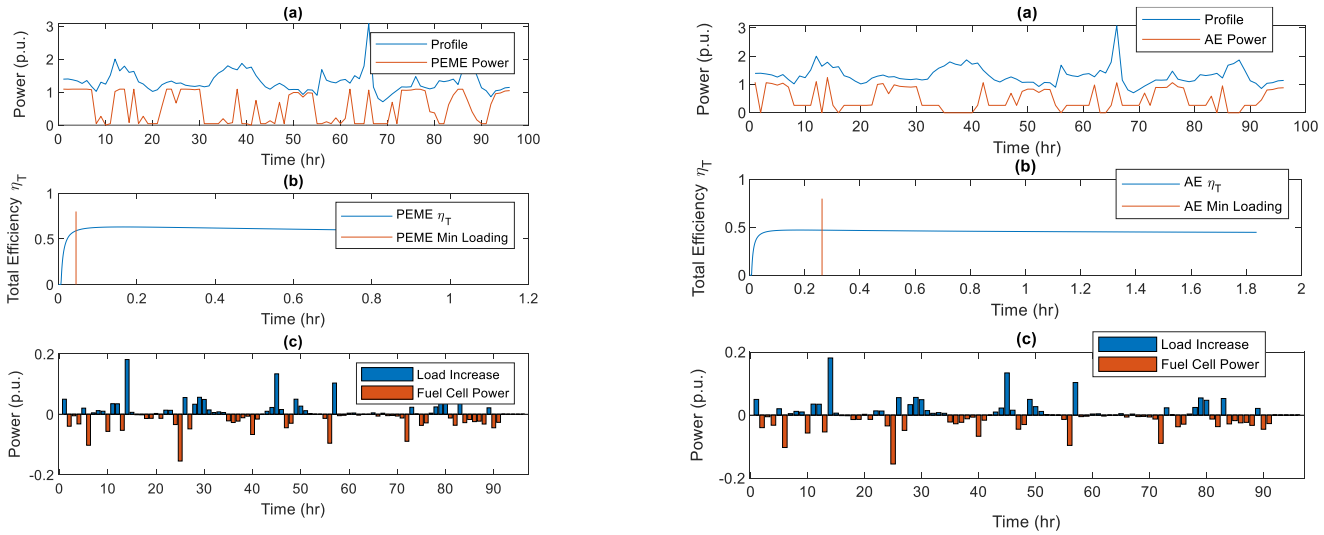

Table 18 |Optimal Sizing of AE and PEME without and with Renewable Smoothing Services

Component	AE without Renewable Smoothing	AE with Renewable Smoothing	PEME without	PEME with Renewable Smoothing

			Renewable Smoothing	
Electrolyzer Size (p.u.)	0.749471	1.837041	1.041281	1.091399
Fuel Cell Size (p.u.)	0	0.154877	0	0.154877
Converter Size (p.u.)	0.772651	1.099348	1.073472	1.124709
Compressor Size (p.u.)	0.240228	0.450218	0.126359	0.126534
Hydrogen Storage Size (100 kg)	216.248	263.6325	277.8159	279.067
LCOH $/kg	9.042414	10.92648	8.315092	9.043258

Facility ratings have been decided for cases as follows: 1) without contribution to the renewables smoothing services, and 2) with contribution to the renewables smoothing service. Similar to utilization of the facility for DR and OR services, the numbers in the table indicate that larger ratings and different designs are needed for various components when the facility is scheduled to provide renewables smoothing to the grid. In addition, LCOH has increased when the facility is operated to provide renewables smoothing. This is because the excess CAPEX needed to size and design the facility for renewables smoothing exceeds the extra revenue collected from contribution to renewables smoothing services.

3.4.4. Addition of Fuel Cell to Participate in OR

Fuel cells could be utilized to convert the produced clean hydrogen into electricity. However, there is a need to understand the value of adding fuel cell units in a GHP to participate in grid services such as OR. In order to understand the capability and economic viability of fuel cells to contribute to ancillary services, the LCOH for the GHP is computed and depicted versus the ratio of the fuel cell to electrolyzer in Figure 25 (a). As shown in the figure, when the fuel cell is integrated with the electrolyzer to operate as an energy storage similar to BSS, the LCOH increases due to the added CAPEX of the fuel cell. Figure 25 (b) shows the required selling price in $/MWh of electricity for the GHP to be able to breakeven its original LCOH. The figure shows that the optimal ratio of the fuel cell to electrolyzer resides between 70% to 90% which requires the least amount of incentive needed to breakeven.

Figure 25 | (A): LCOH for GHP and (B): Required Incentive for Contribution to OR Services

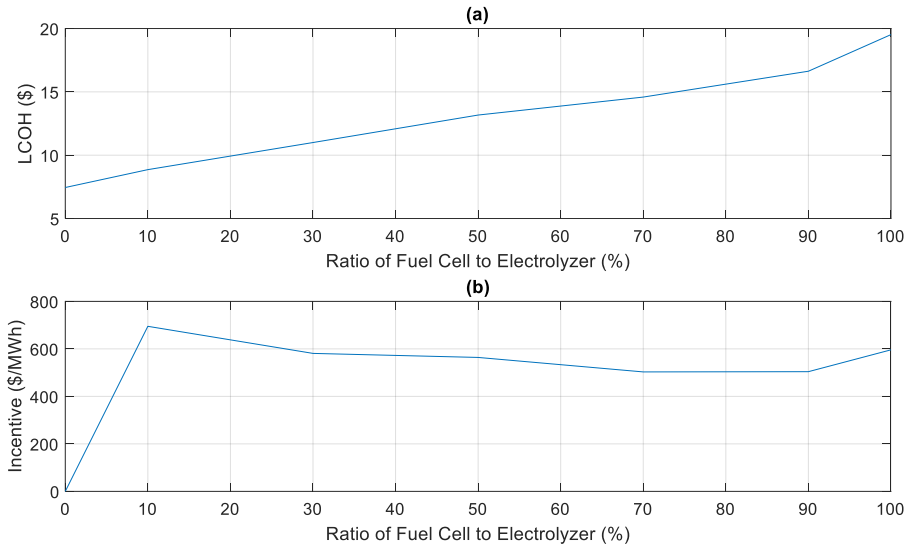

3.4.5. Impact of CAPEX and Efficiency on the LCOH of GHP

In this section, the LCOH vs the CAPEX and efficiency of the GHP is computed to indicate how the LCOH can be positively impacted as the technology materializes resulting in lower CAPEX and higher efficiency. The cost components of the GHP are given below.

1. **Electrolyzer Stack and BOP**
    - **Capital Costs Considering:**
        - Total Uninstalled Capital Cost ($/kW):
            - Stack Capital Cost ($/kW)
            - BOP Capital Cost ($/kW)
        - Installation Cost (% of uninstalled capital cost).
        - Plant Capacity (kg/day)
        - Replacement Cost of Major Components (% of installed capital cost) [Replacement Interval (years)].
    - **Operating Costs:**
        - Variable and Fixed Operating and Maintenance Costs
    - **Feedstock Fuel Costs [Total Electrical Usage (kWh/kg)]**
        - Net System Electrical Efficiency (percentage (%) of lower heating value (LHV) of H2 input energy)

        - Stack Electrical Usage (kWh/kg) (% of LHV H2)
        - BOP Electrical Usage (kWh/kg)
    - Electrolyzer Power Consumption (MW)
    - Average Electricity Price over Life of Plant (¢/kWh)

2. **Hydrogen Station Compression, Storage, and Dispensing system**
    - **Capital Costs**
    - **Variable and Fixed Operation and Maintenance Costs**

Accordingly, the following equation is formulated for calculating the LCOH ($/kg):

$$LCOH = \frac{\sum_{t\in\mathcal{T}}\sum_{h\in\mathcal{H}}(P_{h,t}^{PtH}.Prc_t^{Elc}).\Delta t + \frac{CAPEX}{PL*8760}*168}{\sum_{t\in\mathcal{T}}\sum_{h\in\mathcal{H}}(F_{h,t}^{PtH}).\Delta t\,.HD}$$

where:

- h: is the index of hydrogen plant
- Δt: is the time interval
- T: is the optimization horizon
- $P_{h,t}^{PtH}$: is the input power of the PtH unit (MW).
- Prc_t^{Elc}: is the electricity prices ($/MWh).
- $CAPEX$: is the capital cost of each hydrogen plant ($).
- HD: is the hydrogen density (kg/m^3), i.e., 0.08375.
- PL: is the hydrogen plant life (years).
- $F_{h,t}^{PtH}$: is the outflow of hydrogen from the PtH unit (m^3/h).

The variation in CAPEX primarily results from changes in the size of the system components including the electrolyzer and storage tank, which are determined according to the hydrogen demand. As the technology materializes, however, it is expected that the same system components can be manufactured as a lower cost. In this study, the base CAPEX is used to compute the base LCOH, and then, for reduced CAPEX values, the corresponding LCOH values are computed. Figure 26 shows the relationship between the CAPEX and LCOH values. As shown in the figure, as the CAPEX decreases, the LCOH decreases accordingly on a linear basis.

Figure 26 | **LCOH vs the GHP CAPEX**

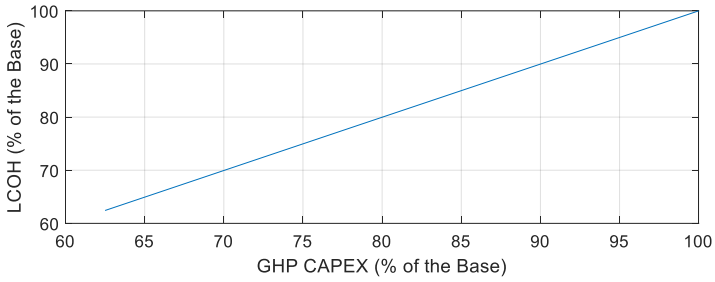

The electrolyzer efficiency impacts the electricity consumption, and in turn the operating schedule and electricity usage cost. This would impact the LCOH values. Similar to the study conducted on the impact of CAPEX on the LOCH, the impact of efficiency changes on the LCOH is evaluated where the base LCOH is computed using the base efficiency value. Then, for increased efficiency values, the corresponding LCOH values are computed, and the results are depicted in Figure 27. As shown in the figure, as the efficiency increases, the LCOH decreases but the relationship between the LCOH and the efficiency values are non-linear.

Figure 27 | **LCOH vs System Efficiency**

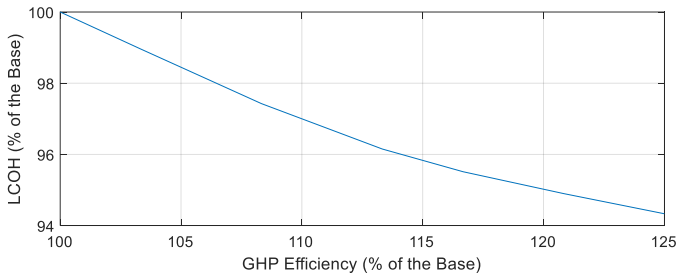

3.5. Feasibility Studies of Distributed Hydrogen Hubs

For this study, distributed hydrogen hubs are aggregated to provide grid services to either bulk transmission systems or LDCs while meeting their local hydrogen demand.

3.5.1. Distributed GHP for Hydrogen Supply and Provision of Grid Services

The main role of hydrogen hubs would be to generate hydrogen, store it, and sell it to consumers as fuel. As such, a hydrogen hub includes PtH, storage, utilization units. The general layout for the integrated hydrogen hubs and power grid is represented in Figure 28.

Figure 28 |Integration of Hydrogen Hubs with the Power Grid

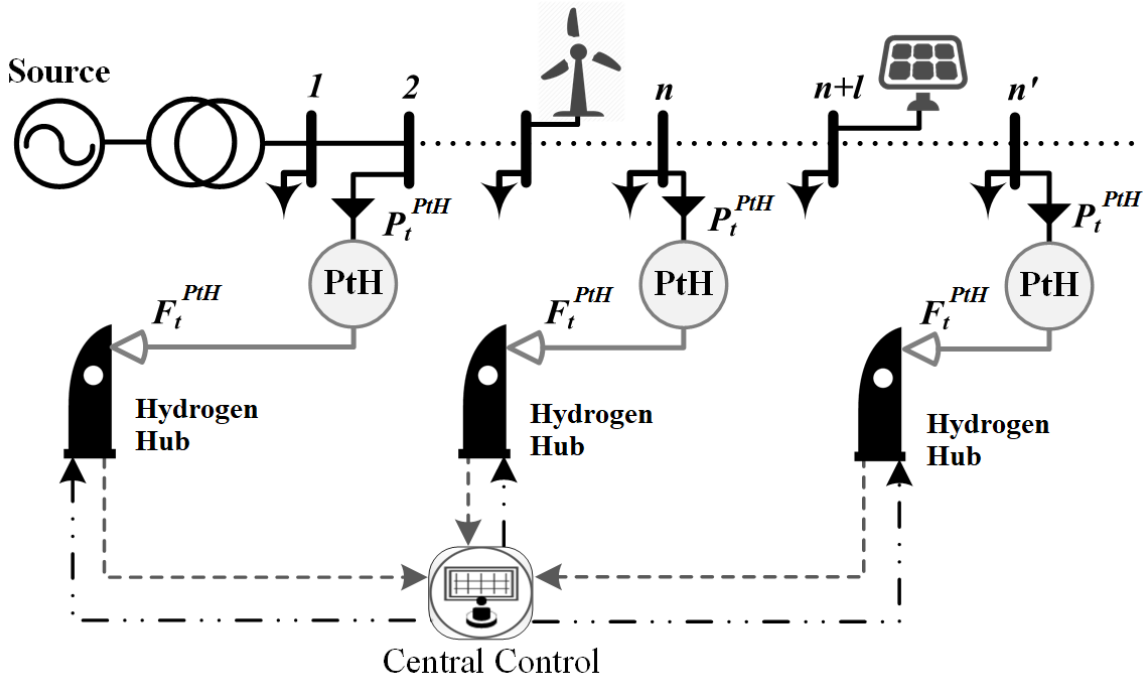

As shown in Figure 28, it is assumed that the PtH unit (i.e., electrolyzer) is placed on site where hydrogen is supplied to the consumer. Several electrolyzers are connected at different locations in the power distribution system that would convert the electricity to hydrogen, which is stored in local storage and supplied to the consumers. In such a set up, there is also a potential for electrolyzers to act as dispatchable loads to provide some services to the power grid. The electrolyzers can participate in various DR programs in the electricity market, thereby achieving a higher revenue level.

3.5.1.1. Participation in the Provision of DR

The economic feasibility of hydrogen hubs for fuel supply to hydrogen consumers and provision of Capacity-Based Demand Response (CBDR) as an ancillary service is investigated. The study has targeted CBDR, which is a promising source of revenue for dispatchable consumers governed by some power system operators in North America including IESO. The CBDR program allows the contracted DR providers to participate in the wholesale market by accepting the DR signals. In particular, the electrolyzers under CBDR are scheduled to take less power from the grid when such an action is demanded by the market operator. The facility would, however, need to be scheduled properly to support consumers since electrolyzers would have to generate less hydrogen when they receive DR signals during peak power demands. Figure 29 shows the 33–bus power distribution system used for studies. As shown in the figure, the power system is integrated with a mix of wind and solar generation, in addition to the distributed hydrogen hubs. The modeling and simulation parameters for the stations are listed in

Table 19.

Figure 29 |33–Bus Power Distribution Test System with High Penetration of Renewable Generation, Integrated with Hydrogen Hubs

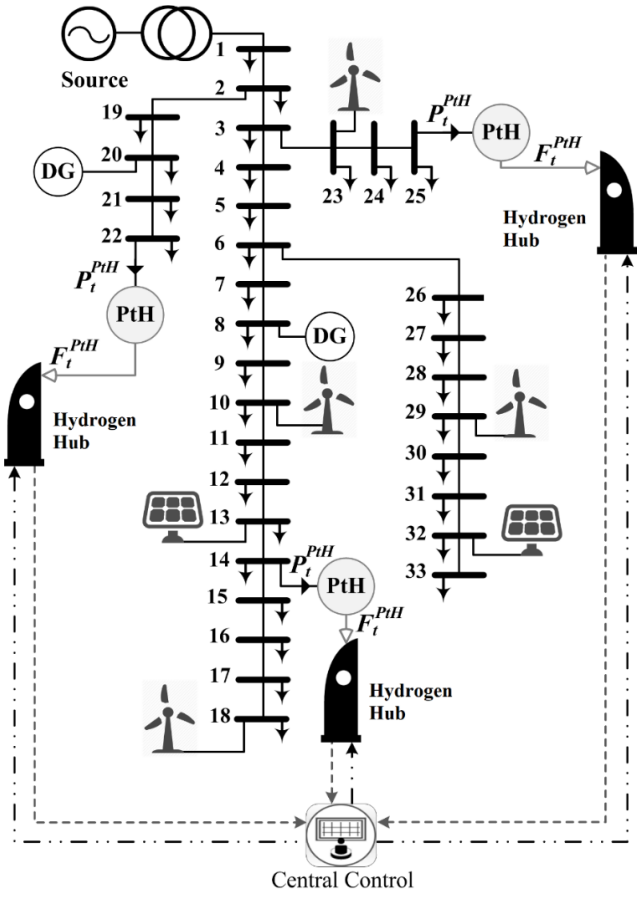

Table 19 |Modeling and Simulation Parameters of the Hydrogen Hubs

$F_h^{max} = 430$ (m^3/h)	$F_h^{min} = 0$
$SOC_h^{max} = 5000$ (m^3)	SOC_h^{min}=10% × SOC_h^{max}
$\Pi^{PtH} = 360$ (m^3/MWh)	$\eta^{PtH} = 60\%$
$\gamma^{Dsp} = 0.006\% \times SOC_{h,t}$	$P_n^{max} = 10$ (MW)
$V_n^{max} = 1.05$ (pu)	$V_n^{min} = 0.95$ (pu)
Total CAPEX = \$2.5 Million	PL = 15 (Year)
C^{PtH}=3% × \$2.5M/(F_h^{max}×8760)	$SOC_t^{CBDR} = 20\% \times SOC_h^{max}$
$DR^{A,Prc} = 30$ (\$/h)	$DR^{U,Prc} = 30$ (\$/MW)
$Prc_h^{H_2,min} = 0.25$ (\$/m^3)	$\beta^{Adj,Prc} = 2$
$R^{Exp} = 13\% \times$ CAPEX	$R^{Dev} = 3\% \times$ CAPEX

CAPEX: Capital Expenditure, PL: Plant Life, and PtH: Electrolyzer

Figure 30 (a) shows the DR signal issued by the market to the central controller of the hydrogen stations. The minimum-allowed SOC, offered CBDR SOC, and the actual SOC are shown in Figure 30 (b)–(d).

Figure 30 | (A) Electricity Market CBDR Signal; Hydrogen Stations SOC at: (B) Station 1, (C) Station 2, (D) Station 3; (E) Aggregated SOC

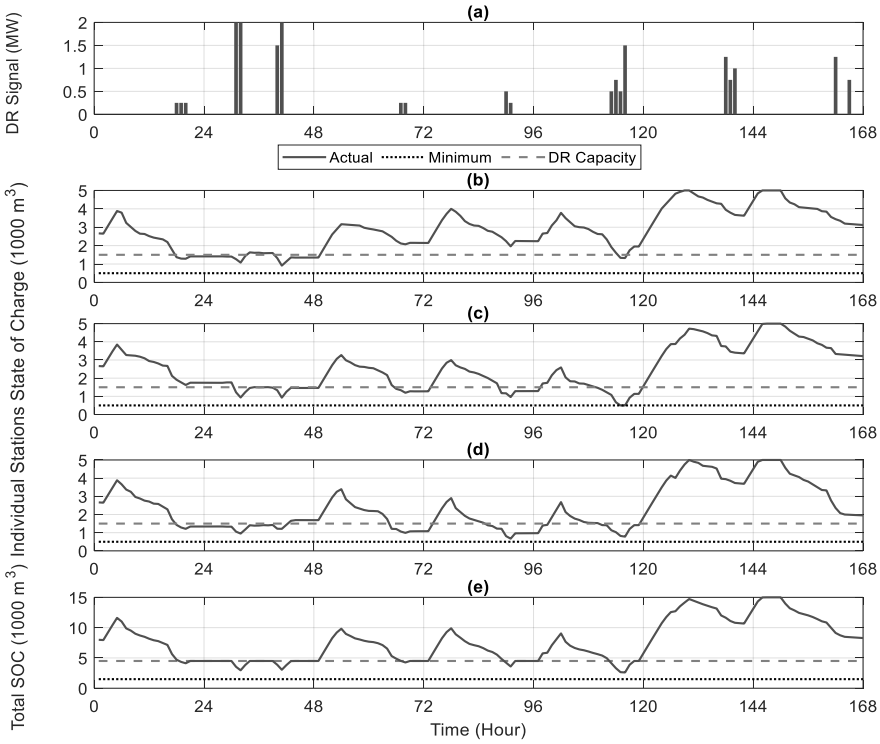

It can be observed that the SOC at each station varies according to the local hydrogen demand at the station. In addition, the CBDR capacity offered to the market is not utilized unless the DR signal is issued; this is to ensure that storage remains ready to follow the signal; i.e., the actual SOC stays above the CBDR capacity. Once the signal is issued, however, the CBDR capacity is released so that the signal can be followed without affecting the hydrogen supply; this can be observed from the figure where the SOC crosses the DR capacity border once the signal is not zero. In such a case, each station would respond differently to the signal depending on the optimal setpoints decided by the optimization problem. Figure 30 (e) shows the aggregated SOC of all the hydrogen stations as a whole, which is offered to the CBDR market. The stations operator receives both the availability payment (via CBDR SOC) and the utilization payment (via operation as per the signal quantity).

The generated revenue is a key factor in every investment, and it has an expected value that should be met. The hydrogen sale price can be considered as a variable in the model that is dynamically adjusted so that the expected revenue could be achieved. The model also profits from contribution to the CBDR program. Therefore, the higher the CBDR prices are, the lower the hydrogen sale prices will be at a given expected revenue value. In such a case, the impact of the CBDR price on the hydrogen sale prices is worth investigating. Accordingly, the required hydrogen sale prices to achieve the

expected revenue of 13% are determined at different prices for the CBDR contribution, and the results are given in Figure 31.

Figure 31 | Average Hydrogen Sale Price at Different CBDR Prices (Note: 1 kg of Hydrogen = 0.08988 × 1 m³)

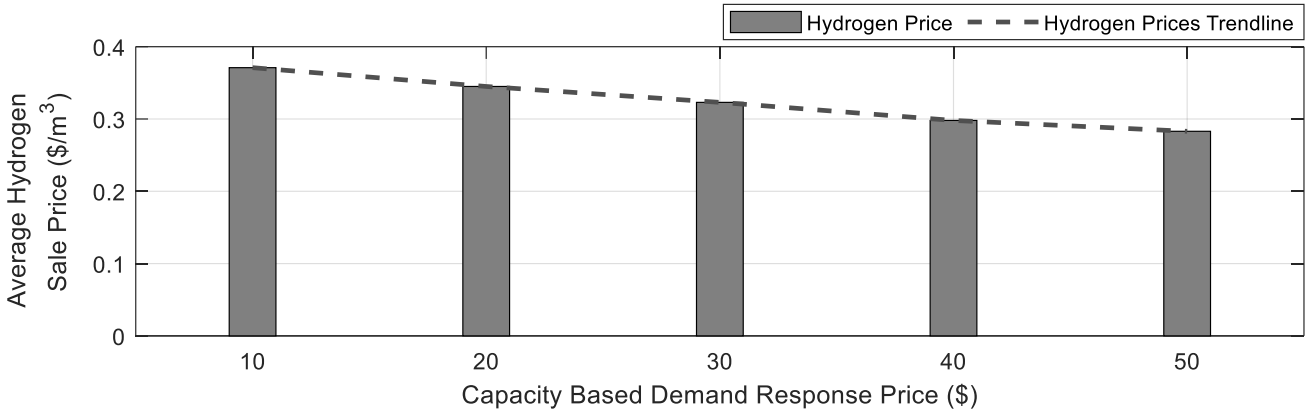

As expected, the hydrogen sale prices decrease as the CBDR price goes higher at a given value for the expected revenue (i.e., 13% of the initial investment per year). This is because the CBDR revenue increases with the increase of its price and, thus, a lower hydrogen price occurs. It is worth noting that hydrogen sale prices in Figure 31 are given in $/m^3, but they can be converted to $/kg, if they are multiplied by 11.2.

The annual revenue, net present value (NPV), internal rate of return (IRR), and the profitability of the investments are computed for the above-mentioned cases and reported in Table 20.

Table 20 | Comparative Revenue and Profitability Values for Hydrogen Hubs

	With CBDR	Without CBDR
Revenue (M$)	1.3	1.126
Profitability (%)	88.14	76.34
NPV (M$)	8.595	6.561
IRR (%)	15.28	12.5

As indicated in Table 20, the participation in the CBDR program enhances the NPV and IRR of the project for the hydrogen stations. In order to investigate the ability of the hydrogen stations to achieve

the expected profit, the profitability of investment needs to be determined. While the expected profit could vary for different projects, it is assumed to be 13% of the CAPEX per year plus the CAPEX value exhausted over the plant life. With the expected CAPEX and plant life, the rate of return of $1.475M per year is expected in order for the plant to be considered profitable. Under the revenue values acquired for all cases, the profitability of the plant is computed and reported in Table 20. The results indicate that the generated revenue is not yet enough to meet the expected profit under either of the cases; however, a higher profitability level is achieved for hydrogen stations with participation in the CBDR program. This would intensify the fact that the stations should be utilized for as many ancillary services as possible in order to become profitable. It should also be noted that as the technology grows, the CAPEX for the stations is expected to shrink; thus, there would be a higher opportunity for the stations to return the expected revenue in the near future.

3.5.1.2. Participation in the Provision of OR

This study investigates the application of distributed hydrogen storage units for fuel supply to consumers and provision of OR services to the grid as an ancillary service. Figure 32 shows a schematic diagram of the framework in which dispersed hydrogen stations are managed by a supervisory scheduling model. Each hydrogen hub contains on-site electrolyzer, fuel cell, and storage units. The optimization problem is executed by the supervisory-based model, and the scheduling setpoints are sent out to the hydrogen hubs. The electrolyzer is in place to both provides hydrogen to consumers and reserve services to the market, i.e., absorbing less as a fictitious supplier or absorbing the surplus energy. The fuel cell unit, however, only aims to provide OR services by supplying energy back to the grid. The required contribution of hydrogen plant to the OR, as an ancillary service, is determined by the market; then, a signal is sent to the market participant, i.e., storage operator. The plant operator would, then, need to follow the signal as received to contribute to the OR market.

Figure 33 shows the operating parameters of the three hydrogen hubs.

Figure 32 | Supervisory Scheduling of Distributed Hydrogen Hubs

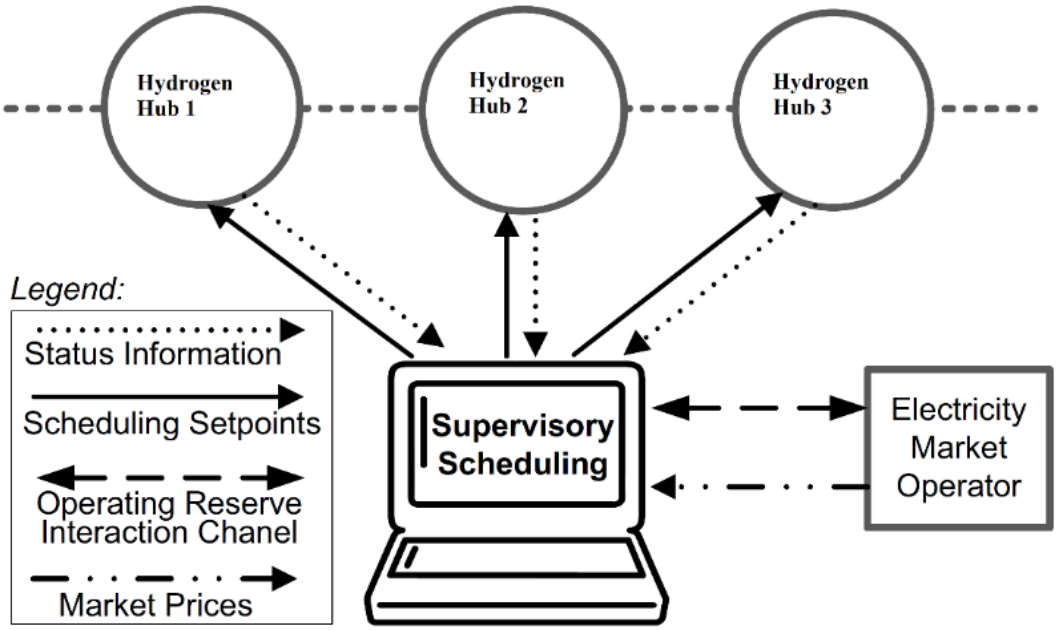

Figure 33 |Operating Parameters of Hydrogen Stations, (A): Electricity Market Prices, (B): OR Signal from the Market, (C): Accumulated Input Powers of All Electrolyzer Units, and (D): Accumulated Output Powers of all Fuel Cell Units

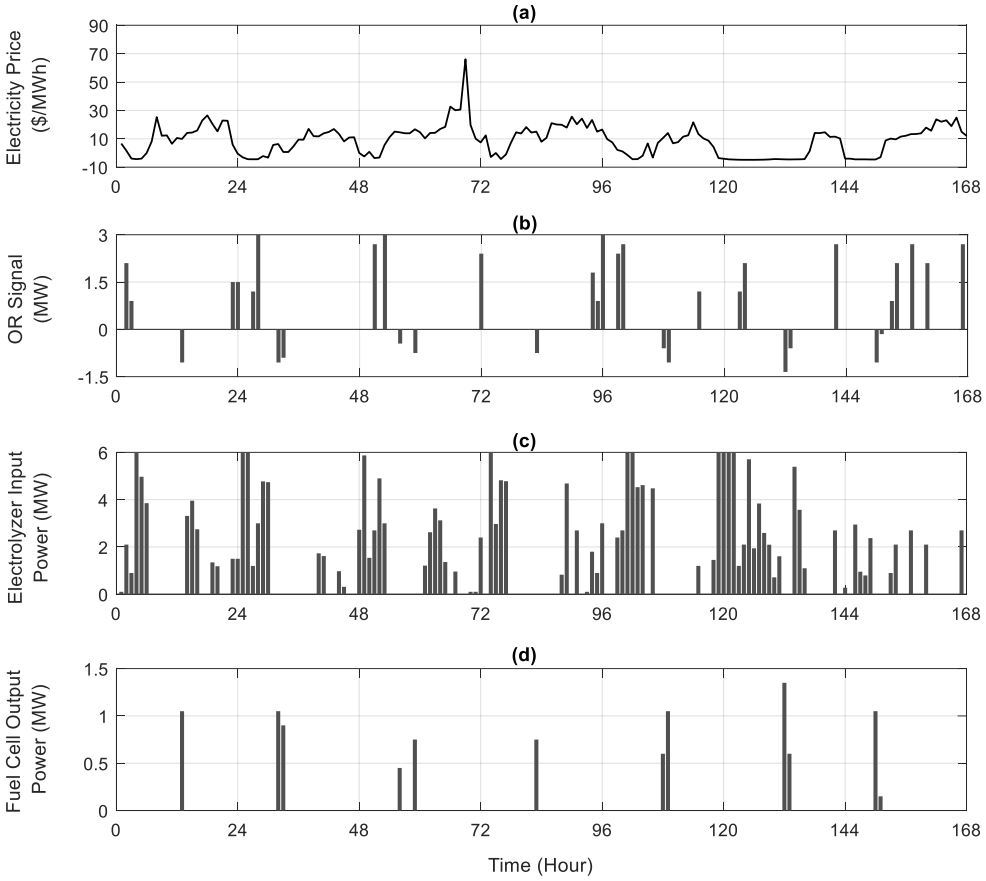

The accumulated operation of the electrolyzer units in Figure 32 (c) is driven by two factors, as follows: (i) negative/lower market prices to minimize the power purchase cost when there is no OR signal; (ii) charging (i.e., positive) quantities of the OR signal to maximize the participation to OR services and accordingly increase the system profit. Besides, the accumulated operation of the fuel cell units is decided by the scheduling model to follow the discharging (i.e., negative) quantities of the signal.

In order to compare the economic viability of the hydrogen hubs under the two cases, various financial parameters are calculated and reported in Table 21.

Table 21 | **Annual Financial Parameters of Hydrogen Hubs Under Two Cases**

Operating Reserve Participation (?)	Gross Income	Net Income	Net Present Value	Break Even Time	Internal Rate of Return	Profitability
No	$528.31 k	$28.31 k	($958.79 k)	14.2 (Years)	0.7%	60%
Yes	$1.27 M	$272.13 k	$724.35 k	11.81 (Years)	3.15%	73%

The capital costs of the plants are exhausted over the plants life in order to determine the gross incomes. In addition, the net present values, assuming the discount rate of 2.5%, and IRR are computed. The break-even time (i.e., the amount of time needed for the generated income to equal the initial capital cost) is also computed. Finally, the system profitability considering the initial cost and expected return is calculated and discussed as elaborated below. The table indicates that the annual gross income is $1.27M when the stations offer OR to the market, while the income is $528.31k when the stations only serve the consumers. In addition, the net income values have come to $272.13k and $28.31k, respectively, as indicated in Table 21. Due to higher gross and net income values, higher net present value and internal rate of return are achieved, and the break-even time shrinks once the facility participates to the OR market, as reported in the table.

It is noteworthy that a higher income when the system offers OR to the market is, in part, expected due to higher capital investment, i.e., electrolyzer plus fuel cell capital costs. When the stations, however, do not participate to OR services, the fuel cell unit is not needed, thereby the capital cost of the electrolyzer is included only. In order to fairly compare the two cases (i.e., considering the capital investments), the profitability of investment needs to be determined, which depends on the expected rate of return, e.g., 5%, 8%, 13% of the capital cost a year. With an expected return equal to 5% of the capital cost per year plus the exhausted capital investment over the plant life, the annual returns of $875k and $1.75M are expected for the electrolyzer only and the electrolyzer plus fuel cell units, respectively. With the gross incomes of $1.27M and $528.31k as mentioned above, the profitability is found to be 73% and 60%, respectively, as reported in the table. As such, a higher profitability is achieved with the OR provision to the market stacked on the benefit from hydrogen sale to consumers. Thus, the contribution of storage facilities in regulation services are, in general, expected to shrink the gap between the current and expected rate of return.

3.6. Feasibility Studies of Hydrogen Hubs to Serve Distribution Grids

GHPs can be utilized to provide various services to LDCs by resolving distribution system issues. The most prominent issues and challenges of distribution systems include voltage regulation, congestion, power losses, and reverse power flow. The application of GHPs for resolving these issues is investigated hereunder. For this study, the GHP facility is sized and rated according to the hydrogen demand in the market as the base application, and its operation is evaluated without and with contribution to ancillary services.

3.6.1. Voltage Regulation

The PtH unit has a unique feature compared to passive voltage regulation devices (e.g., capacitors, reactors, and on-load tap changer in the sense that it can eliminate the voltage rise caused by surplus active power. Similarly, the HfG unit can eliminate the voltage drop issues, caused by lack of active power, via providing the active power to the grid in the vicinity of the consumption area. As shown in Figure 34, the electric energy can be converted directly into renewable hydrogen by the PtH unit during off-peak periods, and then injected to the gas grid. The hydrogen gas can then flow into the gas grid and feed the HfG unit that is connected to another location in the feeder. As shown in the figure, the PtH unit is located in the vicinity of the high renewable generation area; thus, it could eliminate the voltage rise in the system caused by higher renewable generation in one area of the system. Figure 34 shows that the HfG unit can convert the gas into electricity during peak demand periods. As shown in the figure, the HfG unit is located in the vicinity of the high-power demand area; thus, it could eliminate the undervoltage in the system caused by higher power demand in one area of the system. Unlike conventional storage systems (i.e., batteries), energy is not being time shifted in an integrated gas and power grid.

Figure 34|Schematic Diagram for Energy Displacement in the Integrated Gas and Power Grids via Joint Operation of PtH And HfG Units

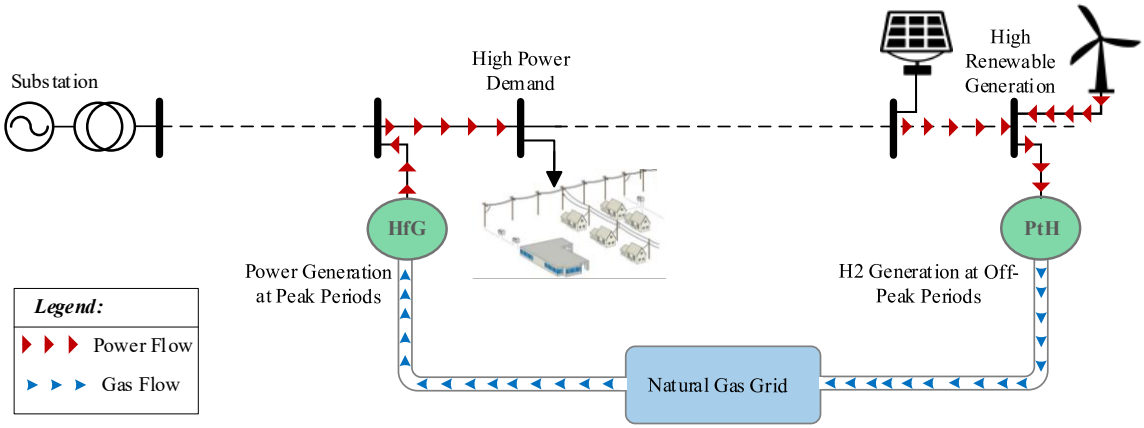

In addition, the system is not impacted by the capacity limitations of a storage system. Such unique features would provide significant advantages for the power grid. It should also be emphasized that the main goal for integrating the PtH unit in the system is to convert the excess/surplus renewable energy-that would otherwise be curtailed-to hydrogen. Once the PtH facility is in place to utilize the surplus energy, it can be operated in coordination with the existing HfG units to regulate the voltage as well. The main motivation for using the PtH-HfG unit for voltage regulation is to increase the functionality of such units via joint applications. The joint operation of the PtH and HfG units under various cases is evaluated, and the results are given hereunder.

In the case where there is no contribution to voltage regulation, referred to as the unconstrained mode, the system behavior is represented without contribution of the PtH-HfG facility to voltage regulation services; i.e., the base case. It is worth mentioning that the power ratings of the PtH and HfG units are selected based on the Active Distribution System (ADS) limitations; i.e., they do not cause voltage rise/drop issues during system normal operation. The cause of the voltage rise and drop are, thus, due to high penetration of Renewable Distributed Generation (RDG) and heavy loading conditions, respectively. Figure 35 and

Figure 36 show the operation of the grids and the PtH-HfG configuration under the unconstrained mode for a week, respectively. As shown in Figure 35 (b) and (c), the gas flow and pressure in the grid are within the specified limits. Nonetheless, the voltage magnitude is out of the normal range as depicted in Figure 35 (a), i.e., 1 +/-5%, as per Range A of the American National Standards Institute (ANSI). The overvoltage is more observable, stemmed from the RDG (mainly wind); because wind units usually generate higher power at off-peak periods when demand is low, causing surplus generation, and thereby causing over-voltages.

Figure 36 (b) and (c) present the operational scheduling of the HfG and PtH units, respectively; where the scheduling depends on the electricity prices shown in

Figure **36** (a).

Figure **36** (b) shows that the HfG unit is operated while the electricity prices are high. In contrast, the PtH unit is operated during low electricity prices as illustrated in

Figure **36** (c). The hourly arbitrage revenue achieved through optimal operation of the PtH and HfG units is represented in

Figure **36** (d). The weekly and annual arbitrage revenue is calculated as $4.73 k and $186.27 k, respectively. One solution to resolve the overvoltage issue in this case, would be curtailment of the surplus RDG; this would, however, undermine the efficacy of renewables and cause considerable financial damages to the investors in RDG units.

In the case where there is contribution to voltage regulation, referred to as the constrained mode, the algorithm schedules the PtH-HfG system towards contributing to voltage regulation. Under this situation, the under/over voltage issues are eliminated as a result of the PtH-HfG operation.

Figure 35 |Gas and Power Grid Operational Parameters Under the Unconstrained Mode; System-Wide (A): Minimum and Maximum Voltage Magnitudes, (B): Maximum Gas Flow, And (C): Minimum and Maximum Gas Pressure

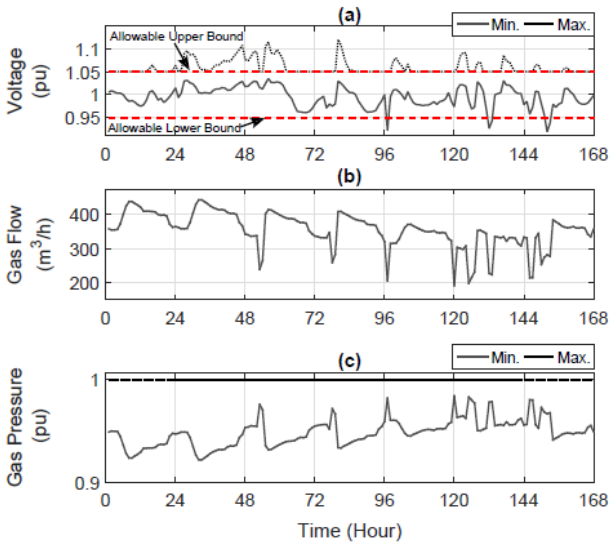

Figure 36 |PtH-HfG Facility Operation Under the Unconstrained Mode; (A): Electricity Price, (B): Generated Power by the HfG Unit, (C): Generated Gas by the PtH Unit, (D): Hourly Arbitrage Revenue of the PtH-HfG Facility

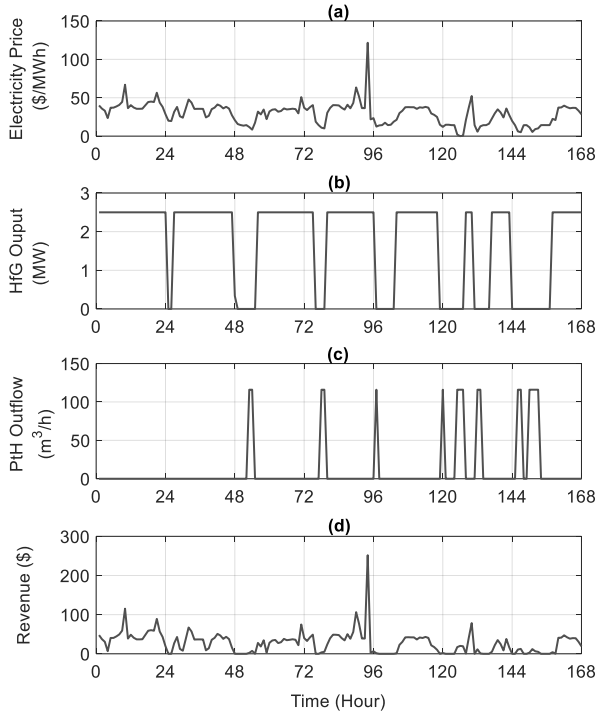

Figure 37 and

Figure **38** represent the grids and PtH-HfG operation in the constrained mode, respectively. Similar to the unconstrained mode, Figure 37 (b) and (c) show that the system-wide gas flow rate and pressure are within the specified limits. Besides, the system-wide minimum and maximum voltage magnitudes are now within the normal range defined by the ANSI code [67], as illustrated in Figure 37 (a). As shown in

Figure **38** (b) and (c), the operation of the HfG and PtH units changes compared to the unconstrained mode (see

Figure **36** (b) and (c)). This change occurs so that the PtH-HfG unit could contribute to the voltage regulation. Comparing the results of both the constrained and unconstrained modes, the following observations can be drawn:

- Once there is an overvoltage issue at a given time step, the PtH unit is operated more in the constrained mode compared to the unconstrained one to absorb the surplus power; which is the reason for the voltage rise. In addition or as an alternative, the HfG unit is operated less to reduce the surplus power, if the HfG operation is not already zero.

- In case of an undervoltage issue at a given time step, however, the HfG unit is operated more in the constrained mode to compensate for the lack of power in the ADS. In such a case, the PtH unit could be operated less to reduce the loading on the ADS, if the PtH operation is not already set to zero. The weekly and annual arbitrage revenue was found to be $4.16 k and $152.51 k, respectively, in this case. The arbitrage revenue is lower in the constrained mode compared to the unconstrained one since the voltage regulation is prioritized to the arbitrage benefit in this case. The annual revenue loss would be 18.12%. The PtH-HfG system will, instead, be financially compensated by the Distribution System Operator (DSO) due to its contribution to the voltage regulation services. The extra voltage regulation benefit in addition to the arbitrage revenue would enhance the overall return on investment in the PtH-HfG system.

Figure 37 |Gas and Power Grid Operational Parameters under the Constrained Mode; System-Wide (A): Minimum and Maximum Voltage Magnitudes, (B): Maximum Gas Flow, And (C): Minimum and Maximum Gas Pressure

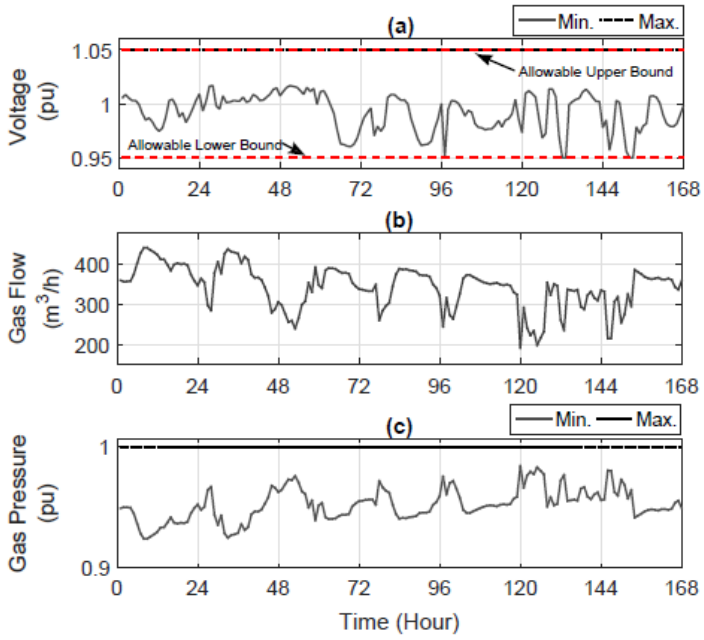

Figure 38 |PtH-HfG Facility Operation under the Constrained Mode; (A): Electricity Price, (B): Generated Power by the HfG Unit, (C): Generated Gas by the PtH Unit, (D): Hourly Arbitrage Revenue of the PtH-HfG Facility

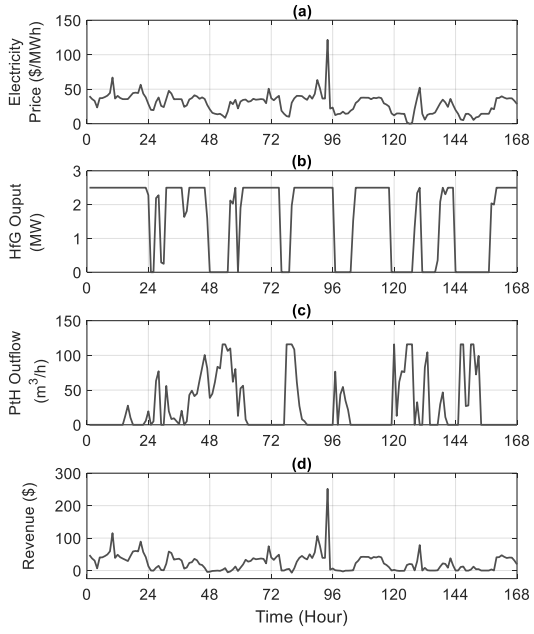

3.6.2. Congestion Management

This section explores how a combination of PtH and HfG can be added to the portfolio of evolving power distribution systems when the motivation is congestion remedy.

In the unconstrained mode when the PtH-HfG unit does not contribute to congestion management, distribution feeder capacity can go up to the maximum value from the nominal one. The operational parameters of the gas and power distribution grids as well as the PtH–HfG facility are studied for one year. However, in order to represent the detailed operation of the grids and the facility, results are shown in Figure 39 and

Figure **40** for one week (out of the studied year) on an hourly basis. The system-wide maximum/minimum parameters are presented for the grids; i.e., the maximum/minimum quantities in the entire system at each time interval. If these quantities are within the allowable limits at each time interval, the operation of the entire system would be acceptable. As shown in Figure 39 (b)-(d), bus voltages magnitudes, gas flow rates in pipelines, and gas pressure values in gas nodes are within the limits.

Figure 39 | Gas and Power Distribution Grid Operational Parameters under the Unconstrained Mode; (A): Maximum Congestion Power in the Distribution Feeder, (B): System-Wide Minimum/Maximum Voltage Magnitudes, (C): System-Wide Maximum Gas Flow, and (D): System-Wide Minimum/Maximum Gas Pressure

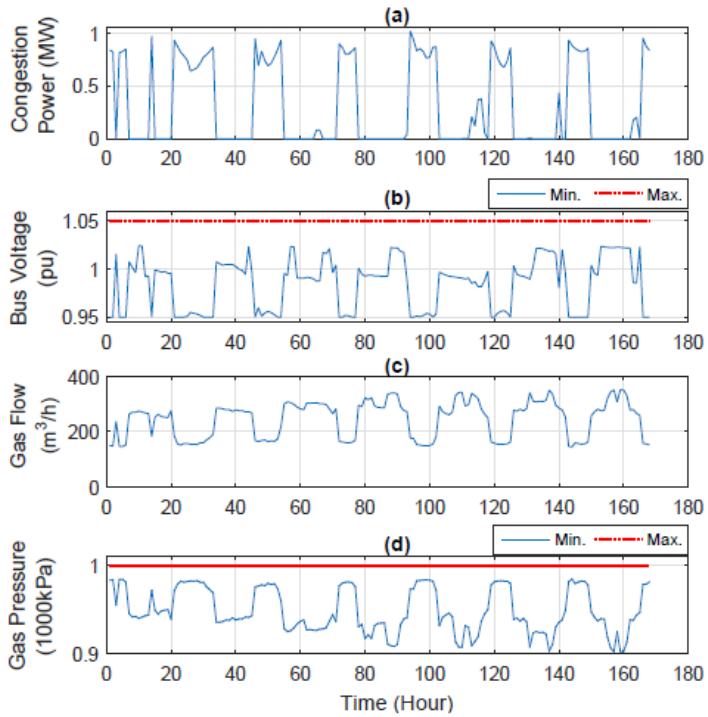

Figure 40 | PtH-HfG Operation under the Unconstrained Mode; (A): Electricity Price, (B): Output Power of the HfG Unit (MW), (C): Gas Outflow of the PtH Unit, (D): Hourly Revenue of the PtH-HfG Facility

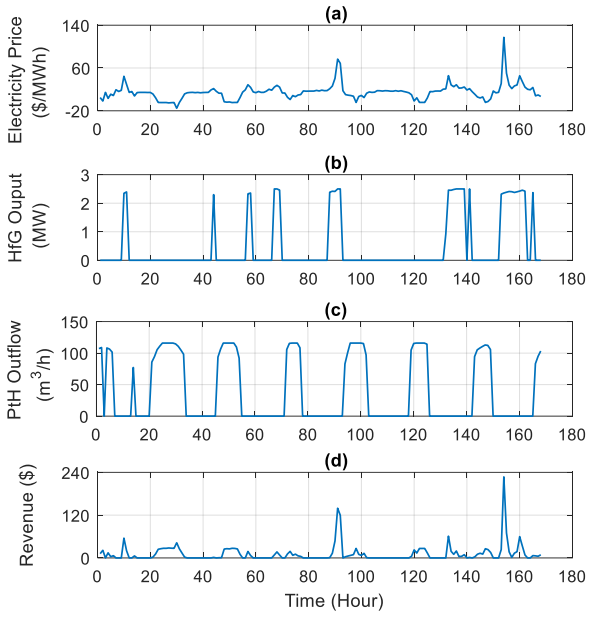

Figure 39 (a) shows the maximum amount of feeder congestion. As depicted in

Figure **40** (a)-(c), HfG and PtH units operate when the electricity price is high and low, respectively, to utilize the electricity price arbitrage. The hourly revenue of the PtH-HfG facility is depicted in

Figure **40** (d), indicating that the revenue at different instances depends upon the prices. The weekly arbitrage revenue is calculated as $1.97 k, i.e., the weekly Base Revenue (BREV). Since the facility is operated in the unconstrained mode, it is not contributing to Distribution System Congestion Management (DSCM) at this stage. As such, it would operate solely towards utilizing the price arbitrage in the integrated power and gas distribution system. The facility, in this case, would achieve the maximum available energy price arbitrage benefit, but no extra profit for contribution to DSCM.

In the constrained mode, when the PtH-HfG unit contributes to congestion management, the upper bound of the feeder capacity cannot go any further than the nominal one unless the PtH–HfG unit cannot contribute to the DSCM. As illustrated in Figure 41 (b)–(d), the bus voltage magnitudes, gas flow rates in pipelines, and gas pressure values in gas nodes are within the limits.

In addition, Figure 41 (a) shows that the congestion is now zero at all instances. As depicted in Figure 42 (a)–(d), the HfG and PtH units operate to utilize the energy price arbitrage. The weekly arbitrage revenue in this case is calculated as $1.54 k, achieved under the unconstrained mode.

Figure 41 | Gas and Power Distribution Grid Operational Parameters under the Constrained Mode; (A): Maximum Congestion Power in the Feeder, (B): System–Wide Minimum/Maximum Voltage Magnitudes, (C): System–Wide Maximum Gas Flow, and (D): System–Wide Minimum/Maximum Gas Pressure

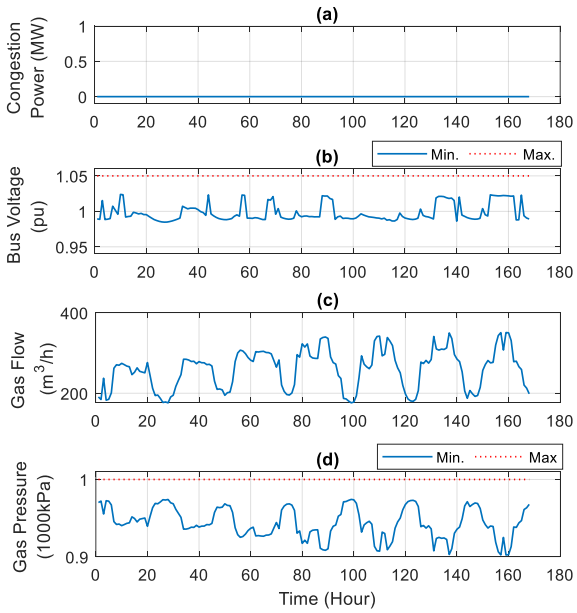

Figure 42 | PtH–HfG Operation under the Constrained Mode; (A): Electricity Price, (B): Output Power of the HfG Unit (MW), (C): Gas Outflow of the PtH Unit, (D): Hourly Revenue of the PtH–HfG Facility

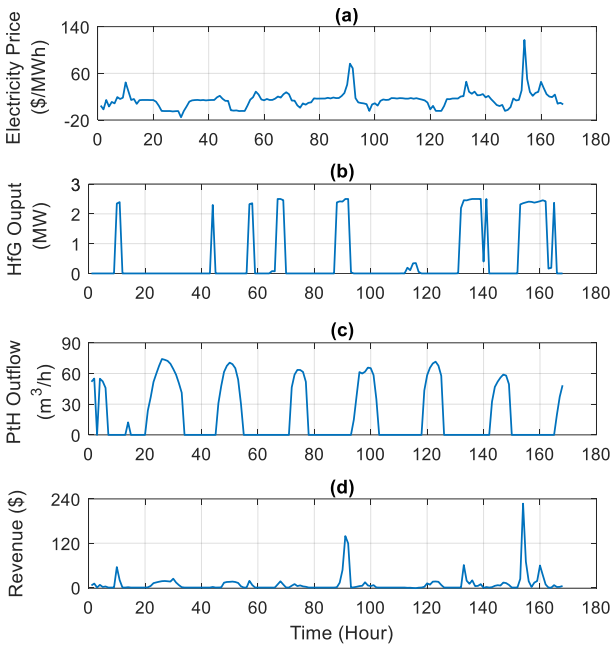

As shown in Figure 39 (a), there is feeder congestion in several instances. In addition, as depicted in Figure 39 (b), the system-wide minimum voltage reaches down to the lower limit of 0.95 pu mainly during the congestion periods; due to the considerable voltage drop over the feeder impedance at the time of congestion.

Figure 41 (a) and (b), however, show that the congestion is zero, and the system-wide minimum voltage is fluctuating around 1 pu; the voltage value in this case, would not approach the lower limit of 0.95 pu. The voltage profile is improved in general as a result of congestion relief. The system-wide maximum voltage, on the other hand, is set to the upper limit of 1.05 pu under both cases of unconstrained and constrained. It is also noteworthy that the voltage values are within the allowable limits as per Range A (i.e., +/-5%) of the ANSI. Besides, as shown in Figure 39 (c) & (d) and Figure 41 (c) & (d), there are only slight differences in the gas grid operation under the two cases. Such an operation is in the favor of the integrated system since the feeder congestion is being alleviated with the minimum impact on the gas distribution grid. It is worth mentioning that the operation of the power and gas grids within the acceptable limits would indicate that the optimal solution is feasible.

Figure 40 (a) and Figure 42 (a) show that the same electricity profile is used to fairly compare the two cases. Figure 42 (b) shows that the HfG unit has a slightly higher operation in the constrained mode to relieve the feeder congestion by providing more local power to the grid. Besides, Figure 42 (c) and

Figure **40** (c) demonstrate that the operation of the PtH unit is limited by the scheduling algorithm to around 75 and 120 (m^3/h), receptively. The lower operation of the PtH facility in Figure 42 (c) is to contribute to the congestion relief by absorbing less power from the grid.

The PtH-HfG facility loses a portion of its arbitrage revenue as a result of the contribution to DSCM. This section aims to analyze the operation of the facility on a monthly basis for a full year. Figure 43 (a), (b), and (c) show the contribution of the facility to DSCM, arbitrage revenue, and arbitrage revenue loss, respectively. As depicted in the figures, on a monthly average, the facility makes around 100MWh contribution to DSCM; whereas the monthly revenue shortfall compared to the BREV is $0.69 k, i.e., 4.68% loss.

The annual arbitrage revenue in this case equals $168.82 k; whereas, the one under the unconstrained mode equals $177.11 k, i.e., the BREV. Thus, the PtH–HfG facility could remedy the congestion with only a very small loss in the base revenue (i.e., 4.68%). The facility in this case is eligible to be financially compensated by the DSO due to its contribution to DSCM. The extra profit, on top of the arbitrage benefit, improves the total return on investments. An index is used that would quantify the contribution of the PtH-HfG facility towards the congestion management, i.e., DSCM index. This index is numerically computed, and the results are represented in Figure 44 on a monthly basis.

Figure 43 | (A): Contribution of the PtH–HfG Unit to DSCM, (B): Generated Arbitrage Revenue and Arbitrage Revenue Shortfall Compared to BREV, and (C): Percentage of the Arbitrage Revenue Loss

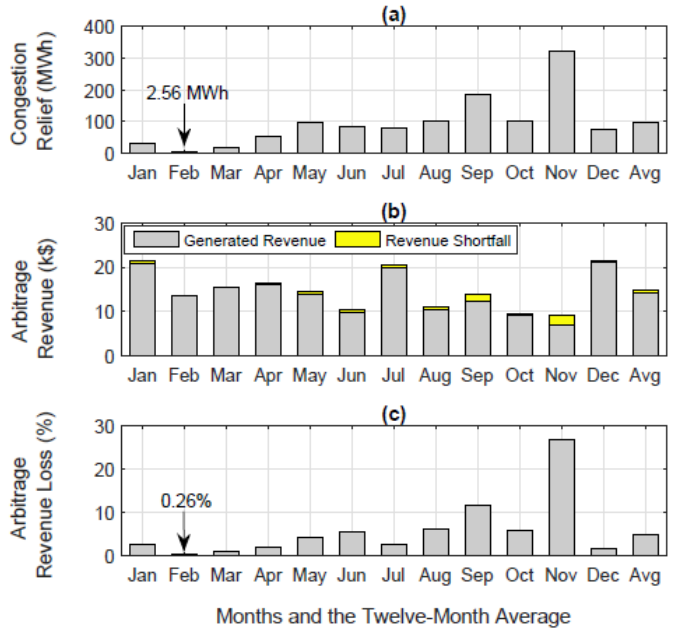

Figure 44 |Monthly and Annual DSCM Index

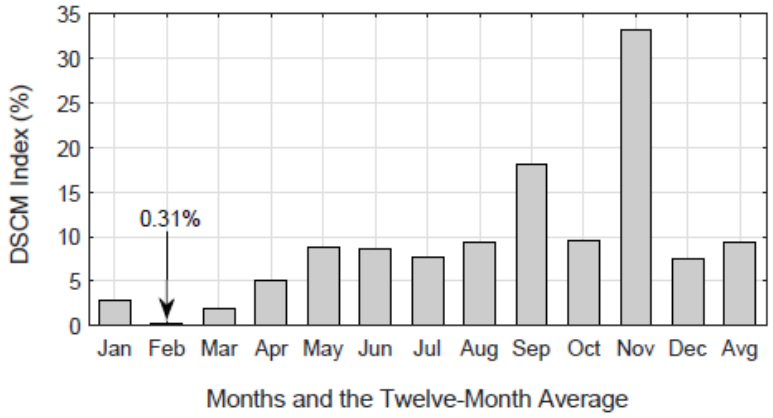

As shown in this figure, the index takes different values at different months. The minimum value of the index is set at 0.31% in February, while the maximum value of 33% occurs in November. The index would have an average value over the year equal to 9.4%. Moreover, it can be observed that there is a strong correlation between the index values and the MWh contribution indicated in Figure 43 (a).

3.6.3. Power Loss Alleviation

In this section, two case studies are given to demonstrate the detailed operation of the PtH-HfG facility for loss alleviation below:

- **Case 1:** No contribution to loss reduction, thereby exploiting the arbitrage benefit only, i.e., the base case.
- **Case 2:** Maximum contribution to loss reduction, in addition to exploiting the arbitrage benefit.

The problem is solved for a complete year, but the snapshot for one week out of the studied year are presented here for the detailed studies. Figure 45 (b) shows that the power losses are alleviated by 23.76MWh on average in Case 2 compared to Case 1.

Figure 45 | Monthly & Annual Average Operation for Cases 1 & 2, (A): Wind Generation/Load Demand Profile, (B): Power Losses, (C): HfG Operation Schedule, (D): PtH Operation Schedule, and (E): Arbitrage Revenue

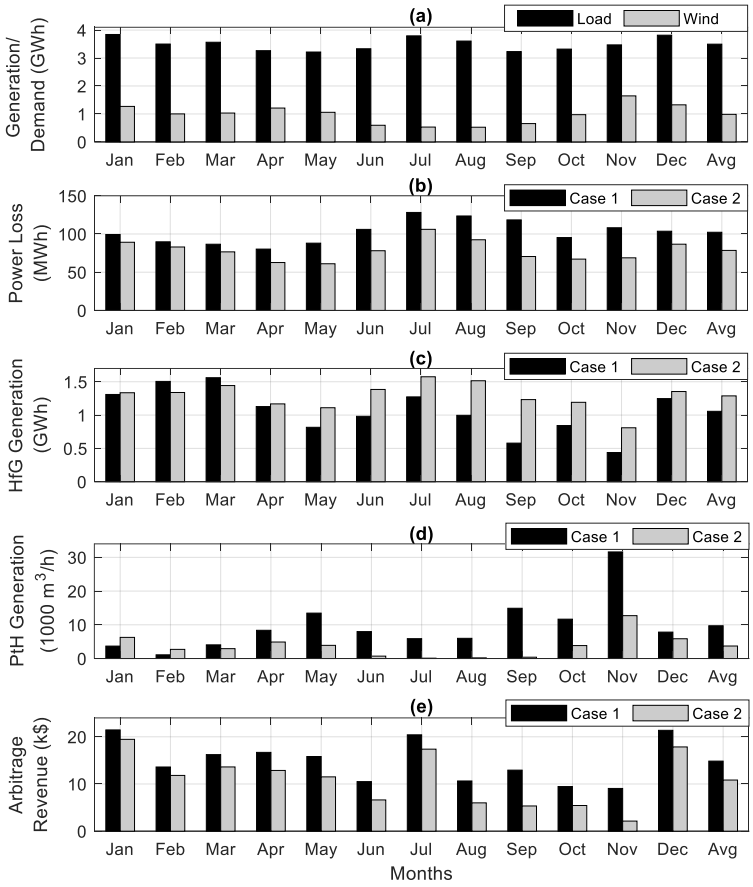

As per Figure 45 (c), in several months and on average, a higher operation is achieved by the HfG unit in Case 2 (21.85% higher on average) to reduce the system losses; while in two months, a lower operation is achieved by this unit. Besides, the PtH unit is operated less under Case 2 in most moths (61.81% less on average), to contribute to the loss alleviation; while in two months it has operated more as shown in Figure 45 (d). Figure 45 (e) shows that the arbitrage revenue under Case 2 is lower than the one compared to Case 1 ($10.84 k versus $14.85 k on average) due to the loss reduction contribution.

Figure 46 (a) shows the loss alleviation while (b) represents the arbitrage revenue shortfall resulted from contribution to loss reduction.

Figure 46 |Monthly & Annual Average Operation Data, (A): Percentage of Power Loss Alleviation, and (B): Percentage of Arbitrage Revenue Shortfall

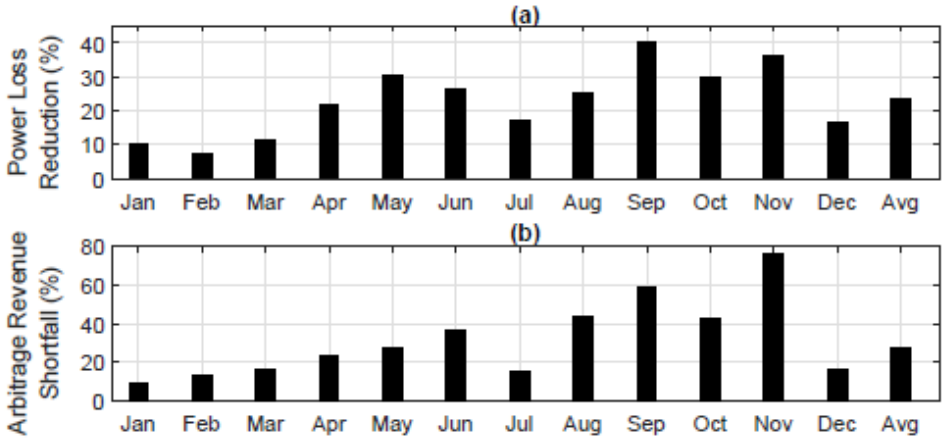

Clearly, there is a strong correlation between the loss reduction and the arbitrage shortfall. During operation for the loss alleviation, the facility has to be operated less than optimality towards the arbitrage benefit. As such, the higher the loss reduction contribution is, the more the arbitrage shortfall would be. The loss reduction is variable at different months from minimum value of 7.54% in February to the maximum value of 40.45% in September; while on an annual average, the PtH–HfG facility reduces the system losses by 23.22%. The arbitrage revenue shortfall, on the other hand, is minimum in January (i.e., 9.3%) and maximum in November (i.e., 76.37%); while, on an annual average, the revenue shortfall is set at 27%. The required charge for loss reduction would need to be $168.9 per MWh loss reduction contribution in order for the revenue shortfall to be compensated. Given the higher rate paid to the facility for contribution to the loss reduction, the overall profitability of investment is boosted. In order to assess the overall profitability, the expected rate of return is to be determined which could vary for each project depending on its risk profit, 5%, 8%, 13%. In this study, a return on investment equal to 13% of CAPEX per year plus the recovery of the CAPEX over the life span of the plant is expected in order for the plant to be profitable. For the CAPEX and life span of $1.7 Million and 20 years, respectively, this would end up in a total expected return as $306 k per year. The actual profit in percentage of the aforementioned expected value is computed as the profitability of investment as illustrated in Figure 47 for the two case studies. The figure shows that the overall profitability of investment in the PtH–HfG facility is boosted in all months under Case 2 as a result of the contribution to the loss reduction.

Figure 47 | **Monthly and Average Profitability of PtH–HfG under Cases 1 & 2**

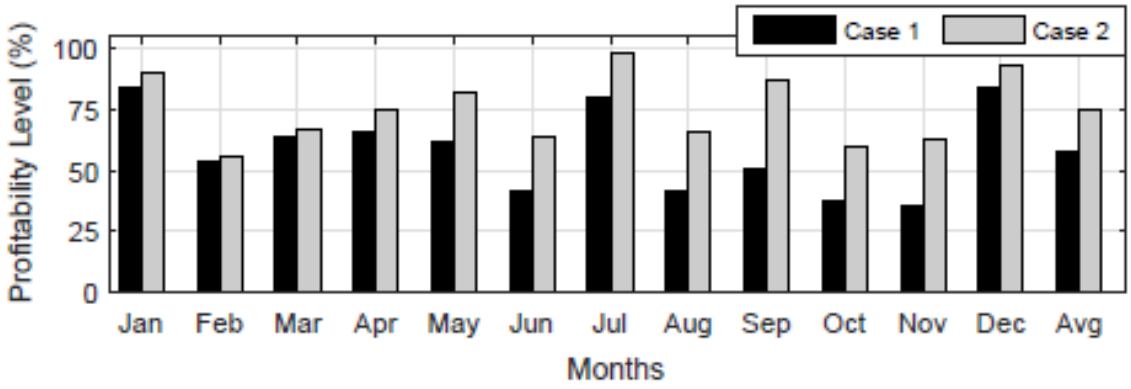

On an annual average, the facility achieves a profitability of 75.1% under Case 2, while it obtains only 58.2% profitability under Case 1. Hence, the joint scheduling of the PtH–HfG facility for multiple objectives could boost the overall profitability, thereby inspiring the private investment more to own and operate such facilities, while also serving the grid via regulation services. In order for the facility to reach to the full profitability level, however, higher compensation would be required, i.e., $617.25 per MWh loss reduction. Nonetheless, as the technology materializes, the facilities with lower CAPEX are expected to emerge, thereby requiring less compensation for the regulation services in order to become fully profitable.

3.6.4. Reverse Power Flow Management

Reverse power flow in distribution systems usually stems from the extra renewable generation. In this section, it is indicated how PtH units could be operated to eliminate the surplus renewable generation in the grid by converting it into the hydrogen. The generated hydrogen is then injected to the gas grid for some useful operations. HfG units are scheduled for less operation when their generation causes reverse power flow. They also support the grid during peak demand by providing local generation as distributed energy resources.

Two case studies are created to reveal the efficacy of the algorithm:

- **Case 1:** The PtH–HfG facility does not contribute to the management of reverse power flow.
- **Case 2:** The PtH–HfG facility provides reverse power flow management services to the power system.

The gas and power grids' operational parameters under the two cases are illustrated in Figure 48.

Figure 48 | System-Wide Operational Parameters of Power and Gas Grids under Case1: No Contribution & Case 2: Full Contribution Towards Reverse Power Management; (A)

Reverse Power; (B) Minimum Voltage Magnitude; (C) Maximum Voltage Magnitude; (D) Maximum Gas Flow; and (E) Gas Pressure

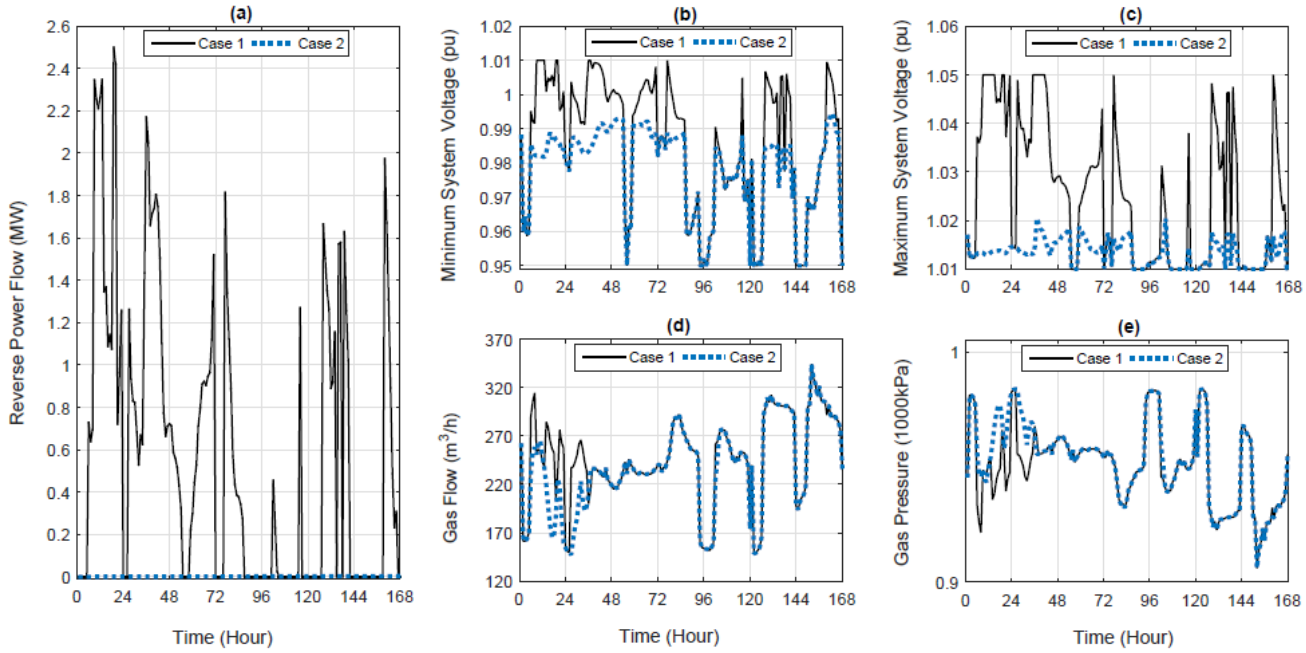

As depicted, Figure 48 (a) shows that the reverse power flow under Case 2 has become zero while there is considerable reverse power flow under Case 1. Figure 48 (b) and (c) illustrate the system-wide minimum and maximum voltage magnitudes. In both cases, the voltage magnitude is within the limit (i.e., +/-5%), as per Range A of the ANSI. However, the maximum system-wide voltage is lower under Case 2 compared to Case 1. This indicates that there would be less voltage rise under Case 2, due to zero reverse power flow in the system. Maximum natural gas flow in the gas grid is shown in Figure 48 (d). While there is a small difference in the flow patterns, the gas flow under both cases is within the limit. In addition, the gas pressure shown in Figure 48 (e) is within the acceptable limit. It is worth noting that the system-wide minimum gas pressure is depicted in Figure 48 (e), while the system-wide maximum pressure is computed at 1000 kPa over the studied period.

Figure 49 shows the operational parameters of the PtH and HfG units under the two cases.

Figure 49 |Operation of HfG and PtH Units under Case 1: No Contribution & Case 2: Full Contribution of the Facility Towards Reverse Power Management; (A) Electricity Price; (B) Output Power of HfG Unit; (C) Outflow Gas of PtH Unit; (D) Arbitrage Revenue Utilized by the PtH-HfG Facility

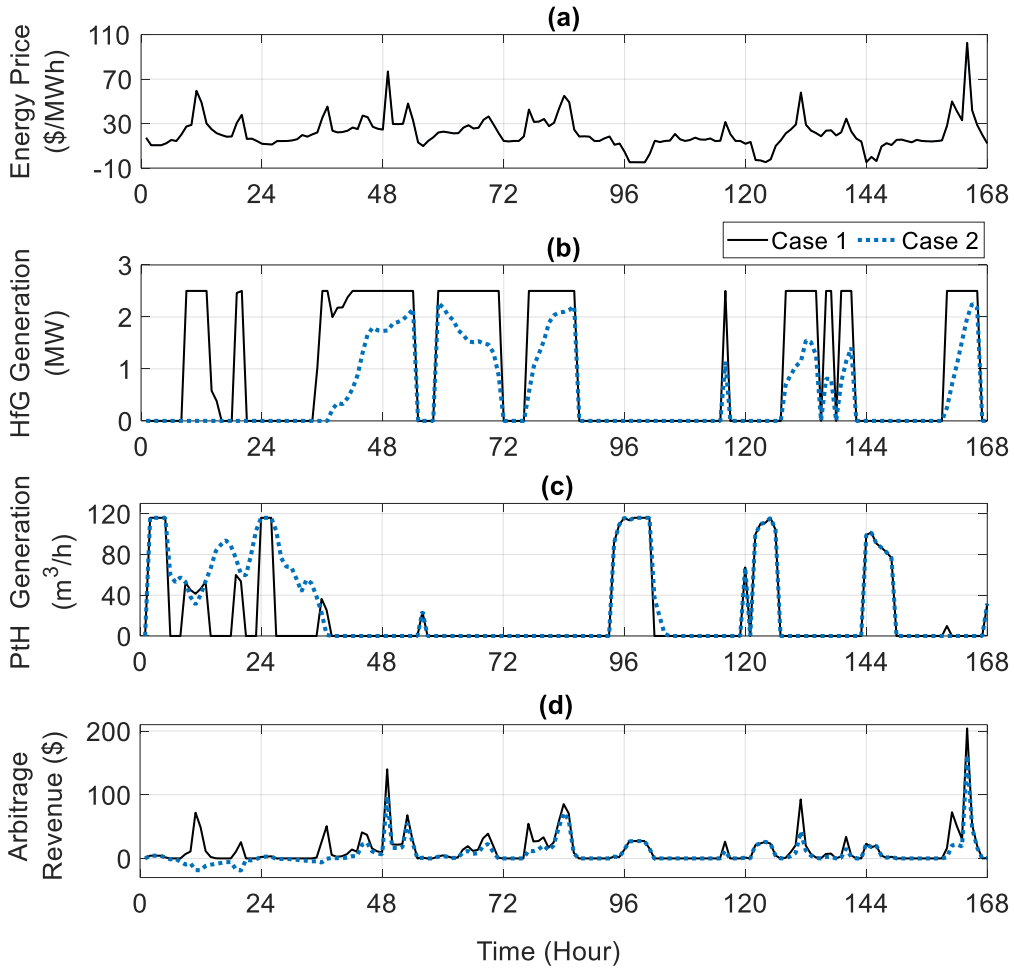

Figure 49 (b) and (c) indicate the HfG and PtH generation, respectively. Under Case 1, the PtH unit operates at lower electricity prices, while the HfG unit works at higher prices to utilize the energy price arbitrage. Under Case 2, however, the operation of the PtH and HfG units are affected and departed partly from the optimal fashion. Figure 49 (d) shows that the arbitrage revenue under Case 2 is lower in some instances compared to Case 1. The weekly arbitrage revenue is calculated as \$2.31 k and \$1.23 k under Cases 1 and 2 respectively. The arbitrage revenue under Case 1 is considered as the base value for the remainder of the studies in this study.

4. Conclusion and Recommendations

This work presents a survey on green hydrogen production and storage technologies. Different technologies for generation of hydrogen are discussed and compared. The technical and economic opportunities and challenges for integration of hydrogen storage technologies with power systems are discussed. The application of GHPs for provision of ancillary services to the grid is investigated, and their technical and economic benefits are discussed. In addition, the application of GHPs for serving LDCs via resolving distribution grid issues is discussed. The main conclusions of this work are given in the following:

- Primarily, there are three electrolyzer technologies (Alkaline, PEME, and solid oxide electrolyzer cell) with different performances.

    - The alkaline water electrolyzer is a mature technology and has a stack lifetime (60,000 operating hours), the lowest degradation rate (0.1%/1000 hr.), and a low electricity consumption (48-53 kWh/kg H_2). It also has the widest capacity range (1-700 Nm^3/hr.) and the lowest CAPEX ($500-$1400/kW), but it offers a low efficiency in the range of 63-70%. It also offers a low response time up to 10 minutes and slow ramp rate of around 0.2-2% per second.

    - The PEME is at the commercial stage and presents a stack lifetime of 50,000-60,000 operating hours, degradation rate of 0.2%/1000 hr, and electricity consumption of 46-55 kWh/kg H_2. It has a low-capacity range (1-100 Nm^3/hr) and a relatively high CAPEX ($1100-$1800/kW). It offers an efficiency of around 60-72%, a very fast start time of up to 1 minutes, and a ramp rate of 100% per second.

    - The solid oxide electrolyzer cell is at the demonstration stage and has the highest efficiency (74-86%), but it operates at a higher temperature range (700-900°C) and introduces a shorter stack lifetime (<20,000 operating hours). It comes with the highest degradation cost (1.9%/1000 hr), and the electricity consumption of 40-45 kWh/kg H_2, provided that a heat source is made available. It offers the lowest capacity (1-10 Nm^3/hr) and the highest CAPEX ($2800-5600/kW).

- The LCOH varies depending on the geographical locations and the applications. The studies conducted in this report suggest that for Ontario, the LCOH would be in the range of $8 to $11/kg of hydrogen.

- The offered clean hydrogen ITC in Canada can reduce the LCOH depending on the CEH. The LCOH can be reduced by up to around 4% for green hydrogen which is produced using RES.

The recommendations and key findings are summarized in Table 22.

Table 22 |Recommendations and Key Findings

Point of interest	Recommendations	Findings
Choice of electrolyzer technology (PEM, Alkaline, or hybrid)	Choose technologies based on project objectives	Hybrid solutions are suitable for hydrogen generation and serving the grid
Hydrogen pricing to meet profitability target	Consider "dynamic pricing"	Hydrogen price range will vary based on targeted profitability
Electrolyzers conversion efficiency varies with loading	Consider appropriate model of conversion efficiency in the design	Appropriate modeling improves the accuracy of results by 10-15% and results in around 25% reduction in LCOH
Elevated LCOH for an application	Consider using GHPs for joint applications and seek incentivization of the technologies	Cost savings depend on the application and compensation/incentivization
Electrolysis manufactures provide typical stack design: membrane thickness, area, pressure	Inquire about customizing the electrolyzer design parameters to best fit the application	Proper electrolyzer designs can result in around 20% reduction in the LCOH
Utilization of BESS to improve the GHP performance and LCOH	Incorporate BESS in the GHP design	BESS can result in more efficient performance of the GHP and up to around 10% reduction in the LCOH

5. Lessons Learned

The main lessons learned in this study are summarised as follows:

- While accurate modeling and simulation of GHPs can take more time and effort than simplified modeling, the effort can result in more accurate simulation results.

- The choice of technology for electrolysis can impact the accuracy of the studies. As such, it is important to select the technologies depending on the application that the GHP is intended to support.

- The elevated CAPEX and moderate efficiency of a GHP are obstacles to its widespread adoption. To reveal its true value, GHPs should be utilized for multiple applications and their contributions to grid services need to be compensated by policy makers and regulatory bodies.

- Repurposing existing gas grid infrastructures for storing and using hydrogen can be considered as a great alternative to other forms of storage, such as compressed gas and liquification.

- The offered clean hydrogen ITC in Canada can help marginally reduce the LCOH depending on the CEH. Yet policy makers and regulatory bodies need to continue supporting the GHP deployment via further incentivization and promote the hydrogen demand increase. In the future, however, it is expected that PtH and HtP technologies become more efficient and cost effective.

6. Next Steps

As the next steps, researchers and industry experts need to collaborate to develop novel solutions to tackle various challenges for integration of GHPs that are yet to be addressed including:

- Higher cost of clean hydrogen compared to existing fossil-based fuels

- Technological uncertainties

- Policy and regulatory issues

- Infrastructure issues

- Supply and demand issues (chicken-and-egg)

- Issues related to mass deployment of GHPs that could alter the existing electricity market programs and initiatives in Ontario, and thus, impact the flexibility and operability of the entire system.

7. Appendix – Mathematical Modeling for Design and Operation of GHPs

7.1. PEME Technology

This section presents a detailed model of PEME and analyze its operation characteristics. The core of the optimization problem contains two main interdependent modules (Cost minimization module, and PEME model), where PEME efficiency is determined by its model based on the PEME' parameters sent by the minimization module. This data exchange is repeated in each optimization iteration. The optimizer core is inputted by the pre–specified hydrogen demand profile and historical data for the grid carbon intensity and the electricity price. To account for the uncertainty of the electricity price, the historical data is used to get a normal Probability Distribution Function (PDF) for each hour in the time period under study. The electricity price PDF functions are discretized into multiple states, and the probability of each state is calculated. Then Monte Carlo cases are generated with their probabilities. The probability of each case is calculated as the average of the hourly probability of the electricity prices in that case given as:

$$\rho_{ElecPrice}^{mc} = \frac{1}{T}\sum_{t=1}^{T}\rho_{ElecPrice}^{mc,t} \forall\ mc \in N_{MCS} \quad (1)$$

The optimizer core is also inputted by the maximum available power from RES and/or the grid to be converted into hydrogen at each time step, which is determined based on the RES generation profile and the grid constraints. Assuming that the GHP is connected to a power transmission system, the objective function of the GHP design optimization problem is formulated to minimize the LCOH as follow:

$$Min \quad \left(\frac{CAPEX + \frac{\sum_{mc=1}^{N_{MCS}} \rho_{ElecPrice}^{mc} OPEX(mc)}{\sum_{mc=1}^{N_{MCS}} \rho_{ElecPrice}^{mc}} + C_{Deg}}{\sum_{t=1}^{T} L_d^t} - \Upsilon \right) \tag{2}$$

The LCOH function consists of four components: CAPEX, weighted average of OPEX, degradation cost (CDeg), and clean hydrogen subsidy represented by Y. CAPEX is a function of the power ratings of the PEME, power converter, and compressor ratings, as well as the BESS and HS capacities expressed as follows:

$$\begin{aligned} CAPEX = {} & P_{elz}^{rate} C_{elz} + P_{BESS}^{rate} C_{BESS} + \\ & P_{Conv}^{rate} C_{Conv} + P_{Cmp}^{rate} C_{Cmp} + E_{HS} C_{HS} \end{aligned} \tag{3}$$

The OPEX of each electricity price case is the summation of the hourly electricity and operational costs given as:

$$\begin{aligned} OPEX(mc) = {} & \sum_{t=1}^{T} P_{grid}^t Price_{elec}^t(mc) + L_{elz}^t O_w + \\ & L_{HS}^t O_{HS} + P_{elz}^t O_{elz} + P_{Cmp}^t O_{Cmp} \end{aligned} \tag{4}$$

The electricity price of the produced hydrogen depends on the agreement between the grid and GHP operators. In this work, the electricity price is assumed to follow a PPA when the GHP produces hydrogen from RES. Otherwise, the price is determined based on the applied electricity market rules. In both cases, GOFs such as delivery charges are added to the costs of electricity. Hence, the electricity price at each time step t could be expressed as follow:

$$Price_{elec}^t = \begin{cases} PPA: Fixed\ PPA\ Price + GOF \\ Grid: Hourly\ Generation\ Price + GOF \end{cases} \tag{5}$$

The hourly electricity cost of the GHP depends on the total power imported from the grid (P^t_{grid}), which is the sum of power consumed by the PEME, compressor, and BESS. The total imported power can be expressed as:

$$P^t_{grid} = P^t_{elz} + P^t_{Cmp} + P^t_{BESS} \tag{6}$$

The compressor power is a function of the PEME cathodic pressure, hydrogen storage pressure, and PEME hydrogen flow L^t_{elz} given as follow:

$$P_{Cmp} = \frac{2RT_{cell}k\ L^t_{elz}}{(k-1)\eta_{Cmp}} \left(\left(\frac{\pi_{HS}}{\pi_{H_2}} \right)^{\frac{k-1}{k}} - 1 \right) \tag{7}$$

The hourly PEME hydrogen flow is a function of its power consumption P^t_{elz} and efficiency η^t_{elz}, which is calculated as follow:

$$L^t_{elz} = \frac{P^t_{elz}\eta^t_{elz}}{\Delta H_{LHV}} \tag{8}$$

The degradation cost C_{Deg} considers both the PEME and BESS as expressed below.

$$C_{Deg} = \sum_{t=1}^{T} |P^t_{BESS}| D^t_{BESS} + P^t_{elz} D_{elz} \tag{9}$$

The BESS degradation cost is function of its SoC given as:

$$D^t_{BESS} = \frac{C_{BESS} - RS_{BESS}}{2(1 - SoC^t)\ Acc^t\ E_{BESS}\ \eta_{BESS}} \tag{10}$$

where,

$$Acc^t = \frac{a}{(1 - SoC^t)^b} \tag{11}$$

The operation of the electrolysis includes constraints on the current densities, cell area, and maximum cathodic pressure, expressed below.

$$\begin{aligned} 0 \le P^t_{elz} \le J^{max} V^{rate}_{elz} A_{elz} \\ A^{min}_{elz} \le A_{elz} \le A^{max}_{elz} \\ \pi^{min}_{H_2} \le \pi_{H_2} \le \pi^{max}_{H_2} \end{aligned} \tag{12}$$

For safety considerations, the percentage of hydrogen in oxygen is restricted by the maximum allowable limit of hydrogen in oxygen, Ψ^{max}_{H2} in O_2 , as follows:

$$\Psi_{H_2 \, in \, O_2} \le \Psi^{max}_{H_2 \, in \, O_2} \tag{13}$$

The excess of hydrogen production is stored in local HS tanks, where the SoH is constrained by the maximum and minimum allowed SoH given as follows:

$$SoH^{min} \le SoH^t \le SoH^{max} \tag{14}$$

where,

$$SoH^t = \frac{\sum_{q=1}^{q=t-1} (1 - \gamma_{HS}) L^q_{HS} + L^t_{HS}}{E_{H_2}} \tag{15}$$

In addition, the hydrogen flow must satisfy the hydrogen balance equation expressed as:

$$L_{elz}^{t} + L_{HS}^{t} = L_{d}^{t} \tag{16}$$

7.2. Alkaline Technology

Modeling of AE consists of two sub-models: the voltage model, and the gas crossover model. The former expresses the voltage-current characteristics and the corresponding voltage efficiency, while the later accounts for the amount of gas cross over and the corresponding Faraday's efficiency. The voltage across the alkaline cell, V_{cell}, consists of three components: the open circuit electrochemical voltage required to split water V_{oc}, activation overpotential Vact, and resistive overpotential V_{res} as given below.

$$V_{cell} = V_{oc} + V_{act} + V_{res} \tag{17}$$

The open circuit voltage is obtained using Nernst equation and varies with the cell temperature, and gases pressure as below:

$$V_{oc} = 1.229 - \frac{9(T_{AE} - T_{ref})}{10^4} + \frac{RT_{AE}}{2F} ln\left(\frac{\pi_{H_2}\sqrt{\pi_{O_2}}}{a_{H_2O}}\right) \tag{18}$$

The electrode kinetic and charge transfer between the electrodes and electrolyte solution is expressed with the activation overpotential [10] as follows:

$$V_{act} = \frac{RT_{AE}}{\alpha_{an}F} ln\left(\frac{J}{J_o^{an}(1-\theta_{an})}\right) + \frac{RT_{AE}}{\alpha_{cat}F} ln\left(\frac{J}{J_o^{cat}(1-\theta_{cat})}\right) \tag{19}$$

where θ is the fractional bubble coverage on the electrodes surface and is calculated through the following empirical formula as explained in [57]:

$$\theta = \left(-97.25 + 182\frac{T_{AE}}{T_{ref}} - 84\left(\frac{T_{AE}}{T_{ref}}\right)^2\right)\left(\frac{J}{J_{lim}}\right)^{0.3} \quad (20)$$

The electrolysis equivalent resistance is determined by the combined resistances of the electrodes (Re), electrolyte (Rel), and separator (Rs). Therefore, the resistive overpotential is calculated as follows:

$$V_{res} = I(R_e + R_{el} + R_s) \quad (21)$$

Electrodes, electrolyte, and separator resistances are expressed below [57].

$$\begin{aligned} R_e &= \frac{\rho_o^{an}\delta_{an}}{(1-\epsilon_{an})^{3/2}A_c}(1 + k_{an}(T_{AE} - T_{ref}))+ \\ &\quad \frac{\rho_o^{cat}\delta_{cat}}{(1-\epsilon_{cat})^{3/2}A_c}(1 + k_{cat}(T_{AE} - T_{ref})) \\ R_{el} &= \frac{\rho_{el}(M)}{A_c(1 + k_{el}(T_{AE} - T_{ref}))} \\ &\quad \left(l_{an} - \beta_{an} + \frac{\beta_{an}}{(1-\theta)^{3/2}} + l_{cat} - \beta_{cat} + \frac{\beta_{cat}}{(1-\theta)^{3/2}}\right) \\ R_s &= \rho_{el}(M)\frac{\tau_s^2\delta_s}{\omega_s\epsilon_s A_c} \end{aligned} \quad (22)$$

In AE, hydrogen crossover consists of three components [58]: diffusion (n^{diff}_{H2}), convection (n^{conv}_{H2}), and electrolyte mixing (n^{el}_{H2}). The total hydrogen crossover, n_{H2}, is determined by summing these three components as below:

$$n_{H_2} = n_{H_2}^{diff} + n_{H_2}^{conv} + n_{H_2}^{el} \quad (23)$$

The hydrogen diffusion and convection flux through the separator is derived by Fick's law and Darcy's law as given below.

$$n_{diff}^{H_2} = \frac{D_{eff}\,\pi_{H_2}\,S_{H_2}(M)}{\delta_s}$$
$$n_{conv}^{H_2} = \frac{Pr_s\,\Delta\pi\,S_{H_2}(M)\,\pi_{H_2}}{\zeta\delta_s} \quad (24)$$

The hydrogen crossover flow by electrolyte mixing is proportional to hydrogen solubility, recirculated electrolyte flow rate and hydrogen pressure [58] as follows:

$$n_{el}^{H_2} = \frac{S_{H_2}(M)\,\pi_{H_2}\,v_{el}}{4} \quad (25)$$

The hydrogen in oxygen percentage, Φ_{H2}, is the ratio between the hydrogen crossover to the sum of the produced oxygen and the hydrogen crossover as given below:

$$\Phi_{H_2} = \frac{n_{H_2}}{N_{O_2} + n_{H_2}} = \frac{n_{H_2}}{\frac{J}{4F} + n_{H_2}} \quad (26)$$

Similarly, the oxygen crossover, n_{O2}, can be obtained. However, the convection component can be neglected considering that the cathodic pressure is higher than the anodic one. The total oxygen crossover is determined as follows:

$$n_{O_2} = n_{O_2}^{diff} + n_{O_2}^{el} = \frac{D_{eff}\,\pi_{O_2}\,S_{O_2}(M)}{\delta_s} + \frac{S_{O_2}(M)\,\pi_{O_2}\,v_{el}}{4} \quad (27)$$

The efficiency of AE consists of two components: voltage efficiency, and Faraday's efficiency. The voltage efficiency is determined as the ratio between the open circuit voltage and the total cell voltage as follows:

$$\eta_V = \frac{V_{oc}}{V_{cell}} \quad (28)$$

Faraday's efficiency mainly depends on the amount gases crossover. The equivalent lost current density, J_{loss}, and Faraday's efficiency are given by:

$$J_{loss} = 2F\, n_{H_2} + 4F\, n_{O_2}$$
$$\eta_F = 1 - \frac{J_{loss}}{J} \quad (29)$$

The total AE efficiency is the multiplication of these two components as below:

$$\eta_T = \eta_V \eta_F \quad (30)$$

References

[1]. Global Hydrogen Review 2022, IEA, Paris, **https://www.iea.org/reports/global-hydrogen-review-2022**.

[2]. Financial Incentives for Hydrogen and Fuel Cell Projects, Office of Renewable Energy. **https://www.energy.gov/eere/fuelcells/financial-incentives-hydrogen-and-fuel-cell-projects**.

[3]. Consultation on the Clean Hydrogen Investment Tax Credit, Department of Finance Canada, Government of Canada. **https://www.canada.ca/en/department-finance/programs/consultations/2022/consultation-on-the-investment-tax-credit-for-clean-hydrogen.html**.

[4]. Upcoming EU Hydrogen Bank pilot auction, Climate Action, European Commission. **https://climate.ec.europa.eu/news-your-voice/news/upcoming-eu-hydrogen-bank-pilot-auction-european-commission-publishes-terms-conditions-2023-08-30_en**.

[5]. Nuclear Power Plants Gearing Up for Clean Hydrogen Production, Office Nuclear Energy. **https://www.energy.gov/ne/articles/4-nuclear-power-plants-gearing-clean-hydrogen-production**.

[6]. German oil refinery to build 30 MW hydrogen electrolysis plant, Reuters. **https://www.reuters.com/article/us-germany-hydrogen-heide-idUSKBN24Z1FO**.

[7]. CUMMINS Powers the Largest PEM In Operation in the World. **https://**www**.cummins.com/news/releases/2021/01/26/cummins-hydrogen-technology-powers-largest-proton-exchange-membrane-pem**.

[8]. NEOM Green Hydrogen Project, Acwa Power. **https://acwapower.com/en/projects/neom-green-hydrogen-project/**.

[9]. Hydrogen Strategy for Canada. **https://www.nrcan.gc.ca/climate-change-adapting-impacts-and-reducing-emissions/canadas-green-future/the-hydrogen-strategy/23080**

[10]. H. Ishaq, D. Ibrahim, and C. Curran, "A review on hydrogen production and utilization: Challenges and opportunities." International Journal of Hydrogen Energy, vol. 47, pp 26238--26264, Jul. 2022.

[11]. Green hydrogen: A guide to policy making, International Renewable Energy Agency, Nov. 2020. https://www.irena.org/publications/2020/Nov/Green-hydrogen

[12]. Green Hydrogen for Industry: A Guide to Policy Making, International Renewable Energy Agency, Mar. 2022, https://www.irena.org/publications/2022/Mar/Green-Hydrogen-for-Industry

[13]. Green Hydrogen Supply: A Guide to Policy Making, International Renewable Energy Agency, May 2021. https://www.irena.org/publications/2021/May/Green-Hydrogen-Supply-A-Guide-To-Policy-Making

[14]. Study on energy storage, Energy Transition Expertise Centre, Mar. 2023, https://energy.ec.europa.eu/studies/preparatory-studies/energy-transition-expertise-centre_en

[15]. K. Zhang, B. Zhou, C. Y. Chung, S. Bu, Q. Wang and N. Voropai, "A Coordinated Multi-Energy Trading Framework for Strategic Hydrogen Provider in Electricity and Hydrogen Markets," IEEE Transactions on Smart Grid, vol. 14, no. 2, pp. 1403-1417, March 2023.

[16]. K. Zhang, B. Zhou, S. W. Or, C. Li, C. Y. Chung and N. Voropai, "Optimal Coordinated Control of Multi-Renewable-to-Hydrogen Production System for Hydrogen Fueling Stations," IEEE Transactions on Industry Applications, vol. 58, no. 2, pp. 2728-2739, March-April 2022.

[17]. C. Feng, C. Shao, Y. Xiao, Z. Dong and X. Wang, "Day-Ahead Strategic Operation of Hydrogen Energy Service Providers," IEEE Transactions on Smart Grid, vol. 13, no. 5, pp. 3493-3507, Sept. 2022.

[18]. L. Zheng et al., "On the Consistency of Renewable-to-Hydrogen Pricing," CSEE Journal of Power and Energy Systems, vol. 8, no. 2, pp. 392-402, March 2022.

[19]. T. Wu and J. Wang, "Reliability Evaluation for Integrated Electricity-Gas Systems Considering Hydrogen," IEEE Transactions on Sustainable Energy, vol. 14, no. 2, pp. 920-934, April 2023.

[20]. P. Zhao, C. Gu, Z. Hu, D. Xie, I. Hernando-Gil and Y. Shen, "Distributionally Robust Hydrogen Optimization With Ensured Security and Multi-Energy Couplings," IEEE Transactions on Power Systems, vol. 36, no. 1, pp. 504-513, Jan. 2021.

[21]. UK Hydrogen Strategy, HM Government, August 2021

[22]. "Fueling the future of mobility: Hydrogen Fuel," Monitor Deloitte, Paris, 2021.

[23]. IEA, "The Future of Hydrogen," IEA, Paris, 2019

[24]. H. Becker, J. Murawski, D. V. Shinde, I. E. L. Stephens, G. Hinds and G. Smith, "Impact of impurities on water electrolysis: a review," Sustainable Energy Fuels, vol. 7, pp. 1565-1603, 2023.

[25]. M. Abomazid, N. A. El-Taweel and H. E. Z. Farag, "Optimal Energy Management of Hydrogen Energy Facility Using Integrated Battery Energy Storage and Solar Photovoltaic Systems," IEEE Transactions on Sustainable Energy, vol. 13, no. 3, pp. 1457-1468, July 2022.

[26]. S. Zhang, N. Zhang, H. Dai, L. Liu, Z. S. Q. Zhou and J. Lu, "Comparison of Different Coupling Modes between the Power System and the Hydrogen System Based on a Power–Hydrogen Coordinated Planning Optimization Model.," Energies, vol. 16, no. 14, p. 5374, 2023.

[27]. J. Simunovic, I. Pivac and F. Barbir, "Techno-economic assessment of hydrogen refueling station: A case study in Croatia.," International Journal of Hydrogen Energy, vol. 47, no. 57, pp. 24155-24168. , 2021.

[28]. P. Benalcazar and A. Komorowska, "Prospects of green hydrogen in Poland: A techno-economic analysis using a Monte Carlo approach," International Journal of Hydrogen Energy, vol. 47, no. 9, pp. 5779-5796, 2022.

[29]. R. Boudries, "Techno-economic study of hydrogen production using CSP technology.," International Journal of Hydrogen Energy,, vol. 43, no. 6, pp. 3406-3417, 2018.

[30]. K. Almutairi, S. S. Hosseini Dehshiri, S. J. Hosseini Dehshiri, A. Mostafaeipour, M. Jahangiri and K. Techato, "Technicaleconomic, carbon footprint assessment, and prioritizing stations for hydrogen production using wind energy: A case study," Energy Strategy Reviews, vol. 36, p. 100684, 2021.

[31]. S. Praveenkumar, A. E. B, J. D. Ampah, S. Afrane, V. I. Velkin, U. Mehmood and A. A. Awosusi, "Techno-economic optimization of PV system for hydrogen production and electric vehicle charging stations under five different climatic conditions in India," International Journal of Hydrogen Energy, vol. 47, pp. 38087- 38105, 2022.

[32]. M. Nasser, T. F. Megaed, S. Ookawara and H. Hassan, "Techno-economic assessment of clean hydrogen production and storage using hybrid renewable energy system of PV/Wind under different climatic conditions," Sustainable Energy Technologies and Assessments, vol. 52, p. 102195, 2022.

[33]. R. Babaei, D. Ting and R. Carriveau, "Optimization of hydrogen-producing sustainable island microgrids," International Journal of Hydrogen Energy, vol. 47, pp. 14375-14392, 2022.

[34]. A. Al-Sharafi, A. Z. Sahin, T. Ayar and B. S. Yilbas, "Techno-economic analysis and optimization of solar and wind energy systems for power generation and hydrogen production in Saudi Arabia," Renewable and Sustainable Energy Reviews, vol. 69, pp. 33-49, 2017.

[35]. N. A. Iskandar and A. Maheri, "Techno-economic Assessment of Hydrogen Refuelling Stations: Case Study of Hydrogen train," International Conference on Environmental Friendly Energies and Applications , vol. 22, 2022.

[36]. O. Tang, J. Rehme, and P. Cerin, "Levelized cost of hydrogen for refueling stations with solar PV and wind in Sweden: On-grid or off-grid?," Energy, vol. 241, 2022.

[37]. R. Bhandari and R. R. Shah, "Hydrogen as energy carrier: Techno-economic assessment of decentralized hydrogen production in Germany, Renewable Energy, vol. 177, 2021.

[38]. El M. Barhoumi, M. S. Salhi, P. C. Okonkwo, I. B. Belgacem, S. Farhani, and M. Zghaibeh, F. Bacha, "Techno-economic optimization of wind energy based hydrogen refueling station case study Salalah city Oman," International Journal of Hydrogen Energy, vol. 48, 2023,

[39]. E. Assareh and A. Ghafouri, "An innovative compressed air energy storage (CAES) using hydrogen energy integrated with geothermal and solar energy technologies: A comprehensive techno-economic analysis - different climate areas- using artificial intelligent (AI)," International Journal of Hydrogen Energy, vol. 48, 2023.

[40]. "The hydrogen strategy: Seizing the opportunities for hydrogen," Government of Canada, https://natural-resources.canada.ca/climate-change-adapting-impacts-and- reducing-emissions/canadas-green-future/the-hydrogen-strategy/23080, Tech. Rep., De- cember 2020.

[41]. Strategy, "The dawn of green hydrogen-maintaining the gcc's edge in a decarbonized world," available from:. [Online]. Available: https://www.strategyand.pwc.com/m1/en/ reports/2020/the-dawn-of-green-hydrogen/the-dawn-of-green-hydrogen.pdf.

[42]. A. Ajanovic, M. Sayer, and R. Haas, "The economics and the environmental benignity of different colors of hydrogen," International Journal of Hydrogen Energy, vol. 47, no. 57, pp. 24 136–24 154, July 2022.

[43]. T. Holm, T. Borsboom-Hanson, O. Herrera, and W. Merida, "Hydrogen costs from water electrolysis at high temperature and pressure," Energy Convers Manag, vol. 237, no. 114106. [Online]. Available: https://doi.org/10.1016/j.enconman.2021.114106.

[44]. C. Minke, M. Suermann, B. Bensmann, and R. Hanke-Rauschenbach, "Is iridium demand a potential bottleneck in the realization of large-scale pem water electrolysis?" Int J Hydrogen Energy, vol. 46, no. 46. [Online]. Available: https://doi.org/10.1016/j.ijhydene. 2021.04.174.

[45]. M. Ozturk and I. Dincer, "A comprehensive review on power-to-gas with hydrogen options for cleaner applications," Int J Hydrogen Energy, vol. 46, no. 62. [Online]. Available: https://doi.org/

[46]. K. Motazedi, Y. Salkuyeh, I. Laurenzi, H. MacLean, and J. Bergerson, "Economic and environmental competitiveness of high temperature electrolysis for hydrogen production," Int J Hydrogen Energy, vol. 46, no. 41. [Online]. Available: https://doi.org/10.1016/j.ijhydene.2021.03.226.

[47]. A. Buttler and H. Spliethoff, "Current status of water electrolysis for energy storage, grid balancing and sector coupling via power-to-gas and power-to-liquids: A review," Renewable and Sustainable Energy Reviews, vol. 82, pp. 2440 – 2454, 2018.

[48]. D. Scamman and M. Newborough, "Using surplus nuclear power for hydrogen mobility and power-to-gas in france," Int J Hydrogen Energy, vol. 41, no. 24. [Online]. Available: https://doi.org/10.1016/j.ijhydene.2016.04.166.

[49]. A. ZAPANTIS, "Global ccs institute," International Energy Agency, https://www.globalccsinstitute.com/wp-content/uploads/2021/04/Circular-Carbon- Economy-series-Blue-Hydrogen.pdf, Tech. Rep., April 2021.

[50]. Fuji Electric Global, online: https://www.fujielectric.com/products/energy/fuelcell/product_series/spec.html

[51]. M. R. Usman, "Hydrogen Storage Methods: Review and current status," Renewable and Sustainable Energy Reviews, vol. 167, p. 112743, 2022.

[52]. I. Hassan, H. Ramadan, M. A. Saleh and D. Hissel, "Hydrogen storage technologies for stationary and mobile applications: Review, analysis, and perspectives," Renewable and Sustainable Energy Review, vol. 149, p. 111311, 2021.

[53]. C. E. Regulator. Market snapshot: How does a refinery turn crude oil into products like gasoline and diesel? [Online]. Available: https://www.cer-rec.gc.ca/en/data-analysis/energy-markets/market-snapshots/2018/ market-snapshot how-does-refinery-turn-crude-oil-into-products-like-gasoline-diesel.html

[54]. V. C. Recycling. Varennes carbon recycling: Plant characteristics. [Online]. Available: https://rcv-vcr.com/

[55]. Essar. Uks first refinery-based hydrogen furnace arrives at essar. [Online]. Available: https://www.essaroil.co.uk/news/uks-first-refinery-based-hydrogen-furnace-arrives-at-essar/

[56]. J. Buckley. Cnn travel: The world's first hydrogen-powered passenger trains are here. [Online]. Available: https://www.cnn.com/travel/article/coradia-ilint-hydrogen-trains/ index.html

[57]. Z. Abdin, CJ. Webb, and EM. Gray, "Modelling and simulation of an alkaline electrolyser cell." Energy, vol. 138, pp 316-347, Nov 2017.

[58]. R. Qi, X. Gao, J. Lin, Y. Song, J. Wang, Y. Qiu, and M. Liu," Pressure control strategy to extend the loading range of an alkaline electrolysis system." International Journal of Hydrogen Energy, vol. 46, pp 35997– 36011, October 2021.

[59]. Engineering Climate Datasets, Environment and Natural Resources, Government of Canada. [Online]. Available: https://climate.weather.gc.ca/prods_servs/engineering_e.html

[60]. Data Directory, Power Data, IESO. [Online]. Available: https://www.ieso.ca/en/Power-Data/

[61]. A. Bergman and A. Krupnick," Incentives for Clean Hydrogen Production in the Inflation Reduction Act", Resources for the Future, November 2022.

[62]. Land-Based Wind Market Report: 2022 Edition, Office of Energy Efficiency and Renewable Energy. [Online], Available: https://www.energy.gov/eere/wind/articles/land-basedwind-market-report-2022-edition

[63]. N. A. El-Taweel,H. Khani, and H. EZ Farag, ”Optimal sizing and scheduling of LOHC-based generation and storage plants for concurrent services to transportation sector and ancillary services market.” IEEE Transactions on Sustainable Energy, vol. 11, pp 1381–1393, July 2019.

[64]. HyLYZER PEM Electrolyzers Spec. Sheet, Cummins Brochures Library. [Online]. Available: https://www.cummins.com/brochures.

[65]. F. Scheepers, M. Stahler, A. Stahler, E. Rauls, M. Muller, M. Carmo, and W. Lehnert,” Improving the efficiency of PEM electrolyzers through membrane-specific pressure optimization.” Energies, vol. 13, pp 612, February 2020.

[66]. M. T. Groot, J. Kraakman, and R. Barros,” Optimal operating parameters for advanced alkaline water electrolysis.” In International Journal of Hydrogen Energy, vol. 46, Sep. 2023.

[67]. American National Standard for Electric Power Systems and Equipment Voltage Ratings (60 hertz), ANSI Std. C84.1, Dec. 2006.